MAREES TERRESTRES

BULLETIN D'INFORMATIONS

1 1 3

15 OCTOBRE 1992

Association Internationale de Géodésie

Commission Permanente des Marées Terrestres

Editeur Prof. Paul MELCHIOR
Observatoire Royal de Belgique
Avenue Circulaire 3
1180 Bruxelles

ATGIA : ACCURATE TIDAL GRAVIMETRY IN ANTARCTICA

a Pre-Project for an International
Coordinated Programme

Pierre Mazzega

UMR39/GRGS/CNES
18 av. E. Belin
31 055 Toulouse Cedex
France.
Fax: (33)61.25.32.05
E.mail: Ciamp@mfh.cnes.fr

0. Summary.

The opportunity is shown of promoting and realizing an International Coordinated Programme of Accurate Tidal Gravimetry In Antarctica (**ATGIA**) before the 2000's, for the overall improvement of our knowledge of the solid, ocean and loading tides and of the various related geodynamical phenomena. The programme of **ATGIA** would consist in the deployment of 35 to 45 Earth Tide gravimeters in the southern islands and numerous stations wintering on the antarctic continent, and on their synchrone operating during one or two complete years.

The complete data sets of all the stations participating the **ATGIA** Programme would be centralized, validated and pre-processed (eg. to compute standard corrections, add the atmospheric pressure parameter,etc) by the International Center for Earth Tides (**ICET**) and then redistributed to all the scientific groups involved in the experiment.

The achievement of such an ambitious programme (fortunately) vitally depends on the agreement and implication of several research laboratories or institutions all around the world. It would give a further opportunity to reinforce a peaceful scientific cooperation between the participating countries, following the true spirit of the Antarctic Treaty.

1. Preamble.

The progresses of geophysical sciences during the last thirty five years (starting with the IGY) definitely prove the necessity to maintain very strong inter-relations between developing theories and ambitious programmes of data acquisition. However, the image of the Earth that could be restored today from the various "empirically observed" geophysical fields would lack a large spherical cap covering the southern latitudes from about 45°S down to the South Pole.

This situation is particularly critical for the present-day studies of the tidal fields: the solid and ocean tides, and their interactions, are planetary phenomena (Melchior 1982) so that the assessment of the models and their theoretical improvements are now entirely dependent on the availability of global and dense networks of high accuracy in-situ observations. The Antarctica and the surrounding Southern Oceans are in a metaphoric sense an "Anti-Earth" (the Antichtone) where our best models are of doubtful accuracy and where at the same time "abnormal" responses of the solid earth and ocean water masses to "normal" forcings are likely to occur (see sec.3).

Tides are also interacting with a lot of other dynamical parameters (e.g. the nutations, length of the day l.o.d., polar motion, structure and rheology of the Earth interior,...) describing the (evolving) state of the planet (eg. Dehant 1991; Groten 1991), which are of interest for several research disciplines (astronomy, geodynamics, geodesy, oceanography; see eg. Melchior 1991). The weakness inherent to the tidal models (their accuracy being almost unknown or their predictions known to be inaccurate, these two cases summarizing the models state of the art for southern latitudes) now hampers identifying the exact mechanisms sustaining these complex interactions and clarifying their relative importance.

In this context, the use of direct observations of the involved fields can be ordered under two general items:

model assessment: the fields as predicted by competing models are compared with "ground-truth" data; at the ultimate stage of this process, at least one model emerges which is recommended as (temporary) standard by the scientific community;

model constraints: the observations can provide a wide range of constraints, from the nature and/or location of physical boundaries (as seen for ex. in the modeling of the core), to the magnitude and/or sampling of coefficients/functions imbedded in the theoretical equations (usually integro-differential).

For both purposes, the reference data set should: -be of good enough quality to allow the proper discriminations; -benefit from a global coverage in order to avoid the over-weighting of specific regions; -gather several kinds of data, differently related to the studied fields and with different error budgets.

In the next section, the three observation techniques providing information on tides and related phenomena, the more likely to be "deployed" within the next decade are reviewed: satellite altimetry, tide gauge measurements and tidal gravimetry. In the following it is shown that:

a- the first two systems will only marginally or scarcely cover the Southern Oceans (and not at all the Antarctic Continent);

b- only an International Coordinated Programme of ATGIA could, within a few years, bring the required observations, combining the necessary accuracy, reliability, "robustness" and coverage, to achieve a decisive breakthrough in our knowledge of tides and related planetary phenomena;

c- all the technical conditions are now put together to actually realise and succeed in an ambitious Programme of ATGIA before the 2000's.

However, it should be well understood that the ATGIA project as described herein for the first time is just a preliminary proposal published in order to provide a "zero order" basis for further discussions and possibly serious amendments. In particular, the exact design of this experiment should rely on quantitative studies to be performed in a preliminary phase.

2. Measurements of Tides and Related Geodynamical Phenomena in the Southern Latitudes: Status and Perspectives.

An exhaustive review of all the existing data related to tides in Antarctica and in the surrounding ocean and islands would be an heavy task which has not been undertaken here. Moreover such an inventory should also consider the availability of these historical data. This report just attempts to give a general overview of the subject.

a- Satellite Altimetry (SA)

Among other oceanographic and geophysical signals, a radar altimeter samples all along the satellite track, the instantaneous sum of the solid, ocean and loading tidal heights, at the rate of one datum per second (about 7 km interval). The spacecraft life-time is usually 2 to 4 years.

In most part of the world ocean, the tidal signal is not the predominant component of the raw SA data. One has to rely on models of the Earth gravity field, of dynamic orbit computation, of the radar wave propagation through the media, etc, before tempting an analysis of the SA data sets. Even with these corrections, the remaining signals (dynamic topography of the general oceanic circulation, mesoscale variability associated with the oceanic eddy fields, dynamic response of the ocean surface to the atmospheric fluctuations, etc) and correction residuals prevent from a direct mapping of the ocean tides (see the review paper by Cartwright 1991). To get a subdecimetric accuracy on the tidal solutions derived from altimetry, rigorous (and "heavy") methods of data analysis (eg. Mazzega and Jourdin 1991) or assimilation scheme within a hydrodynamical model (see eg. Bennett and McIntosh 1982; Zahel 1991) have to be designed.

It should also be mentioned that the solid tide is assumed to be known with a sufficient accuracy (at least with regard to

the other signals) for a theoretical correction to be routinely applied. Therefore, SA is virtually of no use for the study of solid tides.

The situation is much more critical when considering the Southern latitudes. The predicted satellite ephemeris are significantly degraded because of the quasi-absence of tracking stations south of 45°S (note: this problem will be soon overcome for future altimetric missions with the help of global and homogeneous tracking networks, eg. the DORIS network), and of the poorer accuracy of the Earth gravity field models. This last remark should unfortunatly extend to all the geophysical models used in the data processing. Jourdin et al. (1991) have shown that the ocean tides cannot be precisely recovered (except the dominant M2 wave), even on the basis of constraining a priori space-time information, when the signal to noise ratio is too low (in particular when radial orbit errors are larger than 25 cm rms). Moreover, the commonly strong sea states or the sea ice covering large areas around Antarctica, induce perturbations of the radar wave echo which are very difficult to modelize. As a consequence of these limitations, the global mean sea surface models (used as reference surfaces both for SA data validation or as references levels for subsequent analyses), derived from altimetry itself, are truncated near 60°S (see eg. Marsh et al. 1986).

Of the past satellite altimetry missions, only the GEOSAT one may bring useful information on the tides at the southern latitudes (Fig.1). South of 60°S, the GEOSAT data must be processed with much care and validated on the basis of special criteria. With a dedicated effort, a reliable mean sea surface has been very recently computed at Toulouse (A. Cazenave, pers. communication June 1992), a preliminary step before any kind of tidal analysis (note: a map of the gravity field south of 60°S has also been derived from Geosat altimetry by McAdoo and Marks 1992),

At the present time (Spring 1992), we have no exact information on the way the ERS-1 orbit will be computed, the PRARE tracking system having failed at the beginning of the mission. It seems that a laser network will be used for the orbit computation with a very poor coverage of the southern hemisphere.

With an inclination of 66°, the TOPEX/POSEIDON altimetric mission, optimised for oceanographic purposes (Topex/Poseidon 1991), will deliver high accuracy measurements but will not sample south of 66°. The resulting overall improvement of the global ocean tide models should be drastic (see eg. Vincent et al. 1991), but without further measurements, this new generation of models will suffert the same biases from the existing ones around Antarctica (Woodworth 1985; Knopoff et al. 1989). In turn, this limitation may leave the global tidal energy budgets unbalanced (see sec.3)

b- Tide Gauges (TG)

The gauges, moving with the ocean floor or continental coast, sample only the ocean tides (in fact the filtered local sea level). The harmonic constants deduced from the analysis of the time series made at land-based stations are centralized in a data bank at the International Hydrographic Organization (IHO 1979) in

Ottawa. The constants obtained from pelagic tide gauges are gathered by the Bidston Observatory (UK) under the patronage of IAPSO (Cartwright et al. 1979, Cartwright and Zetler 1985). An updated IAPSO compilation should appear very shortly.

In the following, only those tidal data available from these two data banks easily accessible to the scientific community are considered. More information could be probably gathered by an eclectic scanning of the oceanographic litterature. For example, Lutjeharms et al. (1985) report on 12 records exceeding 5 years duration in Antarctica, among which 7 are located on the Ross Ice Shelf and 5 in the Peninsula. These "potential" data will not be discussed in this preliminary study.

Of the 4090 stations of the IHO 1979 data bank, only 105 are situated south of 45°S and 33 south of 60°S (considering the M2 constituent). These 33 land based TG are plotted on Figure 2 with the 7 pelagic locations south of 45°S as published in the IAPSO reports. The accuracy of the whole data set is probably very heterogeneous, depending on the instrument type, calibration and stability, location of the station with regard to the deep ocean, mechanical device for the waves and swells filtering, method of data analysis, record length, and so on. It is worth noting that at the subdecimetric level of accuracy, the validation of these data is an epic problem.

The IHO data reported on Fig.2 are nearly those interpolated by Schwiderski in his model (1980a,b). The three pelagic constants in the Weddell Sea were obtained later and used by Woodworth (1985) to show that the Schwiderski's model exhibits large errors there. This shortcoming of the best available model would partly result from the model fitting to a spurious TG data of the antarctic coast. Comparing the pelagic constants with the relatively independent tidal models of Schwiderski (1980a,b), Cartwright and Ray (1990) and Wagner (1990) (these last two models being derived from overlapping Geosat data sets but with different analysis methods), Wagner (1991, cf p.137) has clearly shown that the dispersion of the pelagic constants relative to the three models increases as the TG records shorten (some of which being no more than two weeks long). This test suggests that on the average, the tidal records extracted from short records are far less reliable (maximum errors on a single tidal constituent up to 8-10 cm) that was previously thought (~1-2 cm).

This report is once again unfavourable for the southern latitudes where the prevailing meteorological and sea state conditions have always challenged the oceanographers from getting accurate and long time series of measurements. Until now, only a few long records have been obtained along the coasts of Antarctica (the list is probably to be completed; see e.g. Lutjeharms et al. 1985). Let us just give a few examples: the results of the analysis of a nearly 1 year long pressure gauge record at the japanese Syowa station (see Fig.3) was published in 1968 by Hori and Inbe; a several years long series of sea level measurements obtained by the British Antarctic Survey at the Faraday station (west coast of the Peninsula) has been analyzed by Cartwright (1979) and more recently a TG moored beneath the George VI Ice Shelf was operated during one year (Pedley et al. 1986). The records provide an evidence for strong tidal non-linearities at least along the Antarctic Peninsula which may result both from

dissipative mechanisms in the shallow waters and from interactions with the ice shelves.

As was previously said, most of the data plotted on Fig.2 were already available at the time Schwiderski produced its tidal model. Recognizing this lack of quality data at these latitudes and planning to perpetuate a global network of sea level survey, the Global Level Of Sea Surface (GLOSS) programme recommended the upgrading or installation of about 11 permanent stations south of 45°S (see Fig.2; in 1988, only 2 of them have had already provided measurements in the past). About 4 supplementary stations are asked for on the antarctic continent by the World Ocean Circulation Experiment (WOCE) in support to the ERS1 and Topex/Poseidon altimetric missions (WOCE 1992; these are Sanae, Palmer, Russkaya and McMurdo, see Fig.3). In fact, the installation and operation of land based or sea floor TG face with formidable difficulties raised by the extraordinary unfavourable weather and sea state conditions (Intergovernmental Oceanographic Commission 1988). As a consequence, the data are often less accurate than in any other part of the world ocean. Today the status and future of several of these "extreme" stations remains uncertain.

The interests of the GLOSS and WOCE programmes in these new measurements are for the monitoring of the monthly and long term sea level fluctuations and their surveying at the main ocean straits as a measure of the large scales water fluxes. One can imagine that the tidal constituents will be also extracted and made available to the scientific community. In any case, even considering the most optimistic scenario (all the stations implemented, long records, accurate measurements, etc), the scarce coverage of this data base will rapidely appear unsufficient for a high accuracy modeling of ocean tides in a region where this phenomenon reveals particularly complex (naturally, nothing at all will be learned from TG measurements about the solid tides and other geodynamical phenomena).

c- Earth Tide (ET) Gravimetry

An ET gravimeter basically measures the in-time variations of the local gravity, with periods ranging between a few minutes to a few months or years. The direct attraction of the Sun, Moon and planetary bodies can be corrected with a high degree of accuracy (Merriam 1992a). The signal is related to the solid tide and indirectly to the ocean tide through the combination of three gravimetric effects that we shall hereafter call "loading tide" (say the newtonian attraction of the tidally raised water masses plus the gravity perturbations resulting from the crust deformation under the tidal load and from the induced vertical displacement in the Earth gravity gradient; Farrell 1972). Several other geodynamical phenomena like the Earth variable rotation, various loading processes (eg. by the atmospheric pressure), core dynamics, have their own signatures in the data (Hinderer et al. 1991a), as well as much more regional or site-dependent mass redistributions (eg. Goodkind 1986).

If we except the rather crude observations of the antarctic expeditions at the beginning of this century, it seems that the first modern measurements of tides in Antarctica were obtained during the International Geophysical Year with gravimeters set on the Filchner (south of the Weddell Sea) and Ross ice shelves (Thiel et al. 1960). In 1969, the Earth Physics Institute in Potsdam did pioneering work by installing an ET gravimeter at the inner-continental station Vostok (Schneider 1971) while another instrument was operated by japaneses at the Syowa station near the coast (Nakagawa et al. 1970). In 1970, an ET gravimeter was installed at the South Pole station (Jackson and Slichter 1974). Then several yearly records were obtained there, cumulating 9 years of observations in 1989 (Knopoff et al. 1989). Tidal gravimeters were also operated for short periods in 1973-1975 on the Ross ice shelf (Robinson et al. 1977) for the purpose of ocean tide mapping: far enough from the hinge zone where the ice shelf, more or less attached to the grounded glacier, is bending with the tides, the ice shelf is freely floating on the ocean surface so that the instruments directly follow the ocean tide oscillations (with the solid and loading tides added to the oceanic signal).

During the last ten years, tidal gravimetry in Antarctica has only sporadically developed, both on the continent and surrounding ice shelves (eg. Williams and Robinson 1980; Ogawa et al. 1991). As a matter of fact, the International Center for Earth Tides (ICET) at the Royal Observatory of Belgium (Brussels) which centralizes the ET gravimetric data bank, counts only 6 stations south of 45°S among more than 300 stations distributed world-wide (these are: the South Pole n°9998, Ferraz King George -Antarctica n°9910, Kerguelen Isl. n°9904, Lauder -N. Zealand n°4420 plus Ushuaia n°7817 and Com. Rivadavia n°7818 -Argentina reported in Melchior et al. 1992). Some of these data have been obtained in the 70's (eg. Kerguelen Isl.) and may be of poor accuracy when compared with the present measurements. The data available south of 45°S from the ICET data bank are plotted in Figure 4.

Since 3 or 4 years, the gravimetric studies of tides and related phenomena are deeply buoyed up by a definite improvement in the calibration techniques. Indeed, several authors have reported on very high accuracy measurements (of the order of 1 **microgal** or better) obtained with "classical" ET gravimeters converted to electrostatic feedback (Baker et al. 1989; Xu et al. 1989; Hsu et al. 1991; Wenzel et al. 1991). Several research subjects that were only accessible with the help of supraconducting gravimeters, enter now the "jurisdiction" of more classical instruments, provided the calibration and maintenance are achieved carefully (Zürn et al. 1992).

It has been said that with regard to a tide gauge, an ET gravimeter not only samples the ocean tide (through its integral loading effect) but the complete tidal field plus other geodynamical processes with their own gravimetric signatures. But when measurements are performed in highly hostile external conditions, the decisive advantage of the ET gravimeter over a tide gauge lies in the possibility of putting the instrument with its power supply and registration devices in a thermostatized room, sheltered from bad weather. Other environmental parameters (eg. the atmospheric pressure, etc) can also be safely recorded at the same time.

Once the ET gravimeter is operating, the maintenance is relatively easy and quick (daily verifications of the recording

tape, weekly calibration, etc.) so that several year records can be obtained which in turn provide a high spectral resolution in the tidal frequency bands.

With the present data recording devices, the in-time sampling rate could be set for example to 1 datum/ 10 min (or even higher), allowing for the study of gravimetric transient phenomena.

Several other in-situ conditions are specific to Antarctica and may "sound" abnormal with regard to the usual tidal gravimetry. But as these conditions proceed from geophysical orgins (eg. the seasonally varying sea ice coverage, the particular rheology of the continental ice sheet, the dynamic response of the sea ice and ice shelves to tidal forcings, etc) they truly allow to widen the investigation fields and to modelize new effects which directly perturb the tides as known at temperated latitudes (or even at the northern latitudes where the ice-ocean-earth system has a completely different structure).

Three main conclusions can thus be drawn from this section:

first: the ET gravimeter is the best adapted instrument for operating in Antarctica: indeed once sheltered from bad weather conditions, the gravimeter provides very accurate and long series of measurements at the low cost of a relatively easy maintenance;

second: as in the next years satellite altimetry and tide gauge technologies will only marginally provide information on tides (ocean tides only!), a large number of ET-gravimeters should be deployed in Antarctica and in the southern islands in order to get accurate observations of all the tidal fields and related geodynamical phenomena;

third: the only way of installing and operating a sufficient number of gravimeters in the southern latitudes is clearly to coordinate at the international level an ambitious programme of high accuracy tidal gravimetry.

In the next section, the concept of an International Coordinated Programme of ATGIA is highlighted and an overview of the expected scientific investigations and results is temptatively presented.

3. The International Coordinated Programme of ATGIA and its Foreseable Scientific Impact.

The sporadic operations of a few tidal gravimeters in Antarctica or in the surrounding islands constitute worthwile experiments both to derive the basic logistic conditions required to get accurate measurements and to delineate the broad features of the tidal response of this continent. Presently, it seems that some countries are conducting (or plan to do so) such observations independently from each others at these latitudes (e.g. at two stations of the People's Republic of China; at the respectively spanish and italian stations of Deception Island and Terra Nova Bay, at the Syowa japanese station; P. Melchior, pers. communication 1992).

Nevertheless, only a deployment of a large array of 35 to 45 instruments properly calibrated and maintained, simultaneously

recording at the microgal (or better) level the gravity variations during one or two years, could yield a real breakthrough in the tidal and geodynamical studies (or any somewhat equivalent experiment, see below).

In coordinating an International Programme of Accurate Tidal Gravimetry In Antarctica, on the basis of a total exchange of the data under the auspices of the International Center for Earth Tides, the scientific community involved in the study of Earth tides would positively create a precedent in the long story of tidal research and would contribute in an invaluable way the progresses of Geodynamics.

The **simultaneous** operation of so many ET gravimeters distributed all over a large continent would also be a really innovating characteristic of the **ATGIA** Programme. Most of the geodynamical processes observed by a gravimeter have large spatial scales (and so are probably the residuals of "first order" models used to describe them). Practically it means that their gravimetric signatures should be coherent for groups of nearby stations. These properties may reveal highly useful to separate weak or very tenuous geophysical signals (say lower than 1 microgal) from uncoherent noises of higher magnitude. For example, this kind of approach was in fact implicit when Zürn et al. (1987) compared their own gravity time series (superconducting gravimeter at Bad Homburg) with the one obtained simultaneously at Brussels, in search for the transient spectral signature of an inertial oscillation presumably detected by Melchior and Ducarme (1987).

In summary, an **ATGIA** experiment should be designed in order to optimize the realization of the following general criteria:

1- **measurement accuracy**: * controls the signal to noise ratio. The better the accuracy, the wider the range of phenomena that can be studied and constrained by the observations. An accuracy of 1 microgal -or even much better at least in some parts of the frequency spectrum- is surely achievable;

2- **length of the time series**: * controls the spectral resolution. The Earth's rotation tends to alias phenomena from different origins in the diurnal frequency band (eg. tides and Free Core Nutation). The discrimination between them is possible when long time series (several years long) are available or with the use of theoretical a priori information;

* if the instrumental drift can be controlled or modelized (eg. De Meyer and Ducarme 1991), allows the study of long period tides / atmospheric loading, and the slow variations of the gravity;

3- **time-sampling rate**: * a rate of 1 datum/10 min (for example) would allow to recover ocean loading signals generated by the shallow water non-linear ocean tides and the tidal interactions with the ice shelves;

* once the tidal and other stationary signals are removed from the time series, the residuals can be analyzed for non-stationary and transient signatures;

4- **simultaneous recordings**: * allow to discriminate between phenomena with similar spectral signatures but with markedly

different spatial coherences (or wavelength power spectra). This kind of approach relying on a priori theoretical information is somewhat "equivalent" to an increase of accuracy (s/n ratio), time series length and time-sampling rate [this point cannot be further argumented in this context and is a matter of current research];
* gives the opportunity of validation and accuracy assessment of the tidal gravity measurements at nearby stations;

5- large array of ET gravimeters: * samples a wide range of ice/earth structures under and around the stations;
* forming numerous pairs of stations, samples a wide range of distances between simultaneous recordings in order to separate various phenomena on the basis of their respective spatial coherences;
* provides several configurations of the stations relative to the ocean.

The precise design of an ATGIA experiment (considering these 5 general criteria but also the exact number and locations of instruments, the calibration protocol before, eventually during, and after the experiment, and so on) should be a matter of preliminary studies. In the same way, numerical experiments using simulated time series should explore various modeling strategies and illustrate in a rigorous manner the scientific results that could be expected from the ATGIA experiment (for example as a function of the number of participating stations, data accuracy, length of the time series, etc). The optimal in-time deployment of gravimeters, among various possibilities (eg. the scenario here proposed is the synchronic deployment of 35 to 45 gravimeters simultaneously operating during 1 or 2 years; another scenario could be to operate only 20 instrumenst during 1-2 years at 20 sites, then changing their locations for another 1-2 years period at 20 new sites,; etc) should be also discussed on the basis of numerical simulations (see also Sec. 5f).

A lot of scientific investigations based on an ATGIA experiment can already be listed (see below). However within 2 to 3 years, several "ingredients" entering more or less directly tidal and geodynamical research may benefit from substantial progresses which will be very useful for our purpose. The more obvious improvement that is foreseable, is the publishing of a new generation of accurate ocean tides models (except possibly all around Antarctica, see sec.2), including more constituents than presently available. The use of these models for the computation of loading effects will leave lower residuals in the tidal gravimetric records. Another example is concerned with the recent progresses made in the knowledge of the continental ice rheology and of its slow deformations which in turn may affect the gravimetric signals. In the following, we have tried to keep a medium line between obvious pessimism and over-optimism. A preliminary list can be given as follows:

Earth Tides:

- the first point is surely to match the observed gravimetric factors with the Wahr-Dehant theoretical model (which includes ellipticity and rotation) for the southern latitudes;

- the impact over the gravimetric factor of the vertical rheological profile of the continental ice sheet and of the lateral heterogeneities due to the varying ice thickness have to be estimated (from 0 m on the rocky coasts to 3000 or 4500 m in East Antarctica; ice thickness directly relates to a definite rheological state of the ice); if necessary, the predicted site dependent factors should be compared with the observed ones. As will be seen in Sec.4, the proposed ATGIA stations present a wide range of "structural sites";

- the previous analysis would then allow to determine a set of improved load Love numbers fitted to the specific structure of the Antarctic continent;

- the atmospheric loading effect on gravity (eg. Van Dan and Wahr 1987; Niebauer 1988) should be reconsidered both for the response of the continental ice sheet and for the extreme atmospheric conditions of Antarctica (pressure and temperature; see Merriam 1992b), using in-situ pressure measurements and/or the predictions of meteorological models (note that the simultaneous operation of all the ET gravimeters would be highly useful for this kind of study). The number of weather stations is steadily increasing in Antarctica and now reaches 40 (O. Bromwich, pers. communication 1992);

- the tidal energy dissipated by the "body tide" should be re-examined accounting for the thick continental ice sheet;

- the debated question of an eventual correlation between the gravimetric residuals and surface geothermal heat flows (eg. Yanshin et al. 1986; Rydelek et al. 1991; Robinson 1991) should be reconsidered for this very specific "heat flow province".

Ocean Tides / Loading Tides:

- within 3 years several competing new global ocean tide models will be available, with the main discrepancies probably occurring at the southern latitudes. The first really independent test will be to match their loads with tidal gravimetry (the complete ICET bank), in particular with the ATGIA experiment data. The residuals unexplained by the ocean tide models, if not generated by extra geodynamical processes, can then be inverted for an improvement of the cotidal/corange maps (Françis and Mazzega 1991);

- apart from the peri-Antarctica ocean, the Weddell and Ross Seas exhibit more or less unusual tides (see Fig.5): the first one has a mix tidal regime (eg. Thiel et al. 1960) while the Ross Sea tide is dominated by the diurnal waves with a possible resonance effect (see eg. Williams and Robinson 1980; McAyeal 1984). A complexe tidal response is also observed along the west coast of the Peninsula (e.G. Cartwright 1979). Further data are needed to improve the models in these "marginal" basins;

- the ATGIA data would allow to search for eventual seasonal modulations of the tidal regime due to the moving sea-ice front (with an area of ~4 million km2 in summer, up to ~20 million km2 in winter). As a matter of fact, such phenomena have been clearly

identified on the sea-level and velocity components of the tides in the semi-enclosed Hudson Bay (Prisenberg 1988);

- the global ocean tides energy budget may remain uncomplete as long as the dissipation on the ice shelves is not properly modeled (Doake 1978). Until now this energy sink has not been accounted for in the global ocean tide models so that unexplained differences between tidal energetics as deduced from satellite orbit analyses or Lunar laser ranging may originate there. To improve our knowledge of this complex phenomenon and to constrain the proposed models, the ATGIA data would be highly useful (in particular to compare with the predicted non-linear tidal waves of species 3, 4, and so on; see Pedley et al. 1986);

Earth Interior & Geodynamical Parameters:

Though this paragraph is rather artificially separated from the one devoted to the Earth Tides, one can list the following items:

- well identified residuals of the body tides alone with regard to the latitude dependent Wahr-Dehant theoretical model, would suggest the presence of strong lateral heterogeneities in the upper mantle (or crust). These anomalies have not been detected yet and theoretical studies have shown that gravity signal perturbation would be small (eg. Wilhelm 1978). The overall structure of Antarctica being very particular, with the underlying bed-rock (the "continent") loaded by several thousand metres of ice at or below the sea level (see Fig.6), the previous model predictions have to be confirmed;

- the ATGIA data set should further allow to fix an upper bound on the effects of the Earth's inelasticity over the gravimetric factor; recent estimations vary from 0.1-0.2% (Dehant 1987a,b) to 0.7% (given as the maximum effect by Lambeck 1988), with medium values proposed by Wahr and Bergen (1986). Recent gravimetric observations weaken the last two estimations for Europe (Baker et al. 1991);

- the array of ET gravimeters operating simultaneously, the search for gravity signatures of the core normal modes (eg. the Nearly Diurnal Free Wobble and the associated Free Core Nutation; the F"I"CN, etc) could be undertaken with dedicated methods (eg. along the line proposed by Neuberg et al. 1987) and possibly compete - or complete - the scarce "array" of superconducting gravimeters (Zürn et al. 1992);

- the transient responses of the Earth to sollicitations (eg. from earthquakes) are located in the core and could be studied with the ATGIA "array". Note that the inertial gravity waves in the core ("undertones", ~0.1 microgal) are maximum at the poles;

- the analysis of the gravimetric signatures of the nutations, polar motion and l.o.d. would constrain the modeling of these phenomena, independently from other geodetic methods (VLBI, analyses of satellite orbit preturbations, etc);

- the surface signal of the Chandler Wooble is a few microgals with a period of ~430 days and could be detected considering a set of ET gravimeters (with independent instrumental drifts).

Long Period Tides:

- the long period tides item is listed separetly as relatively little is known about them. From the point of view of hydrodynamical modeling, the question is not clear whether the (modified) Laplace Tidal Equations are good approximations for the ocean tides at these frequencies. Schwiderski's solutions for Mf, Mm and Ssa are not so satisfactory. Other authors have proposed to rely on a simple equilibrium relation. The debate is open. The homogeneous set of ATGIA experiment data could be decisive to make definite statements regarding that problem, since the long period body tides are maximum at the poles (Rydelek and Knopoff 1982).

4. ATGIA: a Feasible International Programme Before the 2000's

"It was recognized quite early in Antarctic science that, in order to be effective, research had to be coordinated to come to terms with the immense size of the continent, the magnitude of the scientific problems, and the logistic requirements - all beyond the reach of a single nation. **SCAR** (Scientific Committee for Antarctic Research) was established in 1957 by the International Council of Scientific Unions (**ICSU**), of which it is a component body, to initiate, promote and coordinate scientific activity in Antarctica, with a view to framing and reviewing scientific programs of circumpolar scope and significance. With 18 full and 7 associate member countries [summer 88, P.M.], it meets biennially, and acts through an executive committee, permanent working groups, and more temporary groups of specialists to report on the main Antarctic scientific disciplines. Increasingly **SCAR** is being requested to advise and review issues of concern to the **Antarctic Treaty System** through these mechanisms. Such matters focus on requirements for conservation of marine living resources, waste disposal, and the potential environmental impacts associated with a variety of activities, such as minerals exploitation. **SCAR** will need to be responsive to these and future overtures if science is to continue to have a strong voice in the wider development of Antarctic affairs." (from Drewry 1988).

The **ATGIA** Programme has to be realized with the agreement and advice of **SCAR**. Further information of this subject will be gathered during the next few months [P.M.].

The stations of the **SCAR** nations that were opened during the complete 1991 year are plotted on Figure 3. They are not only located on the continent but also on several southern islands. One extraordinary paradox of Antarctic is that though the continent does not have an autochthon population over its 14 million km2, the only "human beings" are invariably scientists and the military who have the responsability of the logistic support. In general it seems that several scientific experiments are simultaneously conducted at each station, with the scientific personnel operating the instruments and ensuring their maintenance. The approximate

number of persons wintering at each station is listed in Appendix A for each nation, with the geographical coordinates of the sites. 25 to 30 more stations are operating only during the summer time. The access facilities may vary from one station to another, with airplanes landing for example at McMurdo or in the Antarctic Peninsula, but most of the sites being accessible by ship only.

A few meteorological parameters are worth noting to give a general idea of the hospitality of the continent. The mean annual temperature at the Vostok station (Polar Plateau, East Antarctica; ice thickness: 3700 m; 3 488 m above sea level) is about -55.6°C, with a minimal temperature of -89.6°C (-128.6°F) recorded on July 21, 1983. The air temperature is much more lenient near the coasts (about -10°C) but the catabatic winds are quasi-permanent (~20 m/s; higher wind speed recorded at Dumont d'Urville: 88 m/s). Useful information on Antarctica may be found for example in the special issue of Oceanus (Summer 1988, 31-2) or in May's book (1989).

As a preliminary proposition for the ATGIA Programme, 34 sites are identified (see Figure 4). Each "ATGIA site" may group several stations from different nations. These sites include islands in the sub-antarctic zone and two sites slightly north of 45°S (these are Tristan da Cunha Isl -UK or Gough Isl. -SA; Amsterdam Isl. -Fr).

Each of the 34 sites should be equipped with 1 -eventually 2- ET gravimeters to fulfil the scientific objectives listed in the previous section. The redundancy would be extremely useful to make in-situ cross-validations and accuracy assessments of the gravity time series. Indeed, the calibration of all the instruments before their installation may reveal unsufficient owing to the environmental conditions of Antarctica. The possibility and opportunity of further in-situ calibrations, for example with an Absolute gravimeter (Hinderer et al. 1991b), during the ATGIA experiment should also be investigated. A few of the 34 sites have been or are already occupied by an ET gravimeter (eg. Com. Ferraz, South Pole, Syowa and Asuka, etc). Further recordings should be obtained at these sites at the same time all the other measurements will be made.

The sites distribution should also match all the requirements of signal processing: it is homogeneous and covers all the latitudes between 45°S to the South Pole; a few stations are distant from the ocean (n° 13, 18, 19); other sites are near the sea ice shelves (10, 11, 14, 17); the ice thickness beneath the sites is varying from 0m (eg. 4: Syowa) to more than 3500m (eg. 18: Vostok) (see Figure 6); a large variety of meteorological conditions are also "sampled", between the dry Polar Plateau to the windy antarctic coasts or the moisty islands north of 65°S. A bathymetric map of the Southern ocean is also given in Figure 7.

In summary, the possibility actually exists of realizing before the 2000's an ambitious ATGIA experiment if the Scientific Community involved in Earth Tides studies and Global Geodynamics coordinates at the international level a well defined Programme to be submitted to the approval of SCAR.

Contacts will be soon established with SCAR and national authorities to write out a preliminary document (to be amended in the future as the project evolves) containing more detailed

information on the station logistics, conditions for a large scientific experiment to be realized, etc, and actions to be undertaken with regard to SCAR.

5. First Evaluation of a Working Plan for the ATGIA Programme.

The ATGIA Pre-Project will be discussed at the 12th International Symposium on Earth Tides to be held at Beijing (People's Republic of China) on August 1993. Prof. Hsu, the organizer of the Symposium has kindly accepted to dedicate a special session to this project of interest for the community involved in tidal research. A working plan is proposed with two main stages as follows:

1- **Pre-Symposium Phase** (April 92 - Spring 93):

This preliminary paper has been now sent to the international Scientific Community (defined on a large basis) likely to be interested in participating in the ATGIA experiment.

The comments, ideas, proposals, etc, of the Scientific Community during the pre-symposium phase would be centralized by P. Mazzega in Toulouse in order to constitute a first draft to be distributed at the Beijing Symposium or alternatively slightly before. **Prof. Hsu**, the General Secretary of IUGG **G. Balmino** and the International Center for Earth Tides will be informed, month after month, of the current "state" of the project.

2- **Post-Symposium Phase** (Summer 93 - ATGIA experiment?):

If the ATGIA experiment is retained by the Scientific Community at the Beijing Symposium, an **ATGIA Scientific Committee** could be created which will have to further promote, coordinate and prepare the realization of the ATGIA Programme. This Committee would also act as an advisory group stating on the various scientific issues of the ATGIA experiment, and ensuring the necessary coordination with the IUGG organization, the SCAR authorities and eventually the national agencies administrating the antarctic stations.

Three general issues would be under the scope of the ATGIA Scientific Committee [to be detailed and completed]:

A. Scientific Issue:
the Committee would have to ask for pre-experiment scientific investigations in order to:

* promote the project;

* precisely design the ATGIA experiment;

* support on a scientific basis the results that can be expected from the ATGIA experiment;

* recommend standards (standard models to be used for the data analysis and/or corrections -cf the conclusions of the dedicated Working Groups);

* prepare the analysis schemes that will be used at the time the data will be released.

B. Technical Issue:
the Committee should give directives for the technical implementation of the ATGIA experiment regarding the following points:

* instrumentation (how many ET gravimeters could be dedicated to the complete ATGIA experiment ?; further instruments acquisitions ?; eventual transformation of the proposed gravimeters ?, etc);

* choice of the calibration protocol (design of a calibration campaign of all the ET gravimeters involved in the ATGIA experiment? where and how to calibrate? Is an in-situ calibration necessary? etc);

* measurements of environmental parameters (what are the environmental parameters to be measured during the experiment? are some of them to be modelized? etc);

* data validation, pre-processing and release (by ICET);

C. International Cooperation and Logistic Implementation:
regarding the relations between the ATGIA Programme and the involved Institutions, the Committee should:

* (if the sciencitic problems raised by an ATGIA experiment justifies it) eventually widen the circle of the scientists interested in the ATGIA programme to nearby disciplines through more or less punctual cooperations (seismology? glaciology? oceanography? meteorology?).

* act as the ATGIA interlocutor with regard to IUGG, SCAR and the involved national agencies;

* make a dedicated effort to organize effective cooperations and exchanges with "Third World" Nations, based on the opportunity of an international scientific experiment;

Conclusion:

A Programme of Accurate Tidal Gravimetry In Antarctica, coordinated at the international level, would lead to a real breakthrough in tidal and geodynamical studies. The feasability of such an ambitious programme has clearly to be more documented and then organized on a very solid basis, but the possibility of realizing it surely exists. The first step is to get the general agreement of all the Scientific Community involved or that could be interested in its success.

The ATGIA Pre-Project will be discussed during a special session of the **12th International Symposium on Earth Tides** (Beijing, Peolple's Republic of China, August 1993), organized by **Prof. Hsu** from the Institute of Geodesy and Geophysics (Wuhan Hubei). This general forum certainly constitutes the best opportunity to turn the pre-project into an International Coordinated Programme of ATGIA.

Acknowledgments: C. Brossier from UMR39/Toulouse has kindly drawn several polar projections of Antarctica with the Geosat data coverage. I also whish to thank A. Souriau (UPR234, Toulouse), G. Balmino (Intern. Gravimetric Bureau, Toulouse), J.L. Hyacinthe (Univ. St Denis, La Réunion) , J.F. Minster (UMR39, Toulouse) and P. Pâquet (Royal Observatory of Belgium, Brussels) for their encouragements in elaborating this preliminary project. This manuscript has benefited from their useful comments. I am grateful to Prof. H.T. Hsu for accepting to dedicate a session of the Beijing Symposium to the **ATGIA** Pre-Project. I am particularly indebted to Prof. P. Melchior for the many ways he helped in the conception of this project and for its unfailing enthusiasm.

References:

* Baker, T.F., Edge, R.J. and G. Jeffries, 1989, "European tidal gravity: an improved agreement between observations and models", Geophys. Res. Lett., 16(10), 1109-1112.
* Baker, T.F., Edge, R.J.and G. Jeffries, 1991, "Tidal gravimetry and ocean tide loading in Europe", Geophys. J. Int., 107, 1-11.
* Bennett, A.F. and P.C. McIntosh, 1982, "Open ocean modeling as an inverse problem: tidal theory", J. Phys. Oceanogr., 12, 1004 -1018.
* Cartwright, D.E., 1979, "Analyses of British Antarctic Survey tidal records", Br. Antarct. Surv. Bull., 49, 167-179.
* Cartwright, D.E., 1991, "Detection of tides from artificial satellites", in **Tidal Hydrodynamics**, B.B. Parker editor, J. Wiley & Sons, New York, 547-567.
* Cartwright, D.E., Zetler, B.D. and B.V. Hamon, 1979, **Pelagic Tidal Constants**, IAPSO Public. Sci. n°30, 65pp.
* Cartwright, D.E. and B.D. Zetler, 1985, **Pelagic Tidal Constants** (2), IAPSO Public. Sci. n°33., 59pp.
* Cartwright, D.E. and R.D. Ray, 1990, "Ocean tides from Geosat altimetry", J. Geophys. Res., 95(C3), 3069-3090.
* Dehant, V., 1987a, "Tidal parameters for an inelastic Earth", Phys. Earth Planet. Inter., 49, 97-116.
* Dehant, V., 1987b, "Integration of the gravitational motion equations for an elliptical uniformly rotating Earth with an inelastic mantle", Phys. Earth Planet. Inter., 49, 242-258.
* Dehant, V., 1991, "Review of the Earth tidal models and contribution of Earth Tides in Geodynamics", J. Geophys. Res., 96 (B12), 20235-20240.
* De Meyer, F. and B. Ducarme, 1991, "Nontidal gravity changes observed with a superconducting gravimeter", in **Proc. 11th Intern. Symp. on Earth Tides**, Helsinki (Finland), E. Sweizerbart'sche Verlag., Stuttgart, 167-184.

* Doake, C.S.M., 1978, "Dissipation of tidal energy by Antarctic ice shelves", Nature, 275, 304-305.
* Drewry, D.J., 1988, "The challenge of Antarctic science", Oceanus (special issue The Antarctic), summer 88, 31(2), 5-10.
* Farrell, W.E., 1972, "Deformation of the Earth by surface loads", Rev. Geophys., 10, 761-797.
* Françis, O. and P. Mazzega, 1991, "What we can learn about ocean tides from tide gauges and gravity loading measurements", in Proc. 11th Intern. Symp. on Earth Tides, Helsinki (Finland), E. Sweizerbart'sche Verlag., Stuttgart, 287-298.
* Goodkind, J.M., 1986, "Continuous measurements of nontidal variations of gravity", J. Geophys. Res., 91(B9), 9125-9134.
* Groten, E., 1991, "Geophysical interpretation of tidal data", in Proc. 11th Intern. Symp. on Earth Tides, Helsinki (Finland), E. Sweizerbart'sche Verlag., Stuttgart, 23-38.
* Hinderer, J., Legros H. and D.J. Crossley, 1991a, "Global Earth dynamics and induced gravity changes", J. Geophys. Res., 96(B12),20257-20265.
* Hinderer, J., Florsh, N., Mäkinen, J., Legros, H. and J.E. Faller, 1991b, "On the calibration of a superconducting gravimeter using absolute gravity measurements", Geophys. J. Int., 106, 491-497.
* Holdsworth, G., 1977, "Tidal interactions with ice shelves", Ann. Geophys., 33(1/2), 133-146.
* Hori, S. and E. Inbe, 1968, "Tides at Syowa station", Antarctic Record, 32, 48-54.
* Hsu, H.T., Tao, G.Q., Song, X.L., Baker, T.F., Edge, R.J. and G. Jeffries, 1991, "Gravity tidal datum at Wuchang of China", in Proc. 11th Intern. Symp. on Earth Tides, Helsinki (Finland), E. Sweizerbart'sche Verlag., Stuttgart, 187-195.
* Intergovernmental Oceanographic Commission, 1988, "Workshop on Sea Level Measurements in Hostile Conditions", Bidston (UK), 28-31 March, Workshop Report n°54, UNESCO, 80pp.
* International Hydrographic Organization, 1979, Tidal Constituent Bank - Station Catalog, Ocean & Aquat. Sci., Dept of Fish. and Oceans, Ottawa (Canada).
* Jackson, B.V. and L.B. Slichter, 1974, "The residual daily Earth tides at the South Pole", J. Geophys. Res., 79(11), 1711-1715.
* Jourdin, F., Francis, O., Vincent, P. and P. Mazzega, 1991, "Some results of heterogeneous data inversions for oceanic tides", J. Geophys. Res., 96(B12), 20267-20288.
* Knopoff, L., Rydelek, P.A., Zürn, W. and D.C. Agnew, 1989, "Observations of load tides at the South Pole", Phys. Earth Planet. Inter., 54, 33-37.
* Lambeck, K., 1988, Geophysical Geodesy, the Slow Deformations of the Earth, Clarendon Press, Oxford, 718pp.
* Lorius, C., Merlivat, L., Jouzel, J. and M. Pourchet, 1979, "A 30000yr isotope climatic record from Antarctic ice", Nature, 280, 644-648.
* Lutjeharms, J.R.E., Stavropoulos, C.C. and K.P. Koltermann, 1985, "Tidal measurements along the Antarctic coastline", Oceanology of the Antarctic Continental Shelf, Antarctic Res. Series 43, 273-289.
* Marsh, J.G., Brenner, A.C., Beckley, B.D. and T.V. Martin, 1986, "Global mean sea surface based upon the Seasat altimeter data", J. Geophys. Res., 91(B3), 3501-3506.

* May, J., 1989, **The Greenpeace book of Antarctica**, Dorling Kindersley Ltd, London (trad. française Souffles SA, 2d ed. 1990), 192pp.
* Mazzega, P. and F. Jourdin, 1991, "Inverting Seasat altimetry for tides in the NE Atlantic: Preliminary results", in **Tidal Hydrodynamics**, B.B. Parker editor, J. Wiley & Sons, New York, 569-592.
* McAdoo, D.C. and K.M. Marks, 1992, "Gravity fields of the Southern Ocean from Geosat data", J. Geophys. Res., 97(B3), 3247-3260.
* McAyeal, D.R., 1984, "Numerical simulations of the Ross Sea tides", J. Geophys. Res., 89(C1), 607-615.
* Melchior, P., 1982, **The tides of the Planet Earth**, 2d edition, Pergamon Press, 641pp.
* Melchior, P., 1991, "Tidal interactions in the Earth Moon system", Union Lecture, IUGG General Assembly, Aug. 19, Vienna (Austria), to appear.
* Melchior, P., Van Ruymbeke, M., Poitevin, C., Rasson, J. and B. Ducarme, 1992, "Tidal gravity measurements in Latin America", submitted.
* Melchior, P. and B. Ducarme, 1987, "Detection of inertial oscillations in the Earth's core with a superconducting gravimeter at Brussels", Phys. Earth Planet. Inter., 42, 129-134.
* Merriam, J.B., 1992a, "An ephemeris for gravity tide predictions at the nanogal level", Geophys. J. Int., 108, 415-522.
* Merriam, J.B., 1992b, "Atmospheric pressure and gravity", Geophys. J. Int., 109, 488-500.
* Nagakawa, I., Kakinuma, S., Yanai, K. and Y. Endo, 1970, "Observation of tidal variation of gravity made in Syowa station, Antarctica", Comm. Obs. roy. Belg., A(9), 16-19.
* Neuberg, J., Hinderer, J. and W. Zürn, 1987, "Stacking gravity tide observations in Central Europe for the retrieval of the complex eigenfrequency of the NDFW", Geophys. J. R. astr. Soc., 91, 853-868.
* Niebauer, T.M., 1988, "Correcting gravity measurements for the effect of local air pressure", J. Geophys. Res., 93(B7), 7989-7991.
* Ogawa, F., Fukuda, Y. Akamatsu, J. and K. Shibuya, 1991, "Analysis of tidal variation of gravity observed at Syowa and Asuka stations, Antarctica", J. Geodetic Soc. of Japan, 37(1), 13-30.
* Pedley, M., Paren, J.G. and J.R. Potter, 1986, "The tidal spectrum underneath Antarctic Ice Shelves", J. Geophys. Res., 91(C11), 13001-13009.
* Prisenberg, S.J., 1988, "Damping and phase advance of the tide in western Hudson Bay by the annual ice cover", J. Phys. Oceanogr., 18, 1744-1751.
* Robinson, E.S., 1991, "Correlation of tidal gravity and heat flow in Eastern North America", Phys. Earth Planet. Inter., 67, 231-236.
* Robinson, E.S, Williams, R.T., Neuburg, H.A.C., Rohrer, C.S. and R.L. Ayers, 1977, "Interaction of the ocean tide and the solid Earth gravity tide in the Ross Sea area of Antarctica: preliminary results", Ann. Geophys., 33(1/2), 147-150.
* Rydelek, P.A. and L. Knopoff, 1982, "Long-period lunar tides at the South Pole", J. Geophys. Res., 87(B5), 3969-3973.

* Rydelek, P.A., Zürn, W. and J. Hinderer, 1991, "On tidal gravity, heat flow and lateral heterogeneities", Phys. Earth Planet. Inter., 68, 215-229.
* Schneider, M.M., 1971, "Erste beobachtungen des schwere-gzeiten in der zentralen Antarktis", Gerlands Beitr. Geophysik, Leipzig 80(6), 491-496.
* Schwiderski, E.W., 1980a, "Ocean tides I: global ocean tidal equations", Mar. Geod., 3, 161-217.
* Schwiderski, E.W., 1980b, "Ocean tides II: a hydrodynamic interpolation model", Mar. Geod., 3, 219-255.
* Scientific Committee on Antarctic Research, 1991, "SCAR Bulletin n°103, October 1991", Polar Record 127(163), 373-376.
* Tchernia, P., 1978, "Océanographie régionale: description physique des océans et des mers", Ecole Nat. Sup. Tech. Avancées, Paris.
* Thiel, E., Crary, A.P., Haubrich, R.A. and J.C. Behrendt, 1960, "Gravimetric determination of ocean tide, Weddell and Ross Seas, Antarctica", J. Geophys. Res., 65(2), 629-636.
* Topex/Poseidon, 1991, "Science Investigation Plan", Science Working Team, Sept. 1, Jet Propulsion Laboratory, Public. 91-27, Pasadena (Calif.), 176pp.
* Van Dam, T.M. and J.M. Wahr, 1987, "Displacements of the Earth's surface due to atmospheric loading: effects on gravity and baseline measurements", J. Geophys. Res., 92(B2), 1281-1286.
* Vincent, P., Le Provost, Ch. and P. Mazzega, 1991, "Topex / Poseidon opportunity to get a new generation of ocean tide model", in Proc. 11th Intern. Symp. on Earth Tides, Helsinki (Finland), E. Sweizerbart'sche Verlag., Stuttgart, 299-307.
* Wagner, C.A., 1990, "A refined M2 tide from Geosat altimetry", NOAA Tech. Memo. NOS NGS 55, Nat. Geodetic Info. Center, Rockville, MD 20852.
* Wagner, C.A., 1991, "How well do we know the deep ocean tides? An intercomparison of altimetric, hydrodynamic and gage data", Manus. Geod., 16, 118-140.
* Wahr, J. and Z. Bergen, 1986, "The effects of mantle anelasticity on nutations, Earth tides, and tidal variations in rotation rate", Geophys. J. R. astr. Soc., 87, 633-668.
* Wenzel, H.G., Zürn, W. and T.F. Baker, 1991, "In situ calibration of LaCoste-Romberg Earth tide gravity meter", Bull. Infor. Marées Terrestres, 109, 7849-7863.
* Wilhelm, H., 1978, "Upper mantle structure and global earth tides", J. Geophys., 44, 435-439.
* Williams, R.T. and E.S. Robinson, 1980, "The ocean tide in the southern Ross Sea", J. Geophys. Res., 85(C11), 6689-6696.
* Woodworth, P.L., 1985, "Accuracy of existing ocean tide models", Proc. Conf. on the Use of Satellite Data in Climate Models, Alpbach (Austria), 10-12 June, ESA SP-244, 95-98.
* World Ocean Circulation Experiment, 1992, "Summary and Assessment of Resource Commitments", WOCE Intern. Proj. Office, Rep. n° 80/92, Wormley (UK).
* Xu, H.T., Becker, M., Groten E. and G. Tao, 1989, "Comparison of gravity tide observations by ET16 and ET21 at Wuchang station of China", Bull. Infor. Marées Terrestres, 104, 7379-7394.
* Yanshin, A.L., Melchior, P., Keilis-Borok, V.I., De Becker, M., Ducarme, B. and A.M. Sadovsky, 1986, "Global distribution of tidal anomalies and an attempt at its geotectonic interpretation",

in Proc. 10th Intern. Symp. on Earth Tides, R. Vieria ed., Consejo Sup. Investig. Cientificas, Madrid (Spain), 731-755.

* Zahel, W., 1991, "Modeling ocean tides with an without assimilating data", J. Geophys. Res., 96(B12), 20379-20391.

* Zürn, W., Richter, B., Rydelek, P.A. and J. Neuberg, 1987, "Comment: 'Detection of inertial gravity oscillations in the Earth's core...' by Melchior and Ducarme (1987)", Phys. Erath Planet. Inter., 49, 176-178.

* Zürn, W., Wenzel, H.G. and G. Laske, 1992, "High quality data from LaCoste-Romberg gravimeter with electrostatic feedback: a challenge for superconducting gravimeters", Bull. Infor. Marées Terrestres, in press.

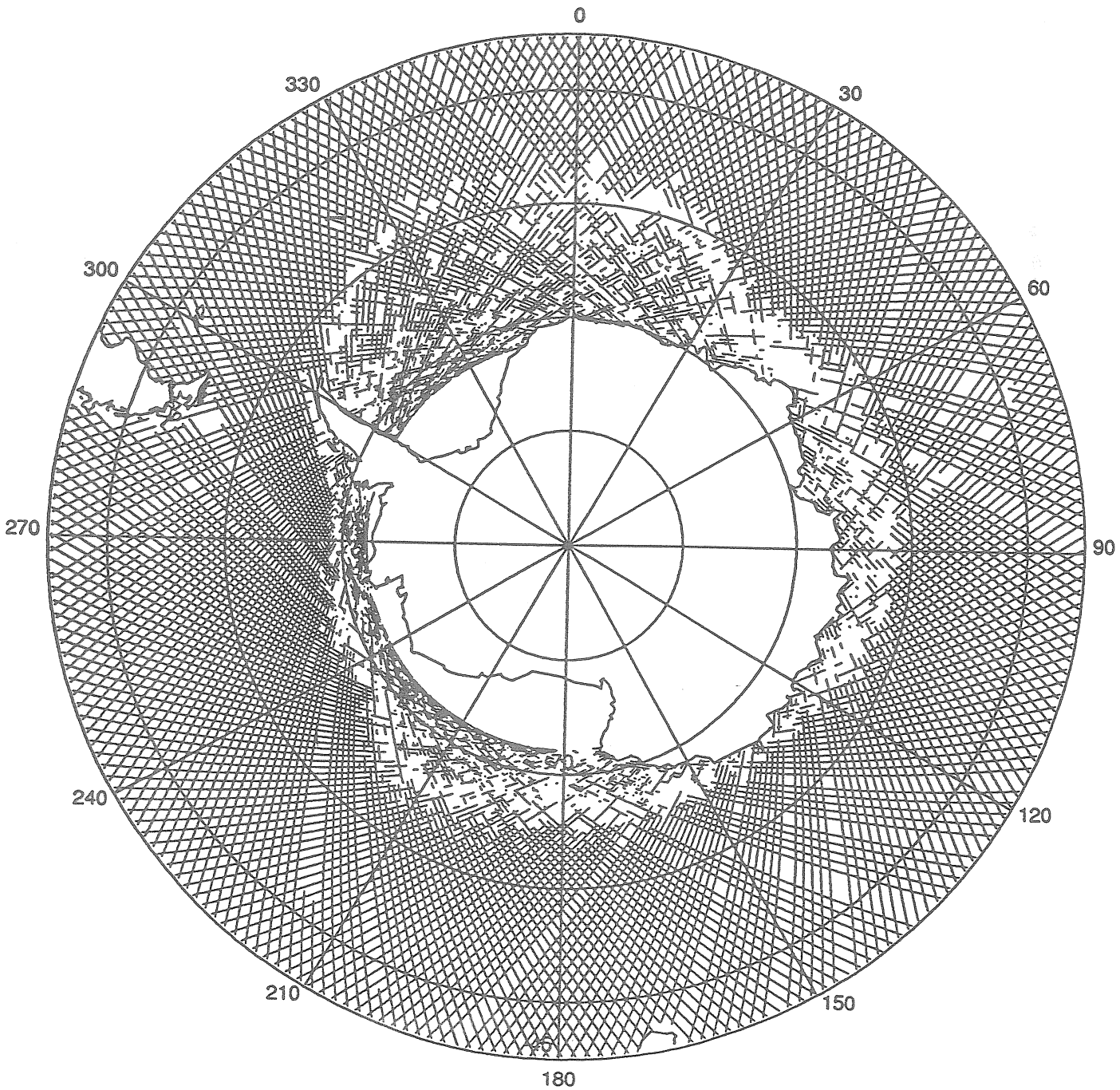

Figure 1: Coverage of the raw Geosat data south of 45°S from 01/11/87 to 18/11/87 (cycle n°22). 43 such cycles of 17 days have been overflown during the released Geosat mission. At these latitudes, the degraded accuracy of the Earth gravity field models induces larger satellite radial orbit errors. Moreover a-the strong sea surface roughness resulting from the heavy sea states, perturbs in a non-linear way the sea height as estimated from the altimeter; b-over the sea ice (with a seasonally moving front), the radar wave back scattering is not yet well understood; c-the mean sea surface models used for routine validations of the raw altimeter data are lacking south oh 60°S. For all these reasons, new statistical criteria of data validation should be defined for these latitudes before any further processing. This coverage of the raw data should be compared with the coverage obtained from the routinely validated Geosat data over the same time period (see Fig.2).

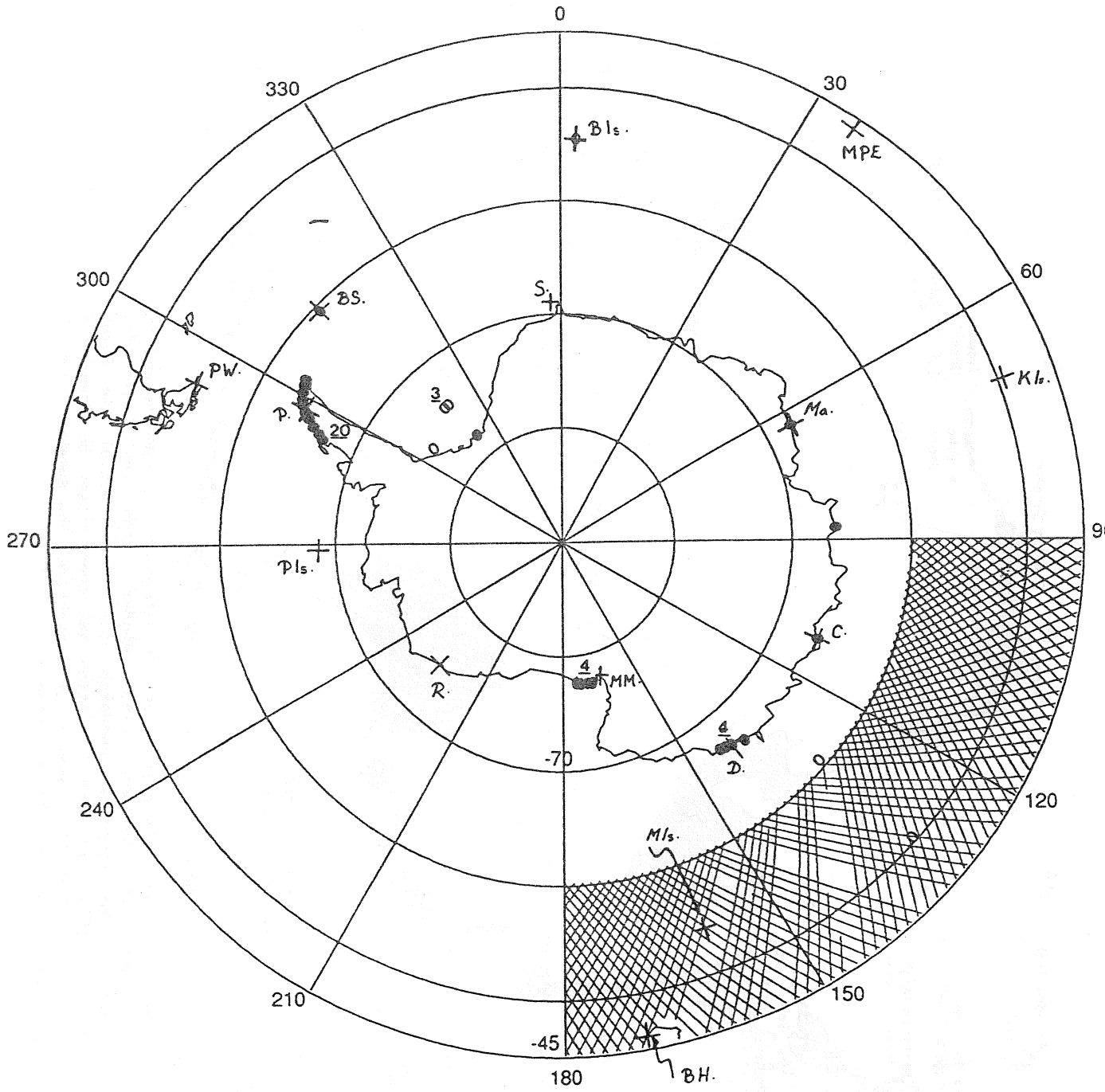

Figure 2: Approximate locations of the land based tide gauge stations (IHO 1979) south of 60°S (●), and of the pelagic stations (Cartwright et al. 1979; Cartwright and Zetler 1985) south of 45°S (O). When stations are grouped, their number is given.

The supplementary stations planned for the GLOSS and WOCE programmes are also plotted (+). Some of them consist in the upgrading, re-equipment with modern instruments and eventually telemetry, of previously existing stations. (BS: Bahia Scotia, C: Casey, MIs: Macquarie Island, Ma: Mawson, PW: Puerto Williams, D: Dumont d'Urville, KIs: Kerguelen Is., BH: Bluff Harbour, BIs: Bouveteya Is., PIs: Peter Is., MPE: Marion Prince Edward Is., S: Sanae, P: Palmer, R: Russkaya, MM: McMurdo).

The coverage of the validated GEOSAT data in a 90° sector is drawn for memory.

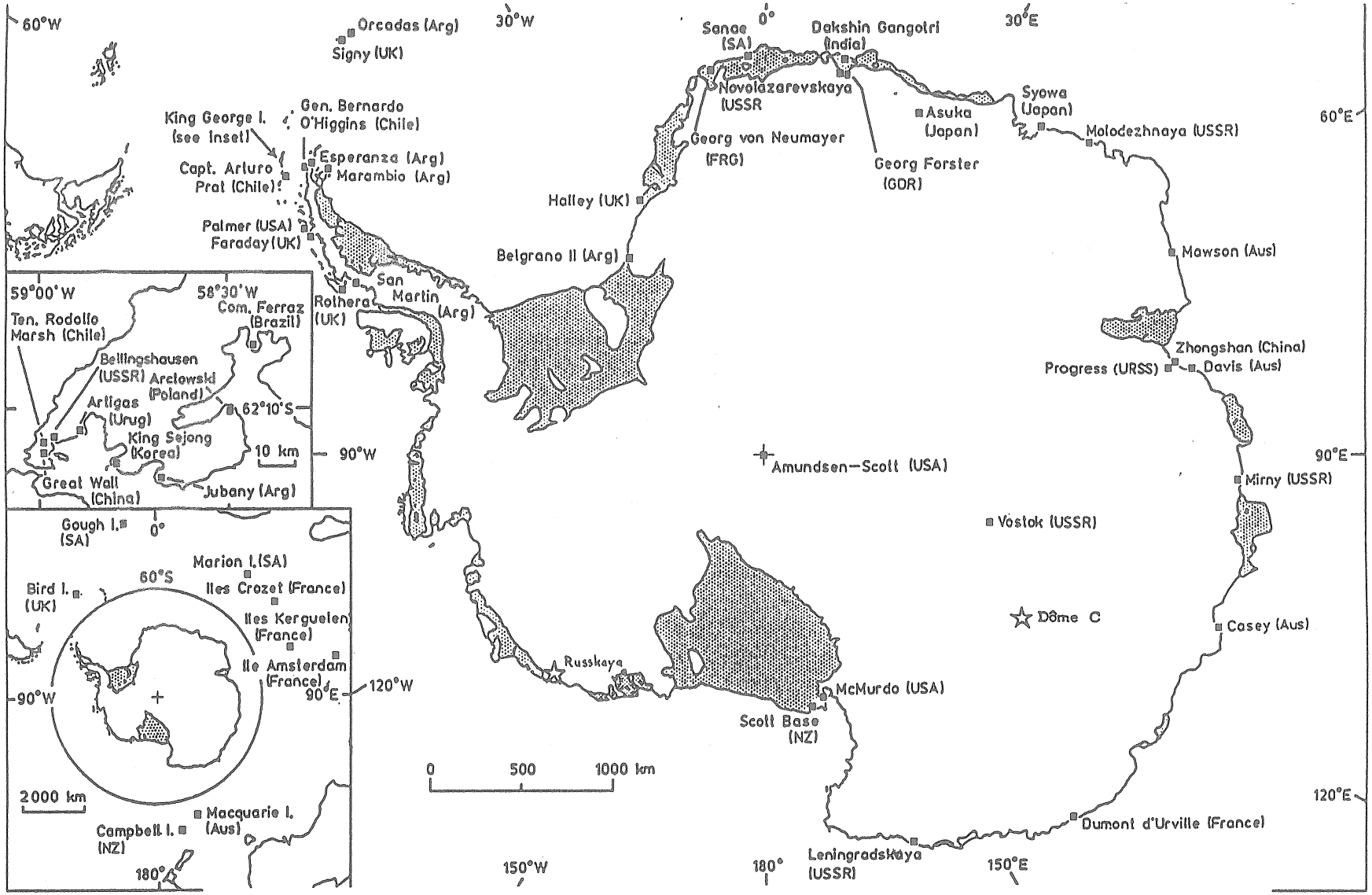

Figure 3 : Stations wintering in the sub-antarctic regions and on the antarctic continent (1991 Winter; from the Scientific Commettee for Antarctic Research Bull. n°103 Oct.91, in *Polar Record* n°163). The Dôme C station has been chosen by France to extend its scientific research in Antarctica. The Russkaya station has been planned by USSR to reoperate in 1992.

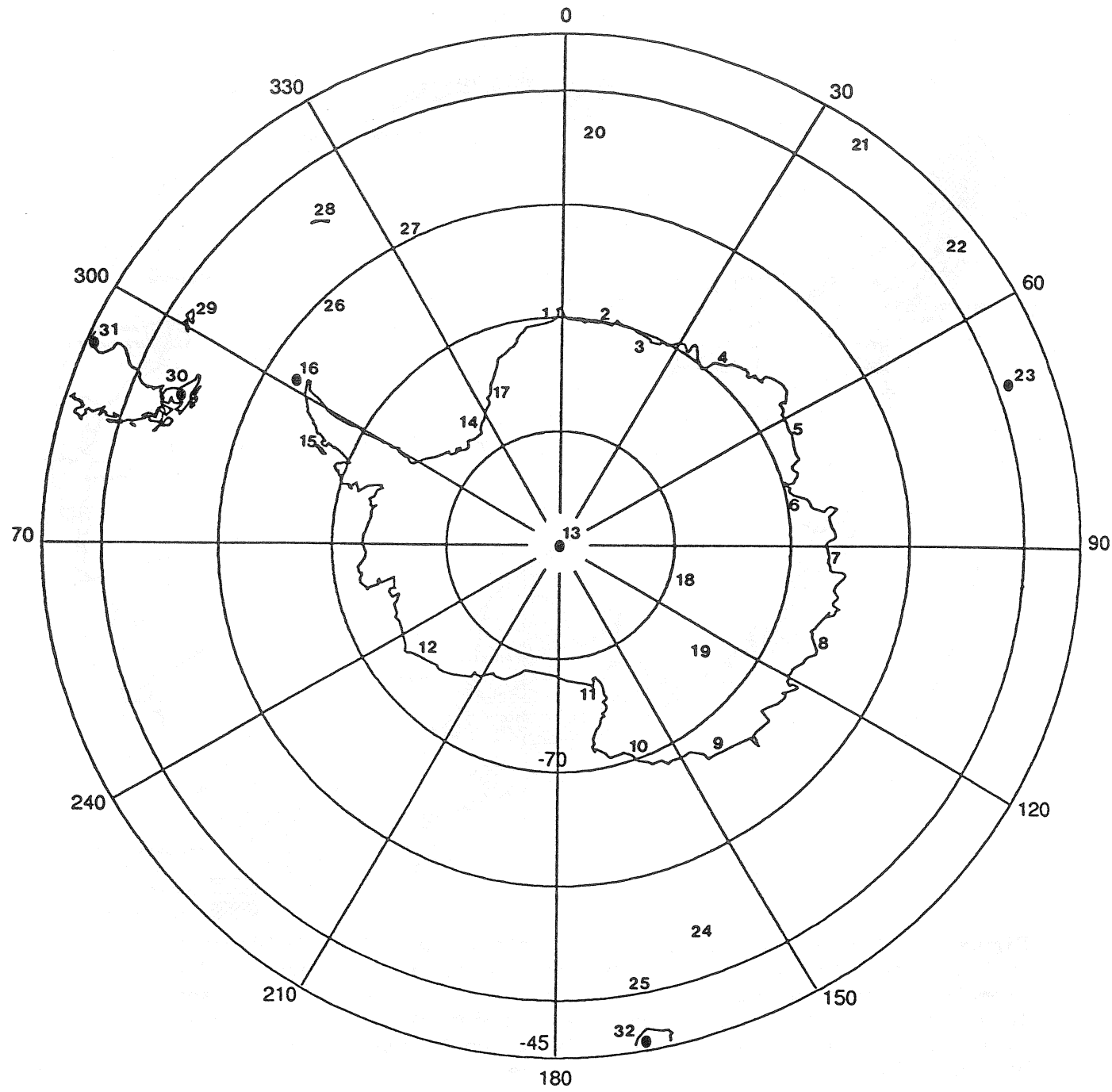

Figure 4: A tentative map of the 34 proposed sites of the ATGIA International Coordinated Programme (2 sites are slightly north of 45°S). The station names and exact locations corresponding to the sites numbers are listed in Appendix A. To a given ATGIA site number may correspond several independent scientific stations (eg. n=16 groups in fact 12 stations from 10 different nations). The operating of 2 ET gravimeters in 2 nearby stations (same site number) may be highly usefull for cross-checks and accuracy assessments.

To each ATGIA site corresponds at least one wintering station (except for n=20, 27 and 29 for which we presently lack information). About 25 more stations are opened for 3 to 4 months during the summer time.

Two supplementary sites are proposed north of 45°S: in South Atlantic, the Tristan da Cunha (UK) / Gough Islands (SA, with n=33) and in the Indian Ocean the Amsterdam Island (France, with n=34). The 6 stations temporary occupied during an ICET campaign (0) are planned to reoperate during the "ATGIA Synchronic Year".

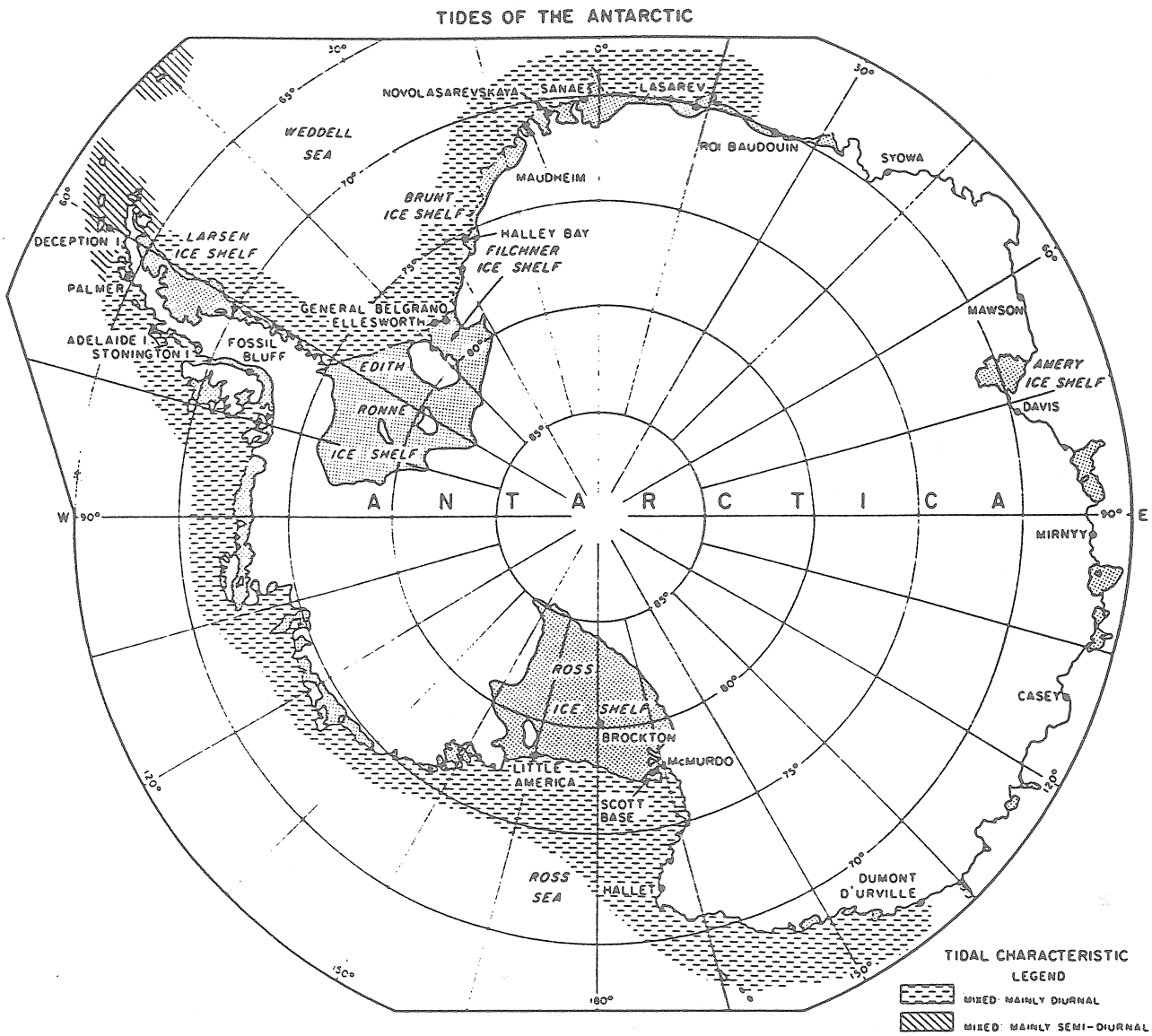

Figure 5: General tidal regime in Antarctica (from Holdsworth 1977). Note this map should be considered with caution: for exemple, Lutjeharms et al. (1985) have published ~1 month sea level records exhibiting mixed but predominantly semi-diurnal tidal characteristics at Sanae and Georg von Neumayer stations, in obvious contradiction with the present map.

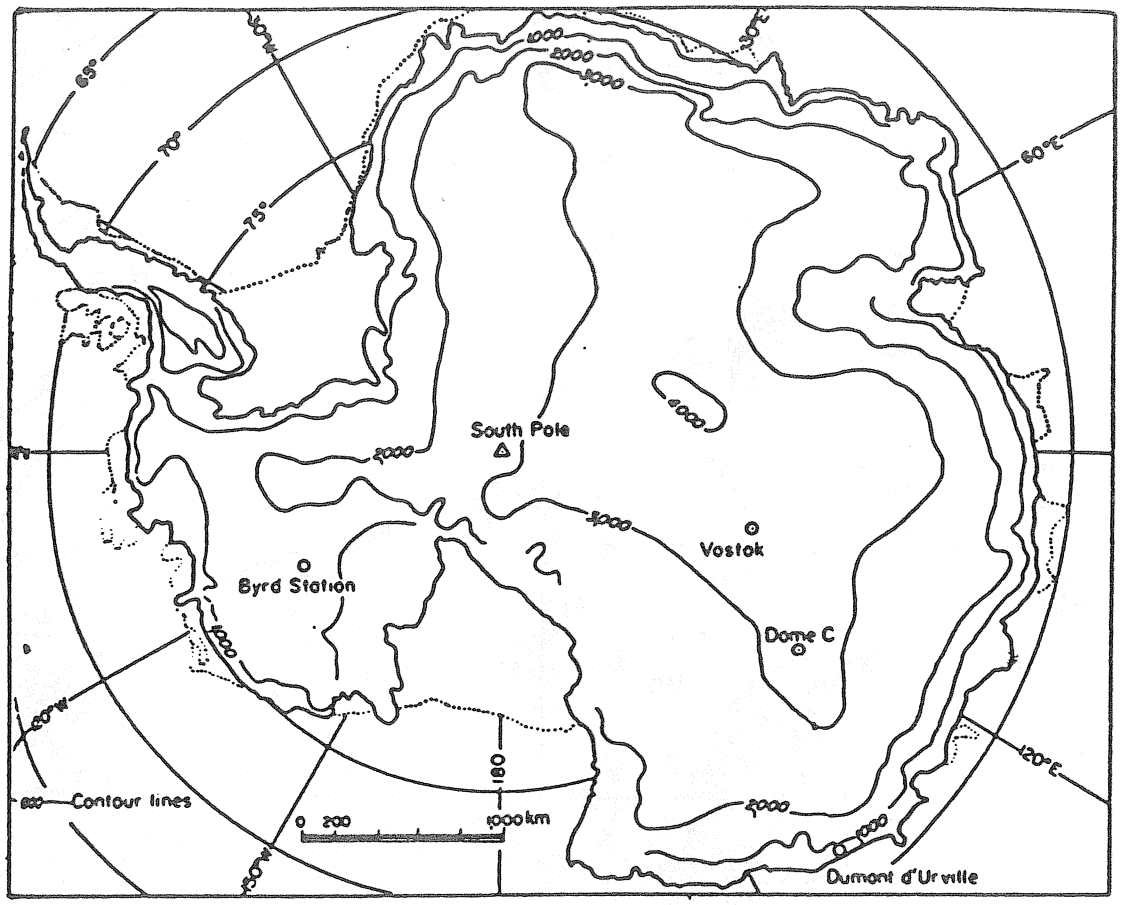

Figure 6 : Heights above sea level in Antarctica (from Lorius et al. 1979). This topography more or less represents the continental ice thickness (the underlying bedrock is often loaded below the sea level).

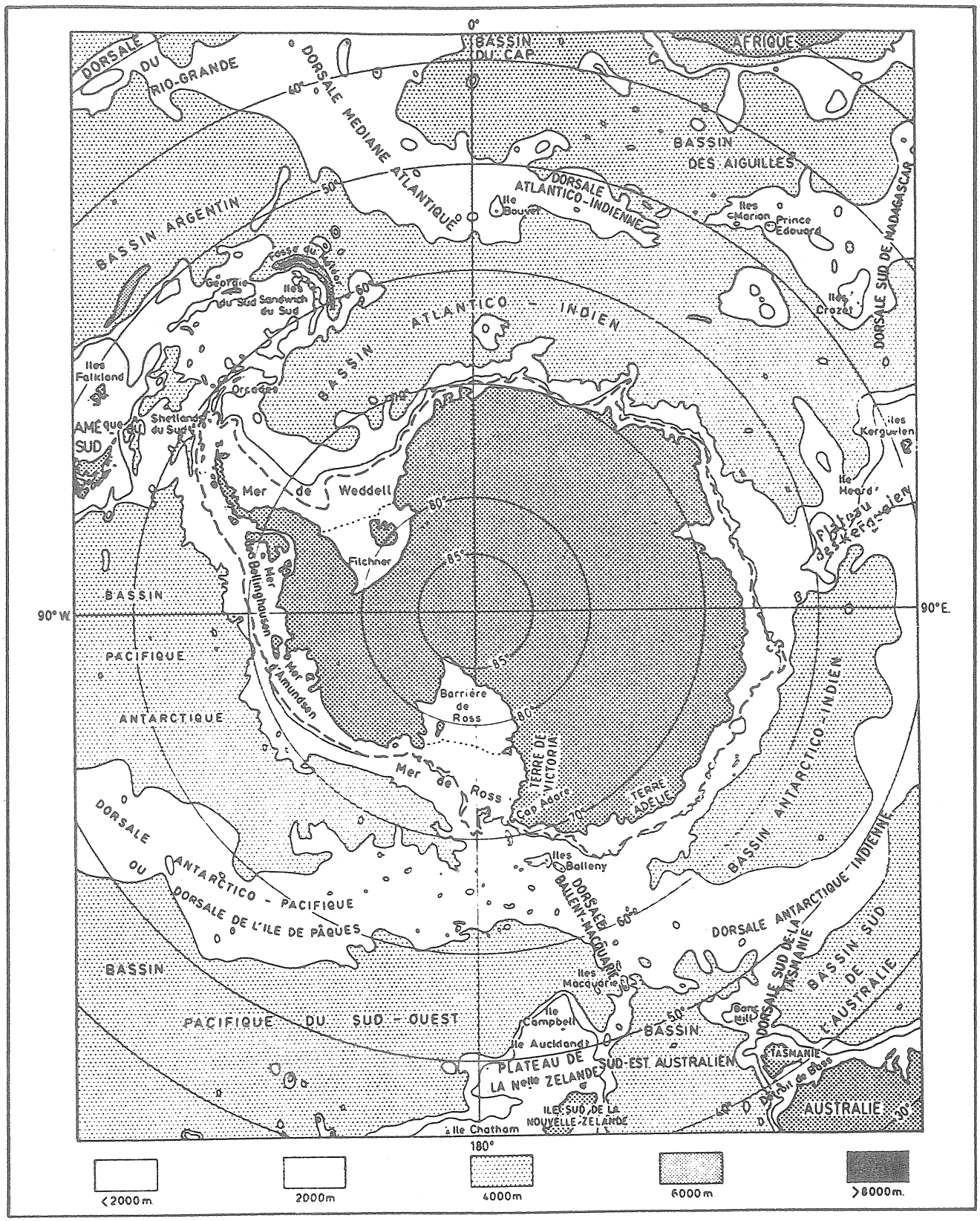

Figure 7: Bathymetric map of the Southern ocean (from Tchernia 1978).

Appendix A: List of the 1991 Wintering SCAR Stations (see Fig.3) and supplementary ATGIA sites.

d : date of installation;
awp : approximative wintering population (in the 90');
n : ATGIA site number (see Fig.4);
*name: site not drawn on Fig.4.

Argentina:

Belgrano II	77°52'S,	34°37'W	d:02.79	awp:18 n14
Orcadas	60°44'S,	44°44'W	d:02.04	awp:14 n26
Esperanza	63°24'S,	57°00'W	d:03.52	awp:29 n16
Marambio	64°14'S,	56°37'W	d:10.69	awp:42 n16
San Martin	68°08'S,	67°06'W	d:03.51	awp:15 n15
Jubany	62°14'S	58°40'W	d:11.53	awp:11 n16

Australia:

Macquarie Is.	54°30'S,	158°57'E	d:?	awp:20 n24
Mawson	67°36'S,	62°52'E	d:02.54	awp:28 n05
Davis	68°36'S,	77°58'E	d:01.57	awp:24 n06
Casey	66°18'S,	110°32'E	d:02.69	awp:32 n08

Brazil:

Com. Ferraz	62°05'S,	58°24'W	d:02.84	awp:12 n16

Chile:

Capt. A.Prat	62°30'S,	59°41'W	d:02.47	awp:08 n16
Gen. O'Higgins	63°19'S,	57°54'W	d:02.48	awp:29 n16
Ten. R.Marsh	62°12'S,	58°55'W	d:03.80	awp:57 n16

France:

Dumont d'Urv.	66°40'S,	140°01'E	d:04.56	awp:28 n09
Crozet Is.	46°26'S,	51°52'E	d: .61	awp:20 n22
*Amsterdam Is.	37°50'S,	77°34'E	d:?	awp:? *n34
Kerguelen Is.	49°21'S,	70°12'E	d:01.50	awp:50 n23
DômeC (exUSA)	74°30'S,	123°00'E	d:11.74	awp:? n19

Germany:

G.von Neumayer	70°37'S,	8°22'W	d:02.81	awp:09 n01
G. Forster	70°47'S,	11°51'E	d:?	awp:? n02

India:

D. Gangotri	70°05'S,	12°00'E	d:01.84	awp:15 n02

Japan:

Syowa	69°00'S,	39°35'E	d:01.57	awp:29 n04
Asuka	71°32'S,	24°08'E	d:01.85	awp:08 n03

New Zealand:

Scott Base	77°51'S,	166°45'E	d:01.57	awp:12 n11
Campbell Is.	52°33'S,	169°9''E	d:?	awp:? n25

People's Republic of China:

Great Wall	62°13'S,	58°58'W	d:02.85	awp:15 n16
Zhongshan	69°22'S,	76°23'E	d:?	awp:? n06

Poland:

Arctowski	62°09'S,	58°28'W	d:02.77	awp:19 n16
Republic of Korea:				
King Sejong	62°13'S,	58°47'W	d:?	awp:? n16
South Africa:				
Sanae	70°18'S,	2°25'W	d:01.60	awp:15 n01
Marion Is.	46°52'S,	37°51'E	d:12.47	awp:? n21
*Gough Is.	40°21'S,	9°52'W	d:01.48	awp:? *n33
United Kingdom:				
Faraday	65°15'S,	64°16'W	d:01.47	awp:12 n15
Halley (IV)	75°36'S,	26°46'W	d:01.56	awp:19 n17
Halley (V)	75°35'S,	26°15'W	d:?	awp:? n17
Rothera	67°34'S,	68°07'W	d:12.76	awp:12 n15
Signy	60°43'S,	45°36'W	d:03.47	awp:12 n26
United States of America:				
Amundsen-Scott	90°	S	d:01.57	awp:17 n13
McMurdo	77°51'S,	166°40'E	d:01.56	awp:132n11
Palmer	64°46'S,	64°03'W	d:01.65	awp:07 n15
Union of Soviet Socialist Republics:				
Mirny	66°33'S,	93°01'E	d:02.56	awp:67 n07
Novolazarevsk.	70°46'S,	11°50'E	d:02.61	awp:57 n02
Molodezhnaya	67°40'S,	45°51'E	d:01.63	awp:129n04
Vostok	78°28'S,	106°49'E	d:02.57	awp:29 n18
Bellingshausen	62°12'S,	58°58'W	d:02.68	awp:25 n16
Leningradskaya	69°30'S,	159°24'E	d:02.71	awp:18 n10
Progress	69°24'S,	76°24'E	d:?	awp:? n06
Russkaya	74°46'S,	136°49'W	d:03.80	awp:12 n12
Urugay:				
Artigas	62°11'S,	58°51'W	d:01.85	awp:10 n16

Supplementary sites proposed for the ATGIA Programme:

Bouvet Is.	54°21'S,	3°20'E	(Norway)	n20
S.Sandwich Is.	60°44'S,	44°39'W	(UK)	n27
Falkland	52°	S, 59°	W (UK)	n29
Lauder	45°02'S,	169°41'E	(N.Zealand)	n32
Ushuaia	54°49'S,	68°20'W	(Argentina)	n30
Com.Rivadaria	45°50'S,	67°29'W	(Argentina)	n31

COMPREHENSIVE RESEARCHES FOR THE EFFECT OF THE OCEAN LOADING ON GRAVITY OBSERVATIONS IN THE WESTERN PACIFIC AREA

He-Ping SUN*
Institute of Seismology
State Seismological Bureau
430071 Wuhan, Xiao Hongshan, P.R. of China

Abstract

The response problems of a radial inhomogeneous elastic earth on gravity measurements in the Western Pacific Area, under the action of the ocean loading, are systematically studied, with both Schwiderski global cotidal maps and chinese local ones, by use of a numerical integral method.

The results show that the discrepancy caused by different earth models can reach up to 10%-15% and difference induced by the consideration of mass conservation is about 10% for tidal loading corrections of M_2 wave. The numerical results obtained from the different regions of South China Sea and East China Sea on four main waves of M_2, S_2, O_1 and K_1 are provided in details. The results show that the tidal loading corrections are dominated by local marine tides. The comparison between calculation loading values and observed tidal gravity residues demonstrates that the loading effects obtained from modified Schwiderski global maps can give an good explanation to the residues which signifies the importance of the modification for Schwiderski global cotidal maps with the local ones. In order to check the calculated results and their related precision, the comparison between our programs and those of ICET is executed in Brussels. The corresponding results show that there exists an excellent agreement between both computations.

1 INTRODUCTION

During the last decades, worldwide studies on the relationship between the deformation of the Earth and ocean loading effects have been successfully carried out in theory and in practice by many scientists as it is believed that they are important for the retrieval of the structural parameters in crust and upper mantle beneath the observation stations where geophysics and geodetic measurements are performed. The corresponding researches in theoretical calculations and in practical observations proved that the highly accurate observations on the Earth's surface are influenced by ocean loading which can contribute to ten percent of the total signal. The continuous earth gravity tide reading is a very good example in this respect. So it is considered that the corrected earth tides data could be used as a significant method to study

* The present address: Royal Observatory of Belgium
3 Avenue Circulaire, 1180 Brussels
Belgium

the Earth's elastic behavior and characteristics of the deformation. On the other hand, many geophysical and geodetic observations for monitoring the yielding of the Earth need accurate earth tidal information for correction in order to improve the corresponding precision, such as the measurements of the distance the Earth and the Moon, the Satellite Laser Range, and the determination of terrestrial baseline lengths by Very Long Baseline Interferometry (VLBI) have now a centimetric precision at a distance of several thousand kilometers, they have to be corrected for ocean tidal loading which causes displacement of several centimeters. Another important example is to monitor the concerned precursor information of gravity changes during the pregnancy of an earthquake event, a lot of efforts have been devoted by Chinese geoscitists to investigate the response problems of an elastic Earth and to tidal loading forces which can induce an additional periodic deformation.

The improvements of geophysics, geodesy and oceanography in theory and in practical observations together with the widely - used advanced electronic computer have made the theory and loading calculations perfectly developed. Many scientists in the world - have successfully realized the research works in this respect. - Longman introduced in 1962 the use of Green's function for determining the deformation of a spherical earth under a concentrated surface mass load instead of expressing the surface mass distribution by a summation of surface zonal harmonics. After that, all the corresponding standard calculation formulas and coefficients are derived by Farrell (1972). By use of advanced electronic computer, we can then begin calculating precisely the ocean loading correction. Melchior and Ducarme (1980) carried out successfully the related calculations and demonstrated the relationship among the corresponding vectors of a tidal gravity theoretical calculation, practical observations and oceanic loading. The use of Schwiderski global cotidal maps promotes the reasonable explanations to the observed residues as it is considered that the Schwiderski global maps are presently the best ones in which the new theoretical and semi-empirical tidal models mixing tidal dynamics and observations are employed.

Nevertheless consider that these global cotidal maps are not sufficiently accurate to study the local responses of the solid Earth to oceanic forcing. It is necessary for us to modify the - global maps with local ones in order to get possibly a more precise response. From the preliminary comparison between the Schwiderski maps and the local ones in the local sea areas along the coast of China, the amplitude differences of the sea tides can - reach up to 5-10 cm, and more than 12 cm for some places in maximum. On the other hand, a lack of tidal information appears in the Bohai Sea region.

We obtained from Institute of Oceanography, State Oceanographical Bureau, the local marine tidal information along the coast of China (unpublished) in 1986 including to the M_2, S_2, O_1 and K_1 waves of Southern China Sea, East China Sea, Yellow China Sea and Bohai Sea regions. The corresponding numerical reading of these maps for the different grid system are completed by us in 1986. Then the both local maps and modified Schwiderski ones are used to

evaluate the loading effects on gravity measurements in the Western Pacific Area with a high resolution.

2 CALCULATION METHOD

The response to the ocean loads depends very much on the locally variable properties of the crust and upper mantle. A model composed of homogeneous, isotopic spherical layers is much more likely to be valid for the body tide, having significant displacements are appreciable only in the crust and upper mantle. Differences in crustal structure, as beneath ocean basins and continents, will therefore affect the load more than the body tides. For example, the surface deformation near the load is very sensitive to properties of the sediments. The calculation of load tides is therefore far more complicate than that of body tides. Celestial mechanics provide us with an extremely precise description of body force, while oceanography can only give us empirical observations or numerical integrations of the hydrodynamical equations which is still far from being perfect for the present and future needs.

Fortunately it is easy to deduce the corresponding calculation formulas for the effects of the ocean loading on tidal gravity vertical and horizontal components, the concerned expression of the convolution integral is as follows

$$\begin{bmatrix} g(\Omega,t) \\ \xi(\Omega,t) \\ \eta(\Omega,t) \end{bmatrix} = -4\pi G\rho_w \sum_{n=0}^{\infty} \frac{(1+k'(n)-h'(n))}{2n+1} \begin{Bmatrix} H_n(\Omega,t) \\ \frac{1}{gR}\frac{\partial H_n(\Omega,t)}{\partial \theta} \\ \frac{1}{gR\cos\theta}\frac{\partial H_n(\Omega,t)}{\partial \lambda} \end{Bmatrix} \quad (1)$$

where ρ_w is the density of sea water, G gravitational constant, g represents surface gravity value, R denotes the radius of earth's equvolume sphere, $\Omega=\Omega(\theta,\lambda)$ are the spherical coordinates of the observation position, t is time, and k'n an h'n surface loading Love numbers, also called loading deformation coefficients, g, ξ and η corresponding loading corrections of the ground gravity, - South-North (NS) and East-West (EW) tilt components respectively, $H_n(\Omega,t)$ represents the nth Laplace series term of the tidal amplitude $H(\Omega',t)$ relative to observation station

$$H_n(\Omega,t) = \frac{2n+1}{4\pi} \iint_{\Omega'} H_n(\Omega',t) P_n(\cos\psi)\, d\Omega' \quad (2)$$

where $\Omega'=\Omega'(\theta',\lambda')$ are spherical coordinates of the load point, $d\Omega'$ denotes the grid element of the loads, $P_n(\cos\psi)$ is nth order Legendre polynomial. Inserting equation (2) into (1), the series of the loading corrections formula can be easily transformed into a integration one

$$L(\Omega,t) = \rho_w \iint_{\Omega'} H(\Omega',t) G(\psi,\beta)\, d\Omega' \quad (3)$$

with

$$L(\Omega,t)=\begin{bmatrix} g(\Omega,t) \\ \xi(\Omega,t) \\ \eta(\Omega,t) \end{bmatrix} \qquad G(\psi,\beta)=\begin{bmatrix} G(\psi) \\ T(\psi)\cos\beta \\ T(\psi)\sin\beta \end{bmatrix}$$

where ψ and β are the corresponding polar distance and azimuth between the observation point and the loading element. $G(\psi)$ and $T(\psi)$ are the corresponding gravity and tilt Green functions as follows

$$\left.\begin{aligned} G(\psi)&=\frac{-G}{R^2}\sum_{n=0}^{\infty}[n+2h'(n)-(n+1)k'(n)]\,P_n(\cos\psi) \\ T(\psi)&=-\frac{1}{M}\sum_{n=0}^{\infty}[1+k'(n)-h'(n)]\,\frac{\partial P_n(\cos\psi)}{\partial\psi} \end{aligned}\right\} \tag{4}$$

where M is the total mass of the Earth. From the spherical triangular relation, we can easily have

$$\left.\begin{aligned} &d\Omega'=R^2\sin\theta'\,d\theta'\,d\lambda' \\ &\cos\psi=\cos\theta\cos\theta'+\sin\theta\sin\theta'\cos(\lambda-\lambda') \\ &\sin\psi\cos\beta=\cos\theta\sin\theta'-\sin\theta\sin\theta'\cos(\lambda-\lambda') \\ &\sin\psi\sin\beta=\cos\theta'\sin(\lambda-\lambda') \end{aligned}\right\} \tag{5}$$

From the equation (3), the ocean loading correction can be obtained by a convolution integral between the corresponding Green functions and tidal amplitudes. The name of Green is given to such function which enable linear differential equations with boundary conditions at the external spherical surface to be solved. Green functions are here the point-load response functions, i.e., caused by the point surface mass load as a function of angular distance from load. The proper weighted sums of the load Love numbers (for each n) must be added up to form these Green functions.

It is obvious that from the properties of the loading Love numbers, the term for n=0 will be omitted naturally in equation (4).The influence takes three forms, (1) the mass attraction of the ocean tides causing the vertical to deviate and g intensity to vary which is called direct effect; (2) a variable flexure of the Earth's crust under the loading effect which is the most important part of indirect effect; (3) a variation of potential of the earth due to this deformation of the crust and upper mantle, an effect which is in the opposite sense to (1) and (2).

Notice that the first term of the summation to Legendre Polynomial is

$$\sum_{n=0}^{\infty} nP_n(\cos\psi)=\frac{-1}{4\sin(\psi/2)}$$

and the first term of the differential to Legendre polynomial is

$$\sum_{n=0}^{\infty}\frac{\partial P_n(\cos\psi)}{\partial\psi}=-\frac{\cos(\psi/2)}{4\sin^2(\psi/2)}$$

The equation (4) can be expressed as follows

$$\left.\begin{aligned} G(\psi) &= G^N(\psi)+G^E(\psi) \\ &= \frac{g}{4M\sin(\psi/2)} - \frac{g}{M}\sum_{n=0}^{N}[2h'(n)-(n-1)k'(n)]P_n(\cos\psi) \\ T(\psi) &= T^N(\psi)+T^E(\psi) \\ &= \frac{\cos(\psi/2)}{4M\sin^2(\psi/2)} - \frac{1}{M}\sum_{n=0}^{N}[k'(n)-h'(n)]\ \frac{\partial P_n(\cos\psi)}{\partial\psi} - \end{aligned}\right\} \quad (6)$$

where $G^N(\psi)$ and $T^N(\psi)$ are the Newton's term and $G^E(\psi)$ and $T^E(\psi)$ are called elastic terms (second terms). In our approach, the Newton's term of the direct attraction of the ocean mass for tidal gravity calculation is expressed as

$$G^N(\psi) = \frac{-1}{M}\left[\frac{h^2+2\sin(\psi/2)}{[4(1+h)\sin^2(\psi/2)+h]^{3/2}}\right] \quad (7)$$

where h is the height of the observation station above the Earth's surface. Comparing with the Earth's average radius, when $h<<R$, then $|h|$ is very small and $G^N(\psi)$ tends to the function

$$\frac{-1}{4M\sin(\psi/2)}$$

which has the same form as the one provided by Farrell (1972b, equation 48).

In general, the instantaneous tidal height can be expressed as a summation of harmonic constituents provided by the cotidal maps

$$\left.\begin{aligned} H(\Omega',t) &= \sum_{p=1}^{N} h_p(\Omega')\cos(\omega_p t+\chi_p+\alpha_p) \\ &= \sum_{p=1}^{N}[H_{cp}(\Omega')\cos(\omega_p t+\chi_p)+H_{sp}(\Omega')\sin(\omega_p t+\chi_p)] \end{aligned}\right\} \quad (8)$$

where h_p α_p, χ_p and ω_p represent the corresponding amplitude, initial phase, argument and angular frequency of pth constituent at loading position respectively, t is universal time, N is constituent sum. When the numerical amplitudes and phases from cotidal maps are obtained, the convolution integral can be directly carried out by use of formulas (3). It is noticed that when the local cotidal maps along the coast of China are employed, the local phase of the cotidal charts have to be taken into consideration in order to match the global ones. The relationship relative to the local phase α_L and the Greenwith phase α_G is

$$\alpha_L = \Phi\lambda^T+\alpha_G$$

where λ^T is the longitude of a field point (usually positive east) and Φ is the order of tides (take 0,1 and 2 for long period, diurnal and semi-diurnal components respectively). Therefore the corrections of the loading tides can be divided into the real and imaginary parts as follows

$$\left.\begin{aligned} A_c &= \rho_w \iint_{\Omega'} H_{cp}(\Omega')\ G(\psi,\beta)\,d\Omega' \\ A_s &= \rho_w \iint_{\Omega'} H_{sp}(\Omega')\ G(\psi,\beta)\,d\Omega' \end{aligned}\right\} \qquad (9)$$

Then the amplitude and phase of the loading corrections are

$$\left.\begin{aligned} L &= (A_C^2 + A_C^2)^{1/2} \\ \lambda &= \tan^{-1}(A_s/A_c) \end{aligned}\right\} \qquad (10)$$

3 DETAILS OF THE PROCEDURE

(1) The choice of Earth's model

In order to calculate precisely the values of loading corrections which dependent very much on the elastic properties of the different Earth's responses to a point mass load, two different Earth models, the Gutenberg-Bullen A and the Preliminary Reference Earth Model (PREM) (Dziewonski and Anderson, 1981) are comparatively used in the present computations. The corresponding load Love numbers and associated Green's function for Gutenberg-Bullen A - Earth Model are adopted according to the determinations published by Farrell in 1972 in which the assumption of the Earth's response is elastic at tidal frequencies. The Green's function for the Preliminary Reference Earth Model (PREM) are calculated in advance depending on the corresponding load Love numbers. These numbers are evaluated by integration of the equations of the tidal motion, the stress-strain relation and Poisson's equation inside the Earth from the center point to Earth's surface.

The comparison of Green's function between G-B and G-D1066A Earth models is given in figure 2. The results show that the difference between different Green's functions is obvious when angular distance $\psi < 0.1^\circ$, it proves that the shallow structure of the Earth can affect the corresponding tidal loading corrections.

The convoluting integral between Schwiderski global cotidal maps and two sets of Green functions are carried out respectively. The corresponding loading corrections are comparatively provided in table 1 and one can see clearly that the discrepancy caused by the use of different Earth's models reaches up to 10 % which in highly precision corrections of the geophysical and geodetical observations has to be taken into consideration, particularly for the stations situated in the coastal lines where the discrepancy between two different Earth models reaches up to 15% and which exactly reflect the sensitivity of the ocean loading in near regions. An easy way to verify the suitability of these Earth models is to fit the observed residues with the values of theoretical - calculations.

(2) Mass Conservation

As of the limits of nonlinear effects, numerical methods, permeability of the coastal lines and global cotidal maps discretization, most of the global cotidal maps based on the ocean tidal model do not conserve mass at all , even in the case of Schwiderski's models in which the new theoretical and semi-empirical tidal models mixing tidal dynamics and observations are employed. In those maps, an $1^\circ * 1^\circ$ grid system in an atlas $41^\circ * 71^\circ$ overlapping charts covering the whole oceanic global are used. This representation is assumed to have a accuracy of better than 5 cm in open sea area for M_2, S_2, O_1 and K_1 constituents.

In order to take into consideration of the mass conservation, in the present paper a uniform correction, which consists in the use of a sheet of water with a constant thickness and phase, is introduced in loading calculation. The corresponding numerical results obtained with original Schwiderski maps are shown in table 2. These results prove that there exists a significant improvement between the model calculations and observations when mass is conserved. Before and after correcting for the deficiency of the tidal mass, the tidal gravity correction values vary of about 10% which can reaches up to the same magnitude with the discrepancy caused by different Earth models, so it is obvious that this is a non-negligible quantity in the correction of high precision tidal gravity measurements.

(3) Use of local maps

For coastal and island stations, the discretization of the Schwiderski models is not sufficient.In the regions along the coast of China there exist some specific tidal phenomena. So it is important to incorporate refined local models into global ones. We obtained, from the Institute of Oceanography, State Oceanographical Bureau, Tianjin, P.R.of China, the local marine tidal information (unpublished) along the coast of China in 1986 including to the M_2, S_2, O_1 and K_1 waves of Southern China Sea, East China Sea, Yellow China Sea and Bohai Sea regions. The corresponding numerical readings of local charts are completed by us in 1986 in which the ocean areas are partitioned into the corresponding spherical elements as $(\frac{1}{6})^\circ * (\frac{1}{6})^\circ$ grid system of about 600km to coastal line in the areas of 19.167°N to 24.0°E, and 106.0°E to 122.0°E, and 24.167°N to 41.0°N and 117.0°E to 126.0°E, and spherical elements as $(\frac{1}{3})^\circ * (\frac{1}{3})^\circ$ grid system between 600 KM to 1000 KM ocean areas to the coastal lines in the regions of 15.0°N to 19.0°N and 106.0°E to 122.0°E, and 24.333°N to 35.0°N and 126.333°E to 130.0°E (see figure 1). All the shallow sea areas along the coast of China are subdivided into 9553 cells. During the numerical works of the local charts, the average tidal amplitude in each cell is represented as tidal height in the center of this element. The corresponding results are show in table 3-6. The loading corrections obtained from the modified Schwiderski global cotidal maps are provided in table 7.

(4) Realization of numerical integral

According to equation (3), the loading corrections can be di-

rectly carried out by using of the following numerical summation form

$$\begin{bmatrix} g \\ \xi \\ \eta \end{bmatrix} = -\rho \sum_{i=1}^{N} H_i(\Omega') \begin{bmatrix} G(\psi_i) \\ T(\psi_i)\cos\beta_i \\ T(\psi_i)\sin\beta_i \end{bmatrix} \sin\theta' \Delta s_i \qquad (11)$$

where $H_i(\Omega')$ is the average tidal amplitude in the center of ith cell, ψ_i represents the corresponding angle distance from the observation point to the center of loading cell, θ_i' is the colatitude of the center at ith loading cell, Δs_i denotes ith loading differential cell. For the local marine regions, Δs_i is taken as $(\frac{1}{6})^\circ * (\frac{1}{6})^\circ$ and $(\frac{1}{3})^\circ * (\frac{1}{3})^\circ$, for the open sea area, Δs_i will be $1^\circ * 1^\circ$. The accuracy of the tidal loading computation can be evaluated as the corresponding Green's functions are obtained dependents on a certain earth model and the errors of the tidal height for a cotidal maps can be predicted in advanced, if the earth radius R (Farrell's table) is taken as the related unit, then the accuracy evaluating formulas will be as follows

$$\begin{bmatrix} \delta g \\ \delta \xi \\ \delta \eta \end{bmatrix} = \left[[\rho_w \Delta s\ h(\Omega')^2] \sum_{i=1}^{N} \begin{bmatrix} [G(\psi_i)]^2 \\ [T(\psi_i)\cos\beta_i]^2 \\ [T(\psi_i)\sin\beta_i]^2 \end{bmatrix} \sin^2\theta_i \right]^{1/2} \qquad (12)$$

4 DISCUSSION

According to the calculation models mentioned above, the tidal gravity corrections for M_2, S_2, O_1 and K_1 waves obtained from different local cotidal maps are given in details in table 3-6 respectively in the region Western Pacific Area. In those tables, L and λ represent the corresponding loading amplitude (in μgal) and phase (in degree). In the first column, the East Sea includes East China Sea, Yellow China Sea and Bohai Sea. The last column shows the total tidal gravity loading corrections of Western Pacific Area, including China, Japan, Korea and Philippine regions. From these tables, it is obvious that the corrections are less 1 μgal in inland stations, however for the stations situated on the coast line and islands, they reaches up to less or more than 3 μgals such as Hong Kong, Shanghai, Chuanzhou and Taibei where the distances of the stations to the sea are about tens of kilometers.

Having some meaningful comparisons with the results in table 7, the importance in the consideration of local tidal loading is presented apparently. The results in table 7 obtained from modified Schwiderski global cotidal maps with local ones are largely improved comparing with the results from original Schwiderski maps (Li Ruihao and Sun He-Ping et al, 1991) and these results can be directly adopted for high precision tidal gravity data corrections.

Making the further corresponding analysis together with

table 3 and table 7 mentioned above, one can see clearly that the tidal gravity corrections in China, Japan and Korea regions are dominated by local marine tides, while the effects for the stations situated in Philippines are not so evident. Take two typical examples of Shanghai and Guangzhou stations which are located at the coastal lines, they are mainly affected by the local oceanic loadings of about (3.24 μgals, -107°) and (1.25 μgal, -81°) while the total loading effects are of about (2.78 μgal, -91°) and (1.31 μgal,-56°) (see table 7). This tendency is also fit the other stations even the ones away from coastal lines, for example of Wuhan, which is situated in the centre of China and about 700 km away from the sea, the total loading effect is about (0.80 μgak, -38°) while the local sea effect occupies about (0.77 μgal, -75°) for the case of M2 wave.

Forthermore, the effect of the oceanic loading depends on the distances between the observations stations and the sea regions. The larger the distances are, the smaller the effects will be. - Shanghai is situated at the east coastal line where the effect is mainly from east sea region, 3.24 μgal, while the effect from south sea area is about 0.11 μgal (see table 3). Guangzhou is another typical example which is located at south coastal line (figure 1), the effect from south sea region is about 0.774 μgal while the - effect from east sea region is about 0.487 μgal. For other stations, there exist nearly the same tendency.

The application of these ocean loading effects on tidal gravity observations is to explain the residues between the values of theoretical calculation and the ones of observations (Melchior, 1980). The corresponding comparison of the M2 wave among the observed residues and loading effects are shown in table 8-1.

The observed residues are listed in column (1) which are - kindly provided by Prof. P. Melchior in which some of results in Chinese stations were published in 1985. The column (2) is calculated tidal loading effects by use of Schwiderski global cotidal maps provided by ICET and column (3) in the same cotidal maps,modified with Bogdanov K.T and Ovtchinnikov V.V.(1968) local maps calculated by Raty (1983, unpublished). The column (4) is the results from modified Schwiderski global cotidal maps with local ones of present paper including to South China Sea, East China - Sea, Yellow China Sea and Bohai Sea (Institute of Oceanography, State Oceanographical Bureau in 1986, unpublished).

The analysis of these results is quite beneficial as the - ocean loading values can be used to better fit the observed residues which proves the success of loading calculations and that the explanation to the tidal gravity observed residues is made forward largely. From the table, one can see that the results of column (4) obtained by modified Schwiderski global maps by local ones - presented by this paper are better to suit the observed residues which proves the importance of introduction of local maps when the global cotidal maps are used.

The final residues vectors $\vec{X}(X,x)=\vec{B}(B,\beta)-\vec{L}(L,\lambda)$ are also calculated and the corresponding results are shown in table 8-2. Comparing the column (2) with column (3), one can possible evaluate the suitability of the local maps between the one of Bogdanov K.T. and Ovtchinnikov V.V. and the one used in this paper. In the co-

lumn (3), the final residues vectors are much impoved than the ones in column (2) for the stations of Shanghai and Qingdao, however for most of other stations, the corresponding residues have not apprently impoved and the residues for the stations of Seoul and Knoya are even large than the ones obtained from the Bagdanov K.T. and Ovtchinnikov V.V. local map. So from these preliminary analysis, a conclusion of the nearly same suitability of the two sets of local maps can be deduced in the calculation of the oceanic corrections for gravity observations. But it seems that the one we used is a little bit better than the Bogdanov local map as the X residues of 9 stations are more or less impoved among the 15 stations calculated in present paper. The one of possible reasons is that a refined local model in South Sea region is used (see figure 1) in present calculation while there is no consideration of the local tide for the Bogdanov T.K. and Ovtchinnikov V.V. local map in that region (see translation in the present Bulletin).

Analysis of the results for O_1 wave obviously shows that the effect of tidal loading corrections at different stations obtained from modified global maps and the ones obtained from the original Schwiderski ones (Sun Heping and Hu Yanchang, 1989) are much approach comparing with the results of M_2 wave, which demonstrates that the suitability of O_1 wave Schwiderski map is better than that of M_2 wave in the use for the West Pacific Area.

In order to check our calculation programs,some comparisons have been done with Dr. B. Ducarme of ICET in the November and December of 1991 in Brussels. The Schwiderski global cotidal numerical original maps are used. The calculations are developed at the computer center of the Royal Observatory of Belgium. Two projects depending on the consideration of the conservation of water mass or not are carried out. The worldwide station in different regions including Lanzhou, Urumiqui, Brussels, Lwiro, Ottawa, Cuiaba, Alice Springs and South Pole are chosen in order to have a throughout view. The corresponding results are listed in table 9. There exists an excellent agreement for two group results, the maximum difference for the loading amplitude is less then 1% and the phase difference is less than 1° except for the station of Urumqui where the phase difference large than 2° as the corresponding loading vector is too small.

5 CONCLUSION

From the corresponding discussion and numerical results, some useful conclusions can be obtained as follows

(1) In the continent and islands of China, Japan and Korea, the tidal gravity loading corrections are dominated by local marine tides, while the effects of the tidal gravity loading for the stations situated in Philippines are not evident, however for the high precision corrections, these factors have to be taken into account. Fortunately, the Schwiderski global cotidal maps cover large part of them (see tables 3-7).

(2) The tidal gravity loading corrections obtained by the

modified Schwiderski global cotidal maps can be used to better explain the corresponding observed gravity residues comparing with the results obtained from original ones which proves the importance of introduction of the local maps along the coast of China when the gravity loading calculations are carried out (see table 8).

(3) The consideration of the different earth models can cause a discrepancy of loading corrections reaching about 10% and 15% for the stations located at the coast lines as the response of tidal load depends very much on the locally variable properties of the crust and upper mantle. So it is absolutely necessary to consider this factor in high precision tidal loading corrections.

(4) Taking into account the mass conservation, the corresponding discrepancy reaches up to 10% especially for gravity loading of M_2 wave which is non-negligible quantity while a small - changes appears for S_2 wave (table 2) and nearly no effects to - tilt loading calculation which is less than 3% for M_2 wave and - less than 1% for other waves (discussion later).

(5) Comparison of the effects of tidal loading corrections of O_1 waves for different station obtained from modified Schwiderski maps with local ones with the results from original maps shows that the corresponding changes are less than those of M_2 wave - which demonstrates that the suitability of O_1 wave for Schwiderski maps is better than that of M_2 wave in the Western Pacific Area.

(6) Two sets of local maps can provide nearly the same suitability in tidal loading computations, however, it seems that the one we used is a little bit better than the Bogadnov T.K. and Ovtchinnikov V.V. local map as the X residues of 9 stations are more or less improved among 15 stations calculated in this paper.

(7) The programs constructed by us give excellent agreement in both loading amplitudes and phases with those obtained by the programs used in ICET (see table 8).

ACKNOWLEDGMENTS

This research is financially supported by the Joint Earthquake Science Foundation of P.R. China and is completed under the guidance of Prof. Li Ruihao, Dr. Jiang Xianhua and Dr. Hu Yanchang gave me a lot of useful helps during calculations, I here give them many thanks.

Prof. Melchior P. provided me the observed residues and results of Raty (1983, unpublished), his patiently read the manuscript and suitable suggestions are also gratefully thanked.

Dr. B. Ducarme and O.Francis who willingly take times to discuss the related problems in the comparison of the programs and the concerned results are also to be acknowledged.

REFERENCES

Agnew, D.C., Conservation of the mass in tidal loading computations, Geophysical Journal Royal Astronomical Society, 72, 321-325, 1983.

Baker T. F., 1977, Earth tides, crustal structure and ocean tides, Proceedings of the International Symposium on Earth Tides (Bonn, 1977), pp.265-280.

Bogdanov K.T. and Ovtchinnikov V.V., Marées de la Mer de Chine Orientale et de la Mer Jaune, Résultats des recherches dans le cadre de projets géophysiques internationaux, Recherches océaniques,Section X du programme de IUGG No.19, Moscou, 1968 (translation in the present Bulletin).

Dziewonski A.M. and Anderson D.L.,1981,Preliminary Reference Earth Model, Phys. Earth Planet. Int., 25, 297-356.

Farrell, W. E., Deformation of the Earth by Surface Loads, Rev. Geophs. Space Phys., Vol.10, 761-797, 1972.

Francis O.& Dehant V., Recomputation of the Green's functions for tidal loading estimations, B.I.M, No. 100, pp 6962-6986.

Hsu H. T., The effect of the ocean tides to gravity and tilt tides observations, Institute of Geophysics and Geodesy, Chinese Academy sinaca., No.4, 1981 (in Chinese).

Jiang Xianhua, 1986, Static deformation response of the Earth to tidal potential concentrated mass loading and shear stress, B.I.M., No. 97, pp 6587-6597.

Li Ruihao, Sun Heping and Jiang Xianhua, Investigation of Ocean loading effect on Earth tidal observations in the Mainland of China, Proceedings of the Eleventh International Symposium Earth Tides, Helsinki (1989), pages 335-343, printed in Stuttgart D-7000,1991.

Li Ruihao, Sun Heping, Chen Dongsheng and Fu Yunhao, On the correction to Observations of Gravity tides and the Indication of Gravity anomaly, ACTA Seismologica sinic, Vol.13, No.2,1991.

Melchior P., The Tides of the Planet Earth, Pergamon Press,Oxford, 2nd edition, 1980.

Melchior P., Fang Tsun, Ducarme B, Hsu Hou-Zse, Van Ruymbeke M, Li Ruihao, Poitevin C. and Chen Dong-Sheng, Studies on the Earth Tidal Observations in China, ACTA Geophysica sinica, Vol.28, No.2, 1985.

Melchior, P., Moens, M and Ducarme, B., 1980, Computations of tidal gravity loading and attraction effects,Obs.Roy.Belgique, Bull. d'Inform. Marees Terr., Vol.IV, Fasc.5, pp. 96-133.

Raty M.F. (1983), Optimisatives des résultats des mesures de marée gravimétrique effectuées en Chine, Memoire, 107 pages, Univ. Cath. de Louvain, Faculte des Sciences.

Schwiderski, E. W., On charting global ocean tides, Rev. Geophys. Space Phys., Vol. 18, 234-268, 1980.

Shen Yujiang, Numerical computation of tides in East China Sea, Journal of Shandong College of Oceanology, Vol.10, No.3,Sept., 1980 (in Chinese).

Shen Yujiang, Hu Dingming and et al, Numerical computation of the tides in South China Sea, Transactions of Oceanology and lomnology, No.1, 1985 (IN Chinese).

Sun He-Ping and Hu Yanchang, Discussion of some problems in tidal loading computation, Crustal Deformation and Earthquake, Vol.9, No. 1, Feb., 1989 (in Chinese with English Abstract).

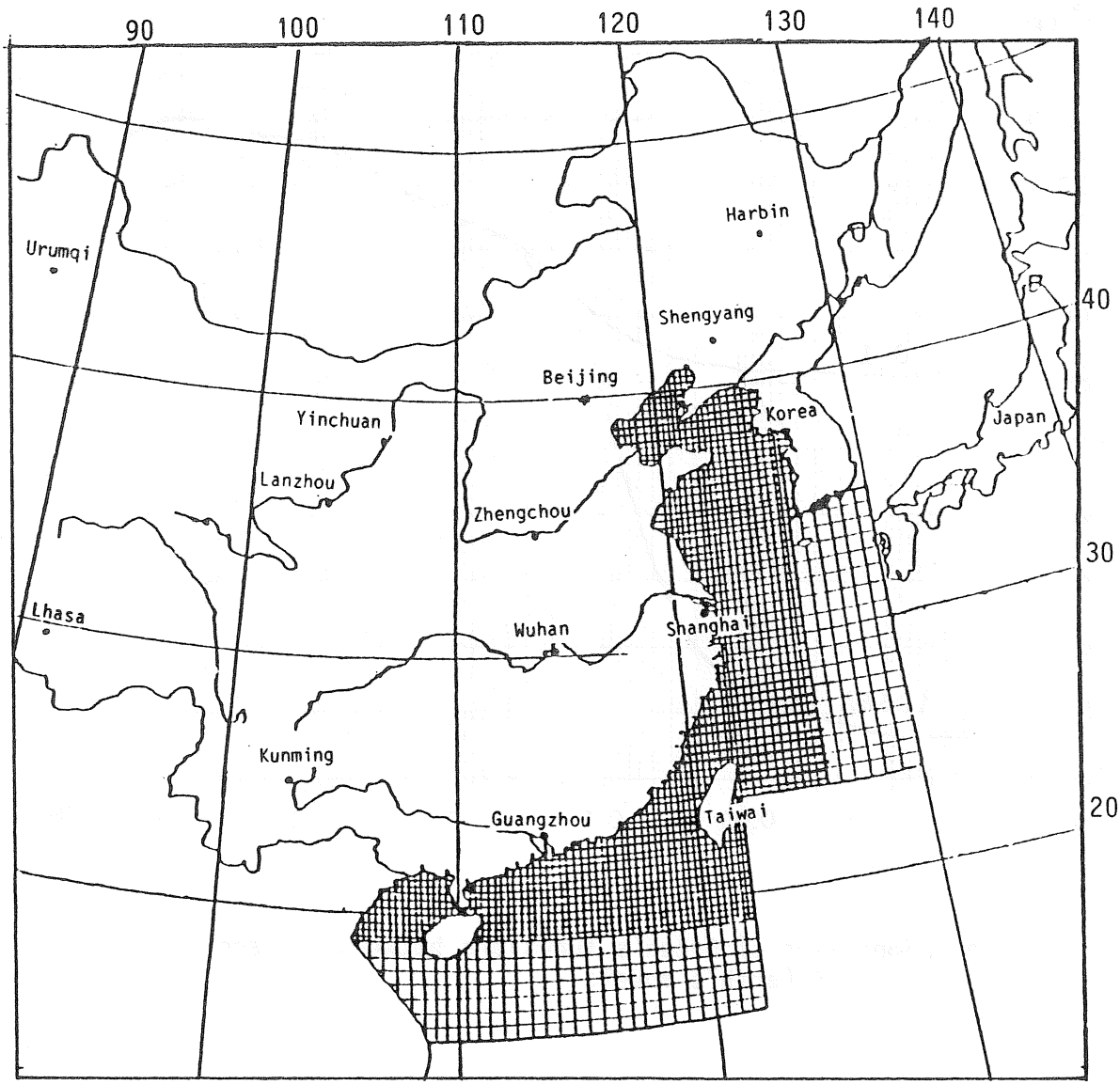

FiG. 1 Local Oceans and its grid system of $(\frac{1}{6})*(\frac{1}{6})$ and $(\frac{1}{3})*(\frac{1}{3})$ along the coast of China

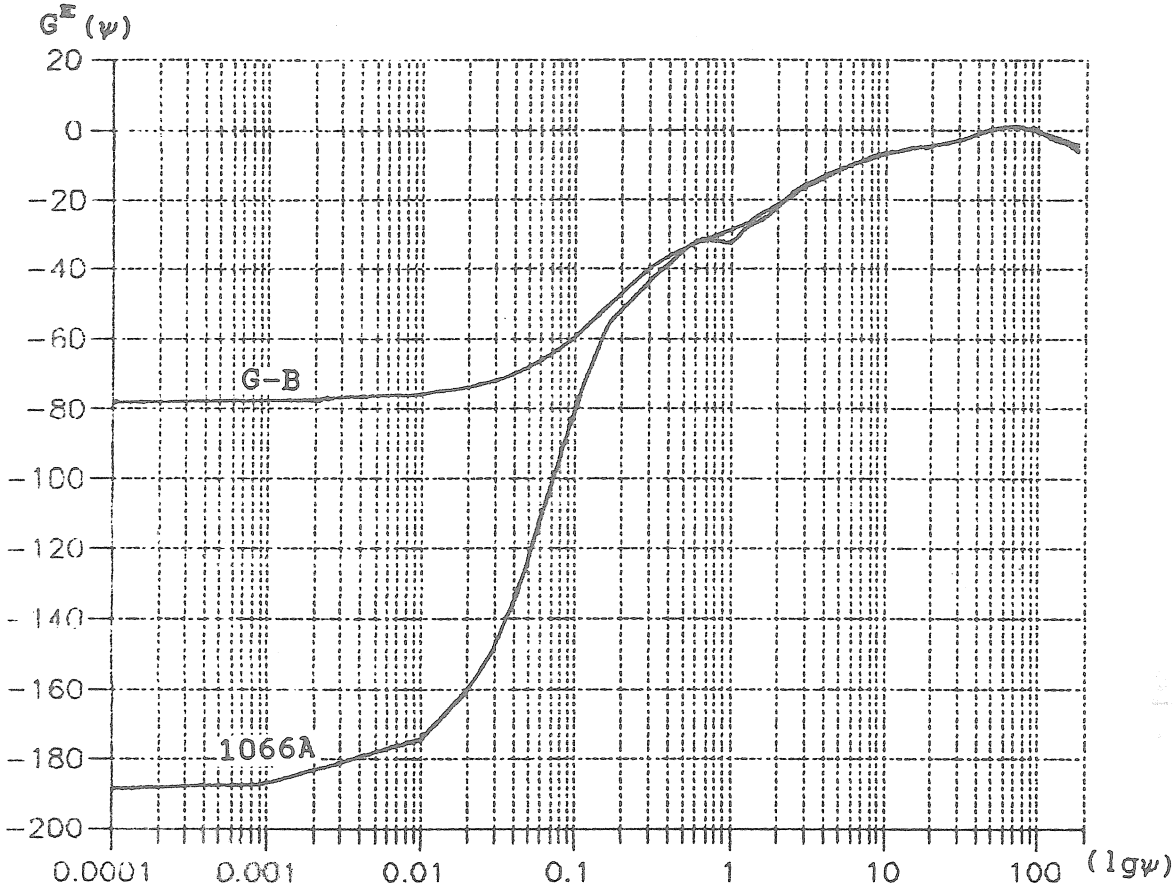

Fig. 2 Comparison of Green's functions between G-B and G-D1066A Earth's models

Table 1 Effect of the different earth models on tidal gravity loading corrections (E.W.Schwiderski maps)
L: amplitude (in microgal) λ : phase (in degree)

Station	M2 wave				S2 wave			
	G-B		G-D1066A		G-B		G-D1066A	
	L	λ	L	λ	L	λ	L	λ
2600 GUANG ZHO	1.07	-55	1.20	-57	0.30	-68	0.32	-76
2603 BEIJING	0.41	49	0.30	23	0.25	27	0.21	22
2604 KUNMING	0.35	-94	0.39	-94	0.11	-176	0.10	-163
2605 LANZHOU	0.01	-17	0.08	-88	0.07	85	0.04	87
2606 URUMQI	0.26	-137	0.39	-144	0.12	172	0.12	-177
2607 WUHAN	0.55	-10	0.63	-24	0.23	-8	0.19	-20
2612 SHANGHAI	1.22	-57	1.41	-55	0.34	-68	0.34	-84
2610 SHENYANG	0.65	46	0.51	27	0.37	18	0.33	16
2633 CHUAUZHOU	2.32	-98	3.09	-63	0.54	-123	0.63	-132
2636 ZHENGZHOU	0.38	23	0.37	-7	0.21	17	0.17	8

Table 2 Effect of the conservation of the mass on tidal gravity loading corrections (E.W.Schwiderski maps)
L: amplitude (in microgal) λ : phase (in degree)

Station	M2 wave				S2 wave			
	original		conserved		original		conserved	
	L	λ	L	λ	L	λ	L	λ
2600 GUANG ZHO	1.30	-48	1.07	-55	0.31	-67	0.30	-68
2603 BEIJING	0.52	25	0.41	49	0.25	25	0.25	27
2604 KUNMING	0.40	-59	0.35	-94	0.11	-175	0.11	-176
2605 LANZHOU	0.23	-1	0.01	-17	0.07	79	0.07	85
2606 URUMQI	0.08	-112	0.26	-137	0.11	171	0.12	172
2607 WUHAN	0.80	-13	0.55	-10	0.23	-9	0.23	-8
2612 SHANGHAI	1.51	-52	1.22	-57	0.35	-67	0.34	-68
2610 SHENYANG	0.71	27	0.65	46	0.37	17	0.37	18
2633 CHUAUZHOU	2.47	-90	2.32	-98	0.54	-122	0.54	-123
2636 ZHENGZHOU	0.57	7	0.38	23	0.22	16	0.21	17

Table 3 Tidal gravity loading corrections of M2 wave (results from different local maps)
L: (microgal) λ : (degree)

Station	South Sea		East Sea		Total	
	L	λ	L	λ	L	λ
2600 GUANG ZHO	0.7738	-87.8	0.4872	-70.4	1.2472	-81.1
2601 HONG KONG	2.3731	-77.2	0.5059	-73.0	2.8779	-76.4
2602 NANKING	0.1111	-104.1	1.4429	-93.7	1.5524	-94.4
2603 PEKING	0.0578	-95.4	0.3040	-58.6	0.3519	-64.2
2604 KUNMING	0.1082	-75.3	0.2185	-40.0	0.3131	-51.5
2605 LANGSHOW	0.0626	-73.0	0.2272	-40.5	0.2820	-47.4
2606 URUMCHI	0.0273	-39.8	0.0996	-4.8	0.1230	-12.1
2607 WUHAN	0.1395	-95.7	0.6403	-70.5	0.7688	-75.0
2610 SHENGYANG	0.0478	-109.0	0.6344	-63.8	0.6690	-66.7
2611 HARBIN	0.0367	-114.6	0.2990	-74.8	0.3281	-78.9
2613 SHANGHAI	0.1133	-107.3	3.1243	-107.4	3.2376	-107.4
2614 QING DAO/	0.0748	-103.6	1.1234	29.6	1.0735	26.7
2616 DATONG	0.0575	-90.2	0.3052	-56.5	0.3545	-61.7
2618 BAODI	0.0588	-97.8	0.2353	-53.8	0.2806	-62.1
2620 WENAN	0.0628	-96.4	0.2637	-52.4	0.3119	-60.5
2623 CHENGDU	0.0856	-74.0	0.2426	-42.0	0.3184	-50.2
2626 YINCHUAN	0.0576	-76.9	0.2382	-44.1	0.2883	-50.3
2629 HUANGSHI	0.1470	-97.6	0.7166	-72.9	0.8524	-77.1
2631 WEIFONG	0.0723	-101.4	0.5633	-59.6	0.6191	-64.1
2633 CHUANCHOU	0.7034	-137.6	3.2249	-126.4	3.9172	-128.4
2634 TAIBEI	0.2933	-110.3	3.4895	-97.7	3.7763	-98.7
2635 NANNING	0.2342	-74.7	0.3036	-53.8	0.5291	-62.9
2636 ZHENGCHOU	0.0871	-92.1	0.4547	-63.7	0.5330	-68.2
2750 SEOUL	0.0574	-114.7	0.4257	-6.4	0.4113	-14.0
2823 KYOTO	0.0461	-129.8	0.5386	-85.1	0.5723	-88.4
2824 NAGASHIMA	0.0465	-130.3	0.5393	-85.2	0.5730	-88.5
2830 SAKUMA	0.0422	-133.5	0.4367	-89.8	0.4681	-93.4
2834 MATSUSHIR	0.0397	-134.6	0.3914	-91.9	0.4214	-95.6
2847 MIZUSAWA	0.0329	-140.8	0.2832	-99.6	0.3087	-103.6
2875 KANOYA	0.0670	-119.5	1.9873	-59.9	2.0220	-61.5
2877 TOKYO	0.0382	-137.4	0.3593	-94.8	0.3884	-98.6
2890 SAPPORO	0.0289	-142.0	0.2328	-101.8	0.2556	-106.0
2898 SENDAI	0.0341	-140.1	0.2996	-98.6	0.3259	-102.6
4010 BAGUIO	0.4161	-67.0	0.3959	-70.3	0.8117	-68.6
4011 MANILA	0.2561	-77.9	0.3335	-69.3	0.5880	-73.0
4020 ZAMBOANGA	0.0907	-95.9	0.1872	-68.9	0.2712	-77.7
4021 BUTUAN	0.0879	-100.7	0.2160	-73.8	0.2970	-81.5
8001 XIAGUAN	0.0872	-69.8	0.1892	-34.1	0.2649	-45.2
8002 MIDU	0.0895	-70.5	0.1911	-34.7	0.2688	-45.9
8003 LIJIANG	0.0836	-69.0	0.1924	-34.2	0.2653	-44.5
8004 CHUXIONG	0.0979	-73.0	0.2015	-37.0	0.2865	-48.6
2450 KATHMANDU	0.0355	-37.4	0.0931	-1.5	0.1236	-11.2

Table 4 Tidal gravity loading corrections of S2 wave (results from different local maps)
L: (microgal) λ : (degree)

Station	South Sea		East Sea		Total	
	L	λ	L	λ	L	λ
2600 GUANG ZHO	0.3334	-118.2	0.1500	-90.5	0.4714	-109.7
2601 HONG KONG	1.0060	-110.9	0.1539	-92.7	1.1533	-108.5
2602 NANKING	0.0416	-123.7	0.4209	-118.7	0.4624	-119.2
2603 PEKING	0.0237	-118.4	0.1203	-74.7	0.1384	-81.5
2604 KUNMING	0.0491	-100.1	0.0730	-61.1	0.1153	-76.6
2605 LANGSHOW	0.0270	-97.5	0.0775	-62.1	0.1007	-71.1
2606 URUMCHI	0.0120	-65.0	0.0347	-26.8	0.0447	-36.3
2607 WUHAN	0.0545	-117.3	0.2049	-92.8	0.2556	-97.9
2610 SHENGYANG	0.0195	-131.6	0.2255	-99.0	0.2422	-101.5
2611 HARBIN	0.0151	-137.6	0.1092	-101.3	0.1217	-105.5
2613 SHANGHAI	0.0415	-125.8	0.9327	-141.0	0.9727	-140.3
2614 QING DAO/	0.0296	-125.2	0.4631	-7.9	0.4503	-11.2
2616 DATONG	0.0238	-113.6	0.1088	-76.8	0.1287	-83.1
2618 BAODI	0.0240	-120.6	0.1241	-62.5	0.1383	-71.0
2620 WENAN	0.0256	-119.2	0.1322	-64.0	0.1483	-72.2
2623 CHENGDU	0.0376	-99.0	0.0814	-63.4	0.1141	-74.5
2626 YINCHUAN	0.0245	-101.1	0.0818	-65.8	0.1028	-73.7
2629 HUANGSHI	0.0564	-118.5	0.2279	-95.5	0.2807	-100.0
2631 WEIFONG	0.0289	-123.3	0.1764	-78.5	0.1979	-84.4
2633 CHUANCHOU	0.1320	-163.5	0.6972	-167.2	0.8290	-166.6
2634 TAIBEI	0.0706	-109.3	1.0758	-117.5	1.1457	-117.0
2635 NANNING	0.1235	-104.9	0.0991	-74.5	0.2150	-91.4
2636 ZHENGCHOU	0.0354	-114.8	0.1515	-84.4	0.1829	-90.0
2750 SEOUL	0.0229	-136.4	0.2602	-45.0	0.2606	-50.0
2823 KYOTO	0.0186	-151.9	0.2165	-111.6	0.2310	-114.6
2824 NAGASHIMA	0.0188	-152.5	0.2162	-111.6	0.2308	-114.6
2830 SAKUMA	0.0172	-155.9	0.1723	-115.6	0.1857	-119.1
2834 MATSUSHIR	0.0162	-157.2	0.1533	-117.6	0.1660	-121.1
2847 MIZUSAWA	0.0135	-163.7	0.1086	-124.6	0.1194	-128.7
2875 KANOYA	0.0263	-140.2	0.8618	-90.0	0.8789	-91.3
2877 TOKYO	0.0156	-160.0	0.1398	-120.1	0.1521	-123.9
2890 SAPPORO	0.0119	-165.0	0.0879	-126.6	0.0975	-131.0
2898 SENDAI	0.0140	-162.9	0.1153	-123.6	0.1264	-127.7
4010 BAGUIO	0.1954	-99.5	0.1340	-89.6	0.3282	-95.5
4011 MANILA	0.1205	-113.2	0.1145	-89.1	0.2298	-101.5
4020 ZAMBOANGA	0.0437	-126.8	0.0656	-89.5	0.1038	-104.3
4021 BUTUAN	0.0409	-130.4	0.0764	-94.5	0.1121	-106.8
8001 XIAGUAN	0.0395	-94.9	0.0636	-55.4	0.0974	-70.3
8002 MIDU	0.0406	-95.6	0.0642	-55.9	0.0989	-71.1
8003 LIJIANG	0.0377	-94.2	0.0648	-55.5	0.0971	-69.5
8004 CHUXIONG	0.0443	-97.8	0.0676	-58.1	0.1056	-73.7
2450 KATHMANDU	0.0161	-63.3	0.0320	-23.1	0.0455	-36.3

Table 5. Tidal gravity loading corrections of O1 wave (results from different local maps)
L: (microgal) λ : (degree)

Station	South Sea		East Sea		Total	
	L	λ	L	λ	L	λ
2600 GUANG ZHO	0.7306	-77.5	0.1209	-1.4	0.7687	-68.7
2601 HONG KONG	1.4124	-71.1	0.1269	-2.6	1.4636	-66.5
2602 NANKING	0.1426	-82.3	0.2297	0.7	0.2846	-29.0
2603 PEKING	0.0742	-84.6	0.0736	2.6	0.1069	-41.2
2604 KUNMING	0.1322	-111.6	0.0548	9.8	0.1135	-87.3
2605 LANGSHOW	0.0762	-81.5	0.0556	6.5	0.0958	-46.1
2606 URUMCHI	0.0344	-64.9	0.0251	22.6	0.0434	-29.6
2607 WUHAN	0.1672	-82.0	0.1419	-1.7	0.2367	-45.8
2610 SHENGYANG	0.0635	-89.7	0.0895	-57.0	0.1470	-70.5
2611 HARBIN	0.0491	-93.1	0.0718	-27.7	0.1025	-53.5
2613 SHANGHAI	0.1489	-82.2	0.5602	13.8	0.5641	-1.3
2614 QING DAO/	0.0977	-85.4	0.4006	-93.1	0.4976	-91.6
2616 DATONG	0.0730	-83.4	0.0724	-4.1	0.1119	-44.0
2618 BAODI	0.0759	-85.2	0.0782	23.9	0.0893	-29.3
2620 WENAN	0.0805	-84.6	0.0884	11.9	0.1125	-33.3
2623 CHENGDU	0.1006	-88.6	0.0597	7.8	0.1110	-56.3
2626 YINCHUAN	0.0711	-80.9	0.0581	3.4	0.0962	-43.9
2629 HUANGSHI	0.1766	-81.3	0.1565	-1.8	0.2565	-44.5
2631 WEIFONG	0.0937	-85.2	0.1389	-35.0	0.2116	-54.9
2633 CHUANCHOU	0.5727	-68.6	0.5642	-25.6	1.0576	-47.3
2634 TAIBEI	0.3847	-69.3	0.8264	-12.1	1.0844	-29.5
2635 NANNING	0.4692	-159.4	0.0762	4.6	0.3965	-156.4
2636 ZHENGCHOU	0.1080	-83.3	0.1037	-5.5	0.1647	-45.3
2750 SEOUL	0.0780	-90.6	0.4032	-48.8	0.4643	-55.2
2823 KYOTO	0.0654	-97.8	0.1554	-20.8	0.1816	-41.3
2824 NAGASHIMA	0.0663	-98.0	0.1550	-20.2	0.1810	-41.2
2830 SAKUMA	0.0602	-99.9	0.1249	-22.9	0.1504	-45.9
2834 MATSUSHIR	0.0563	-100.7	0.1117	-24.8	0.1367	-48.3
2847 MIZUSAWA	0.0464	-104.3	0.0795	-29.1	0.1018	-55.3
2875 KANOYA	0.0957	-91.2	0.5590	-6.6	0.5760	-16.2
2877 TOKYO	0.0546	-102.1	0.1021	-25.4	0.1264	-50.3
2890 SAPPORO	0.0404	-105.6	0.0643	-31.2	0.0846	-58.6
2898 SENDAI	0.0483	-103.8	0.0844	-28.3	0.1072	-54.1
4010 BAGUIO	0.9677	-72.6	0.1092	-5.1	1.0145	-66.9
4011 MANILA	0.5085	-75.9	0.0920	-5.2	0.5459	-66.7
4020 ZAMBOANGA	0.1519	-83.8	0.0515	-5.9	0.1703	-66.6
4021 BUTUAN	0.1479	-85.6	0.0600	-8.8	0.1719	-65.7
8001 XIAGUAN	0.1052	-100.1	0.0476	12.2	0.0976	-73.3
8002 MIDU	0.1083	-101.8	0.0481	12.0	0.0991	-75.5
8003 LIJIANG	0.0999	-95.9	0.0482	12.0	0.0965	-67.6
8004 CHUXIONG	0.1191	-106.9	0.0507	11.1	0.1052	-81.7
2450 KATHMANDU	0.0445	-68.9	0.0237	26.8	0.0483	-39.7

Table 6 Tidal gravity loading corrections of K1 wave (results from different local maps)
L: (microgal) λ : (degree)

Station	South Sea		East Sea		Total	
	L	λ	L	λ	L	λ
2600 GUANG ZHO	0.9837	-128.7	0.1556	-36.0	0.9887	-119.7
2601 HONG KONG	2.7635	-121.0	0.1634	-37.2	2.7858	-117.7
2602 NANKING	0.1866	-132.2	0.3215	-34.9	0.3505	-66.7
2603 PEKING	0.0981	-132.0	0.0954	-24.1	0.1139	-79.1
2604 KUNMING	0.1504	-138.6	0.0696	-23.9	0.1368	-111.1
2605 LANGSHOU	0.1007	-124.1	0.0694	-26.9	0.1149	-87.3
2606 URUMCHI	0.0454	-107.6	0.0312	-10.8	0.0519	-70.9
2607 WUHAN	0.2210	-129.7	0.1826	-36.0	0.2774	-88.7
2610 SHENGYANG	0.0837	-138.3	0.1129	-104.2	0.1881	-118.6
2611 HARBIN	0.0647	-141.6	0.0843	-63.6	0.1164	-96.5
2613 SHANGHAI	0.1936	-133.0	0.7546	-27.8	0.7281	-42.7
2614 QING DAO/	0.1284	-134.4	0.4566	-155.1	0.5786	-150.6
2616 DATONG	0.0966	-129.9	0.0882	-35.8	0.1260	-85.6
2618 BAODI	0.1002	-132.9	0.1274	-0.4	0.0950	-51.5
2620 WENAN	0.1064	-132.2	0.1218	-14.8	0.1193	-67.1
2623 CHENGDU	0.1312	-127.4	0.0754	-25.8	0.1375	-95.0
2626 YINCHUAN	0.0942	-125.0	0.0720	-29.9	0.1134	-85.7
2629 HUANGSHI	0.2331	-129.7	0.2023	-36.4	0.2998	-87.3
2631 WEIFONG	0.1235	-133.7	0.1257	-96.1	0.2359	-114.7
2633 CHUANCHOU	0.7081	-120.8	0.7428	-61.1	1.2586	-90.2
2634 TAIBEI	0.4652	-122.6	1.0147	-50.3	1.2380	-71.3
2635 NANNING	0.3346	165.5	0.0975	-29.5	0.2418	171.6
2636 ZHENGCHOU	0.1430	-130.1	0.1283	-38.4	0.1892	-87.4
2750 SEOUL	0.1022	-140.4	0.4954	-89.3	0.5653	-97.4
2823 KYOTO	0.0854	-148.6	0.1911	-53.2	0.2019	-78.1
2824 NAGASHIMA	0.0865	-148.9	0.1919	-52.5	0.2015	-77.8
2830 SAKUMA	0.0785	-150.7	0.1544	-55.4	0.1667	-83.4
2834 MATSUSHIR	0.0735	-151.3	0.1374	-57.5	0.1514	-86.4
2847 MIZUSAWA	0.0608	-154.5	0.0976	-62.1	0.1127	-94.7
2875 KANOYA	0.1242	-142.6	0.7243	-37.7	0.7026	-47.5
2877 TOKYO	0.0712	-152.8	0.1263	-58.0	0.1398	-88.6
2890 SAPPORO	0.0530	-155.3	0.0784	-64.6	0.0941	-98.8
2898 SENDAI	0.0632	-154.1	0.1038	-61.2	0.1186	-93.3
4010 BAGUIO	1.1110	-132.2	0.1402	-38.8	1.1115	-125.0
4011 MANILA	0.6362	-133.3	0.1180	-38.7	0.6376	-122.7
4020 ZAMBOANGA	0.1969	-135.9	0.0658	-39.2	0.2002	-116.8
4021 BUTUAN	0.1911	-138.5	0.0767	-41.9	0.1976	-115.8
8001 XIAGUAN	0.1279	-130.9	0.0603	-21.5	0.1219	-103.1
8002 MIDU	0.1303	-131.9	0.0610	-21.7	0.1234	-104.3
8003 LIJIANG	0.1245	-128.9	0.0611	-21.7	0.1213	-100.2
8004 CHUXIONG	0.1392	-135.2	0.0643	-22.7	0.1291	-107.8
2450 KATHMANDU	0.0580	-108.2	0.0298	-6.7	0.0598	-78.9

Table 7 Tidal gravity loading corrections
(Schwiderski global maps + local ones)
L: (microgal) λ : (degree)

station	M2		S2		O1		K1	
	L	λ	L	λ	L	λ	L	λ
2600 GUANG ZHO	1.31	-56	0.38	-83	1.23	-52	1.21	-97
2601 HONG KONG	2.96	-64	1.05	-97	1.97	-56	3.01	-108
2602 NANKING	1.37	-65	0.36	-70	0.83	-3	0.90	-25
2603 PEKING	0.38	-6	0.19	-3	0.51	17	0.53	3
2604 KUNMING	0.48	-82	0.13	-153	0.35	-40	0.25	-84
2605 LANGSHOW	0.19	-48	0.02	39	0.30	7	0.21	-4
2606 URUMCHI	0.22	-118	0.09	-176	0.17	56	0.17	84
2607 WUHAN	0.80	-38	0.23	-41	0.63	-13	0.59	-36
2610 SHENGYANG	0.69	-23	0.26	-28	0.64	16	0.66	1
2611 HARBIN	0.35	6	0.24	0	0.74	25	0.82	8
2613 SHANGHAI	2.78	-91	0.67	-118	1.23	4	1.45	-24
2614 QING DAO/	1.69	29	0.74	1	0.61	-30	0.29	-52
2616 DATONG	0.32	-12	0.14	1	0.45	16	0.44	2
2618 BAODI	0.40	7	0.24	-1	0.54	20	0.61	6
2620 WENAN	0.42	2	0.23	-4	0.53	16	0.57	1
2623 CHENGDU	0.30	-61	0.03	-134	0.32	-13	0.20	-39
2626 YINCHUAN	0.19	-30	0.05	22	0.33	13	0.27	3
2629 HUANGSHI	0.88	-41	0.26	-45	0.67	-14	0.63	-37
2631 WEIFONG	0.75	-19	0.30	-18	0.63	2	0.55	-15
2633 CHUANCHOU	3.12	-115	0.39	-148	1.67	-33	1.73	-67
2634 TAIBEI	3.73	-72	1.19	-81	1.95	-20	2.09	-50
2635 NANNING	0.63	-51	0.13	-87	0.40	-90	0.26	-106
2636 ZHENGCHOU	0.53	-28	0.18	-21	0.51	0	0.48	-18
2750 SEOUL	1.18	14	0.62	-13	1.02	-5	1.03	-28
2823 KYOTO	2.03	2	1.02	-19	1.69	12	2.03	-7
2824 NAGASHIMA	2.72	2	1.34	-19	1.98	11	2.40	-8
2830 SAKUMA	2.32	11	1.21	-12	1.97	14	2.38	-5
2834 MATSUSHIR	1.60	17	0.89	-8	1.69	16	2.03	-2
2847 MIZUSAWA	1.81	46	1.00	8	2.02	22	2.42	4
2875 KANOYA	4.27	-21	1.83	-45	2.10	3	2.57	-18
2877 TOKYO	2.09	23	1.14	-5	2.02	16	2.45	-2
2890 SAPPORO	1.22	53	0.71	10	1.76	24	2.05	6
2898 SENDAI	1.92	42	1.06	7	2.06	21	2.48	3
4010 BAGUIO	2.60	-17	0.98	-37	2.14	-52	1.90	-88
4011 MANILA	2.50	-15	0.94	-34	1.83	-51	1.70	-81
4020 ZAMBOANGA	3.10	-4	1.59	30	1.67	-56	1.84	-79
4021 BUTUAN	3.99	-8	1.69	-33	1.70	-35	2.01	-53
8001 XIAGUAN	0.55	-93	0.19	-158	0.30	-34	0.19	-91
8002 MIDU	0.56	-92	0.19	-158	0.31	-36	0.20	-91
8003 LIJIANG	0.48	-91	0.16	-159	0.29	-28	0.16	-81
8004 CHUXIONG	0.53	-89	0.17	-157	0.33	-39	0.23	-89
2450 KATHMANDU	0.84	-106	0.35	-152	0.14	53	0.28	136

Table 8-1 The comparison of the tidal gravity loading corrections of M2 wave and observed residues

		(1)		(2)		(3)		(4)	
		B	β	L	λ	L	λ	L	λ
2401	NEW DELHI	1.84	-110	0.94	-121			0.91	-118
2450	KATHMANDU			0.87	-111			0.84	-106
2600	GUANG ZHO	1.11	-75	1.09	-55	1.48	-63	1.31	-56
2601	HONG KONG	2.78	-19	1.83	-67	2.24	-70	2.96	-64
2603	PEKING	0.89	14	0.42	49	0.41	-21	0.37	-6
2604	KUNMING	1.19	-45	0.39	-95	0.59	-82	0.46	-80
2605	LANGSHOW	0.78	-55	0.02	-27	0.27	-57	0.19	-48
2606	URUMCHI	0.68	-2	0.27	-137	0.25	-112	0.22	-118
2607	WUHAN	1.03	-36	0.56	-10	0.99	-50	0.80	-38
2610	SHENGYANG	1.11	1	0.66	46	0.68	-29	0.69	-23
2613	SHANGHAI	2.36	-100	1.16	-64	3.94	-91	2.67	-84
2614	QING DAO/	2.67	34	2.38	68	1.76	8	1.88	30
2750	SEOUL	3.03	33	1.68	50	2.34	28	1.18	14
2875	KANOYA	4.37	-30	4.20	-12	4.14	-28	4.27	-21
2823	KYOTO	2.45	-1	2.22	10	1.96	-1	2.02	2
2847	MIZUSAWA	2.56	35	2.07	47	1.79	47	1.81	46
2877	TOKYO	2.51	20	2.33	27	2.04	22	2.09	23
4011	MANILA	1.35	-21	2.47	-13			2.50	-15

B and β: amplitude and phase of observed residue;
L and λ: amplitude and phase of loading correction;
(1) Observed tidal gravity residues;
(2) Schwiderski map/ICET (provided by Prof. P.Melchior);
(3) Schwiderski map +local one (Raty 1983, unpublished);
(4) Schwiderski map +local one (present paper);

Table 8-2 X residues(X,x) in West Pacific aera

		(2)		(3)		(4)	
		X	x	X	x	X	x
2401	NEW DELHI	0.93	81.06			0.95	77.68
2600	GUANG ZHO	0.38	-152.05	0.46	147.34	0.45	178.22
2601	HONG KONG	2.07	22.16	2.22	32.79	2.20	52.83
2603	PEKING	0.60	-9.81	0.60	37.00	0.56	27.13
2604	KUNMING	0.99	-27.36	0.80	-18.71	0.85	-27.02
2605	LANGSHOW	0.76	-55.71	0.51	-53.94	0.59	-57.24
2606	URUMCHI	0.89	10.36	0.80	15.06	0.80	12.29
2607	WUHAN	0.58	-60.99	0.25	37.84	0.23	-29.09
2610	SHENGYANG	0.79	-34.96	0.62	34.12	0.56	31.33
2613	SHANGHAI	1.58	-125.62	1.65	101.92	0.76	154.32
2614	QING DAO/	1.50	-28.36	1.33	69.34	0.81	43.37
2750	SEOUL	1.51	13.96	0.73	49.27	1.95	44.35
2875	KANOYA	1.35	-103.86	0.27	-61.86	0.69	72.87
2823	KYOTO	0.50	-58.41	0.49	-1.00	0.45	-14.73
2847	MIZUSAWA	0.69	-3.80	0.89	10.30	0.86	11.21
2877	TOKYO	0.35	-35.20	0.48	11.41	0.44	5.50
4011	MANILA	1.15	-3.59			1.17	-8.05

Table 9(a) Tidal gravity loading corrections of M2 wave
(results from Schwiderski map from this paper)
L: amplitude (microgal) λ : phase (degree)

(A) consideration of non conservation of the mass with G-B model

		(1)		(2)		(3)	
		L	λ	L	λ	L	λ
2605	LANZHOU	0.177	11.01	0.116	-12.34	0.228	-0.61
2606	URUMQUI	0.044	-8.35	0.098	-138.62	0.077	-112.90
201	BRUXELLES	0.601	80.94	1.046	65.18	1.632	70.92
3420	LWIRO	0.946	80.80	1.221	74.12	2.164	77.04
6803	OTTAWA	0.965	-369.15	1.154	-377.99	2.113	-13.97
7309	CUIABA	0.642	25.66	0.994	62.01	1.559	47.87
4209	ALICE SPRINGS	0.268	-47.25	0.570	-83.88	0.802	-72.37
9998	SOUTH POLE	0.334	-84.01	0.432	-46.76	0.727	-62.92

(B) consideration of conservation of the mass with G-B model

		(1)		(2)		(3)	
		L	λ	L	λ	L	λ
2605	LANZHOU	0.064	160.68	0.080	-18.25	0.016	-13.92
2606	URUMQUI	0.138	-135.05	0.124	-140.43	0.261	-137.59
201	BRUXELLES	0.726	66.09	1.129	61.00	1.853	62.99
3420	LWIRO	0.899	69.32	1.210	71.66	2.109	70.66
6803	OTTAWA	0.763	-371.47	1.087	-379.10	1.846	-15.96
7309	CUIABA	0.587	43.74	1.006	64.96	1.568	57.17
4209	ALICE SPRINGS	0.082	-15.23	0.511	-86.94	0.542	-78.70
9998	SOUTH POLE	0.316	-50.64	0.443	-42.23	0.757	-45.73

Table 9(b) Tidal gravity loading corrections of M2 wave
(results from Schwiderski map from ICET)
L: amplitude (microgal) λ : phase (degree)

(A) consideration of non conservation of the mass with G-B model

		(1)		(2)		(3)	
		L	λ	L	λ	L	λ
2605	LANZHOU	0.117	9.60	0.116	-12.95	0.228	-1.61
2606	URUMQUI	0.046	-12.14	0.099	-137.93	0.081	-110.77
201	BRUXELLES	0.614	80.86	1.058	65.20	1.628	70.94
3420	LWIRO	0.953	80.68	1.225	74.09	2.172	76.97
6803	OTTAWA	0.979	-9.39	1.167	-18.04	2.140	-14.10
7309	CUIABA	0.644	25.49	0.998	61.95	1.563	47.79
4209	ALICE SPRINGS	0.269	-47.88	0.570	-83.83	0.804	-72.49
9998	SOUTH POLE	0.327	-85.10	0.423	-46.79	0.709	-63.40

(B) consideration of conservation of the mass with G-B model

		(1)		(2)		(3)	
		L	λ	L	λ	L	λ
2605	LANZHOU	0.064	163.24	0.080	-19.04	0.016	-28.37
2606	URUMQUI	0.141	-133.76	0.126	-139.79	0.266	-136.60
201	BRUXELLES	0.740	66.18	1.142	61.05	1.880	63.07
3420	LWIRO	0.901	68.19	1.211	71.67	2.111	70.61
6803	OTTAWA	0.775	-11.72	1.100	-19.13	1.871	-16.06
7309	CUIABA	0.588	43.71	1.010	64.95	1.573	57.16
4209	ALICE SPRINGS	0.081	-16.83	0.510	-86.87	0.543	-78.86
9998	SOUTH POLE	0.307	-50.71	0.434	-42.16	0.738	-45.70

*: (1) direct attraction of the water mass;
(2) elastic effect caused by deformation of the earth;
(3) total effect;

Traduction

Marées de la Mer de Chine Orientale et de la Mer Jaune

K.T. Bogdanov, V.V. Ovtchinnikov

Résultats des recherches dans le cadre de projets géophysiques internationaux

Recherches océaniques
Section X du programme MGG N° 19, pp 105-115 - Moscou 1968.

L'étude des marées de la Mer Jaune et de la Mer de Chine Orientale et la construction des cartes cotidales sont devenues le sujet de plusieurs travaux parmi lesquels les plus connus sont les travaux de Ogura et Dietrich [1, 2].

Parmi les recherches soviétiques sur cette région le travail le plus complet est celui de L.Y. Boris [3] consacré aux marées et aux courants de marée de la Mer Jaune.

Le travail de S. Ogura publié dès 1933 n'a pas perdu à présent sa valeur et répond à beaucoup de questions quant au caractère et aux processus de formation des oscillations de marée dans la Mer Jaune et dans la Mer de Chine Orientale. Les cartes cotidales de Ogura ne peuvent prétendre à une haute précision à cause de la petite quantité de données incorporées dans la réduction, ce que l'auteur lui-même indique.

L'erreur importante de ce travail est la méthode imparfaite de composition des cartes cotidales qui ont été établies sans tenir compte de la propagation des ondes de marées dans la mer libre, principalement la variation des heures cotidales près des rives. Cependant la carte générale des marées (la direction de la propagation de l'onde de marée, les valeurs des amplitudes des marées, la rotation des lignes cotidales autour des points amphidromiques) a été notée par Ogura et coïncide sûrement et complètement avec les schémas les plus avancés. Ogura donne des cartes cotidales uniquement pour les deux composantes M_2 et K_1. Tenant compte de leur exactitude en général il convient de montrer que la position des lignes cotidales est quand même nécessaire avec plus de précision. Les emplacements de beaucoup de points amphidromiques soulèvent le doute, notamment en ce qui concerne les amphidromes A, B et D pour l'onde semi diurne M_2.

Le travail de L.Y. Boris donne les cartes cotidales des ondes M_2 et K_1 et également les schémas des courants de marées d'écoulement pour la Mer Jaune établis par la méthode des valeurs limites.
Bien que les cartes cotidales de L.Y. Boris soient plus précises, éclairant de façon plus détaillée le schéma des mouvements de marées dans la Mer Jaune, certains détails de ce schéma sont litigieux. Les coordonnées de certains points amphidromiques éveillent aussi des doutes aussi bien sur la carte de la composante semi diurne, que sur la carte de l'onde diurne. La carte du caractère de la marée est également imprécise. En outre, le travail de Boris se limite à la surface de la Mer Jaune, en restant derrière les limites de la recherche des bassins de la Mer de Chine Orientale, un lien avec les phénomènes de marées est évident.

Avec l'augmentation de la quantité des données d'observations sur la côte et dans les îles des mers de Chine Orientale et Jaune on a constaté la possibilité d'établir des cartes plus précises et d'essayer de combler la lacune dans l'étude des phénomènes de marées de ce vaste bassin.

Ainsi, le problème de ce travail consiste dans l'établissement des cartes de marées pour les mers Jaune et de Chine Orientale sur la base des constantes harmoniques des points côtiers et insulaires dans le but d'éclaircir le caractère et les particularités des ondes de marées dans ces mers.

Pour établir les cartes cotidales on a employé la méthode des isohypses s'utilisant à maintes reprises pour les différentes mers et des océans et se justifiant tout à fait comme objective et assez précise [4].

La surface des mers Jaune et de Chine Orientale est idéale pour l'application de la méthode des isohypses. Elle est favorisée par la surface relativement petite des mers, la grande étendue de la ligne de côtes, la présence d'îles si bien que dans les deux mers il y a d'assez nombreux points avec des constantes harmoniques de la marée pour les composantes principales des ondes. La disposition des points permet de dessiner complètement tous les traits principaux du relief des marées.

Les constantes harmoniques des ondes M_2, S_2, K_1, O_1 tirées des tables de marées [5] ont servi de données de départ pour l'établissement des cartes. On a entré d'abord les constantes harmoniques pour 297 points situés sur la côte et les îles du bassin étudié. Pour la facilité des calculs toutes les données ont été ramenées à un système unique de calcul des angles de la position (g_{pp}). Lors du report sur la carte des points pris pour les calculs préliminaires il est apparu utile d'éliminer une série entière de points situés à une distance très proche l'un de l'autre et ayant des valeurs presque identiques pour les constantes harmoniques. Ainsi on a pris finalement dans la réduction les constantes harmoniques en 196 point.

Leur répartition est assez régulière mais leur réseau est assez raréfié sur le bassin Ouest en comparaison avec la côte Est (respectivement 75 et 113 points). Sur les îles, dans la partie libre de la surface étudiée, il y a 19 points de constantes harmoniques connues. Les données, obtenues sur les îles situées dans les parties les plus libres n'ont intentionnellement pas été prises dans la réduction afin de les utiliser pour estimer la régularité de l'établissement et de la précision des nouvelles cartes de marées. Pour que les cartes de marées soient comparables avec les cartes des autres régions de l'océan mondial et en particulier avec les cartes des régions contiguës, tous les calculs et l'établissement des cartes de marées ont été faits en temps solaire du méridien de Greenwich. Le calcul préliminaire de la hauteur du niveau pour chaque onde en particulier a été fait pour les conditions astronomoiques moyennes où les corrections, corrigeant la valeur des amplitudes et des phases étaient égales à B = c = 1 et b = c = o.

Pour construire les cartes des isoamplitudes on a utilisé les valeurs de la constante harmonique H (amplitude de l'onde) aux points situés sur la côte et dans les îles en tenant compte des valeurs nulles des amplitudes aux points amphidromiques.

Il est utile d'examiner préalablement les traits généraux dans la propagation de toutes les composantes des ondes de marées et ensuite les

particularités de propagation de chacune des composantes des ondes. Il convient d'abord de mentionner que dans notre travail on n'a pas examiné la propagation des ondes de marées et des oscillations de marées dans les baies peu profondes et les golfes déterminées principalement par les conditions locales. Les marées de la surface de niveau de la Mer Jaune ont un caractère progressivement vertical ce qui s'explique apparemment par la complexité des contours du bassin par rapport aux grandes chutes de profondeurs et se confirme par la présence d'une grande quantité de systèmes amphidromiques sur les cartes de marées des ondes M_2, S_2, K_1, O_1. On peut supposer que dans le bassin de la Mer Jaune les marées se forment par la réflexion de l'onde directe depuis la rive Nord et de l'interférence des ondes directes et réfléchies.

Pour expliquer les différentes particularités des marées de la Mer de Chine Orientale et de la Mer Jaune il est utile de comparer les schémas des ondes particulières (M_2, S_2, K_1 et O_1) simultanément avec des cartes plus anciennes des autres auteurs.

La carte de marée de l'onde M_2 (fig. 1) indique que cette onde provenant de l'océan, se propage dans la Mer de Chine Orientale partout comme une onde progressive, à l'exception de la région Sud Ouest c'est à dire de la région située au Nord Ouest de l'île de Taiwan où on observe une déformation de l'onde de marée sous l'influence du peu d'eau de la partie Ouest de la mer. Ici le schéma des lignes cotidales prend un aspect en éventail ce qui est caractéristique d'une onde complexe.

En quatre heures, c'est à dire avec une assez grande vitesse, l'onde M_2 coupe toute la Mer de Chine Orientale depuis le Sud Est jusqu'au Nord Ouest. La profondeur relativement grande de la partie Est du bassin et par conséquent la faible influence de la friction provoque incontestablement son déplacement si rapide. Lors de la comparaison de la nouvelle carte de marée de l'onde M_2 de la Mer de Chine Orientale avec les cartes cotidales faites précédemment par S. Ogura on ne découvre pas de différences de principe entre elles à l'exception d'une autre situation des lignes cotidales.

Le caractère de propagation de l'onde M_2 dans la Mer Jaune varie sensiblement. L'existence à la surface de la Mer Jaune de quatre systèmes amphidromiques en est le témoignage. L'onde de marée apparaissant dans ce bassin, venant de la Mer de Chine Orientale se déforme sous l'influence du peu d'eau du fond et du démembrement du trait de la rive, ce qui s'exprime par un caractère complexe progressivement vertical des oscillations. L'insignificance de la part de la composante progressive se maintient par rapport au petit déplacement des points amphidromiques depuis la ligne moyenne de la mer si on regarde en direction de la propagation de l'onde directe.

La variante proposée de la carte de marée ne donne pas de nouvelle interprétation de principe du caractère de propagation de l'onde M_2 dans la Mer Jaune mais la position de systèmes amphidromiques et particulièrement de leurs centres est très précisée et correspond bien aux caractéristiques observées des oscillations de marées. Ainsi la différence entre la position des points amphidromiques sur les cartes de L.Y. Boris et S. Ogura et également sur la nouvelle carte atteint en certains endroits (systèmes amphidromiques B et D) des valeurs d'environ 1°. Il convient de noter une concordance presque complète des coordonnées de l'amphidromie C dans les trois cartes mentionnées.

La carte de marée de l'onde S_2 (fig. 2) coïncide fort bien avec la

carte de l'onde M_2. La propagation de cette onde dans ces mers a le même caractère. Sur la carte de l'onde S_2 sont également situés quatre systèmes amphidromiques. Mais si la localisation de trois de ceux-ci, A, B et C correspond assez précisément avec la position des systèmes amphidromiques correspondants de l'onde M_2, par contre les coordonnées du quatrième (D) en diffèrent sensiblement. Préciser leur position par comparaison avec les cartes des autres auteurs n'est pas possible puisque cette carte a été faite ici pour la première fois.
L'analyse des cartes de marées des composantes diurnes, ondes K_1 et O_1 (fig. 3, 4), qu'il est utile d'examiner ensemble indique qu'elles sont moins compliquées que les cartes des ondes semi diurnes. Le caractère de propagation des ondes diurnes est le même que pour les semi diurnes. Cependant sur les cartes des ondes K_1 et O_1 les oscillations verticales ne se décèlent pas seulement dans la Mer Jaune et dans la Mer de Chine Orientale.
Cela se confirme par le fait que les systèmes amphidromiques Sud des ondes semi diurnes et des ondes K_1 et O_1 ne se trouvent pas à la même distance de la ligne moyenne de la mer : les points amphidromiques des ondes M_2 et S_2 sont situés plus à l'Ouest que les points relatifs aux ondes K_1 et O_1. Il s'ensuit qu'une partie de l'onde progressive est plus importante dans les oscillations semi diurnes que dans les diurnes.

Sur les cartes de marées des ondes K_1 et O_1 sont reportés les systèmes amphidromiques de la Mer Jaune. Leurs coordonnées pour l'onde K_1 correspondent presque exactement avec les coordonnées pour l'onde O_1.

La comparaison des nouvelles cartes de marées des ondes diurnes avec les cartes correspondantes des autres auteurs ne peut se faire que pour l'onde K_1, car nous ne disposons pas des cartes de l'onde O_1. La comparaison montre que la position des lignes cotidales dans la Mer de Chine Orientale sur la nouvelle carte correspond bien avec la carte de L.Y. Boris si on ne tient pas compte de certains détails de leur disposition. Lors de la comparaison de la position des lignes cotidales dans ce même bassin sur la nouvelle carte et sur la carte d'Ogura on relève une différence assez importante dans la position des points amphidromiques. Si les coordonnées du point amphidromique Nord correspondent assez bien sur les trois cartes et que les coordonnées du point amphidromique Sud concordent de façon satisfaisante sur la nouvelle carte et sur la carte d'Ogura, elles diffèrent sensiblement des coordonnées relevées sur la carte de L.Y. Boris. La différence aussi bien en latitude qu'en longitude atteint 0.5° ce qui constitue une importante différence si on prend en compte les dimensions relativement petites du bassin. Sur les nouvelles cartes de marées les isolignes des amplitudes des ondes correspondantes sont reportées en traits pointillés.

La réalité des cartes et leur précision a été vérifiée par des calculs préliminaires de contrôle des hauteurs du niveau pour huit points situés sur des îles dans les zones ouvertes du bassin. Ces points n'ont pas été pris en considération lors de l'élaboration des cartes de marées; ainsi certains se trouvent à une distance de plusieurs dizaines de miles des points les plus proches intervenant dans la réduction. Les calculs préliminaires ont été faits aussi bien pour chaque composante de marée que pour les oscillations totales.
Les courbes de l'allure du niveau aux points indiqués, précalculés à une date concrète selon les valeurs des constantes harmoniques, rele-

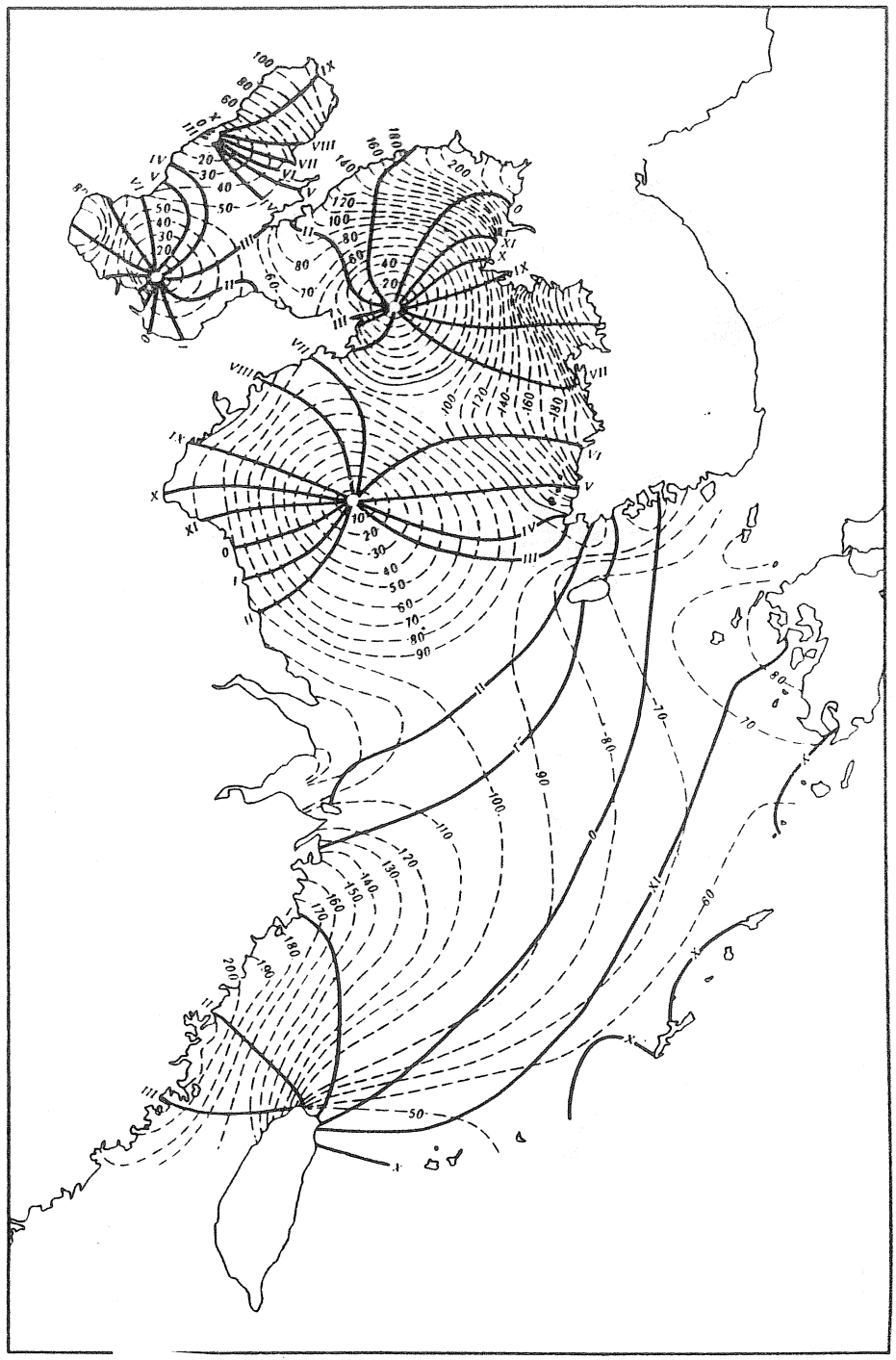

Figure 1 Carte de marée de l'onde M_2.

Les traits continus sont les isophases, les traits pointillés sont les isoamplitudes.

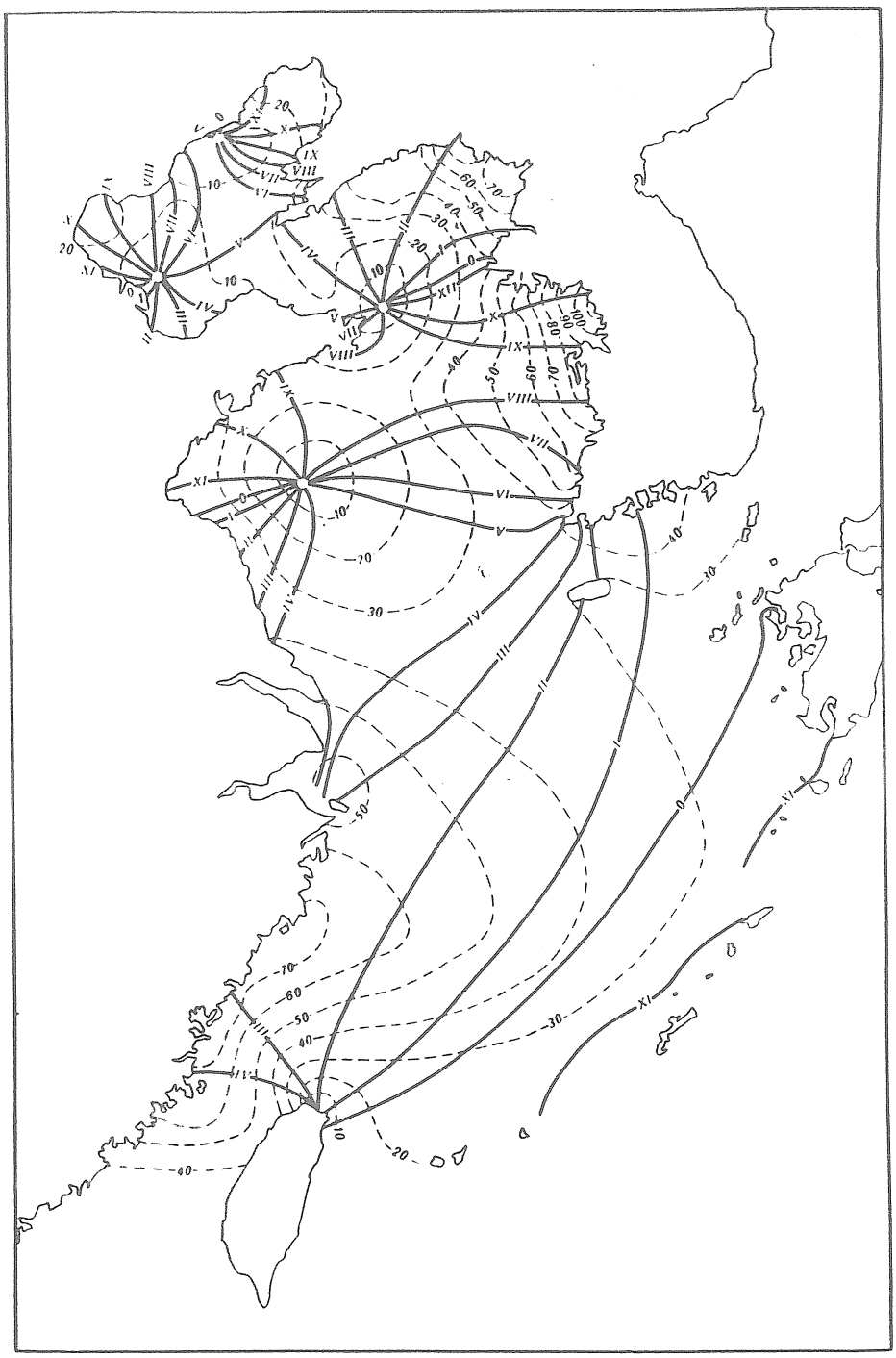

Figure 2 Carte de marée de l'onde S_2

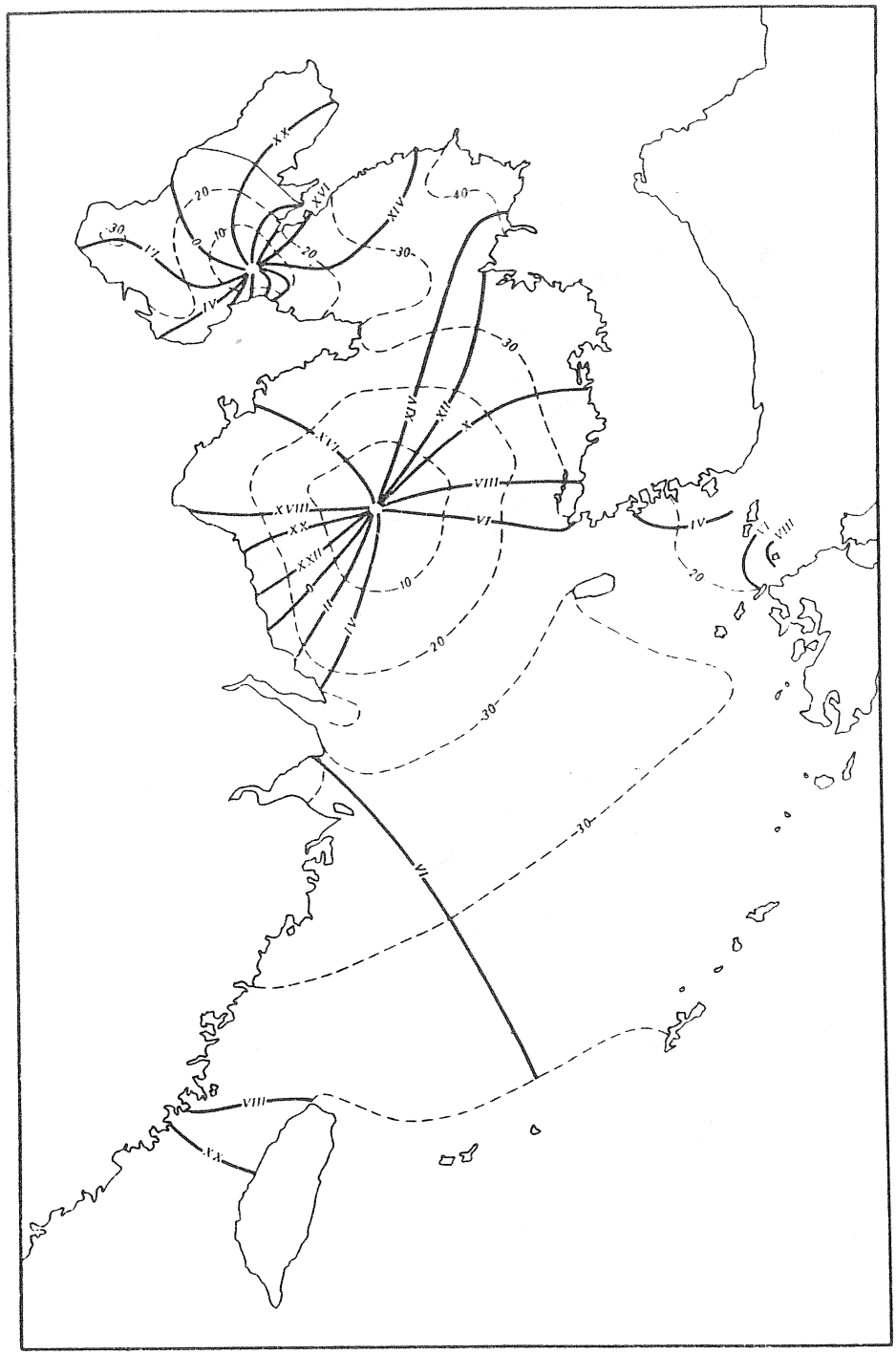

Figure 3 Carte de marée de l'onde K_1

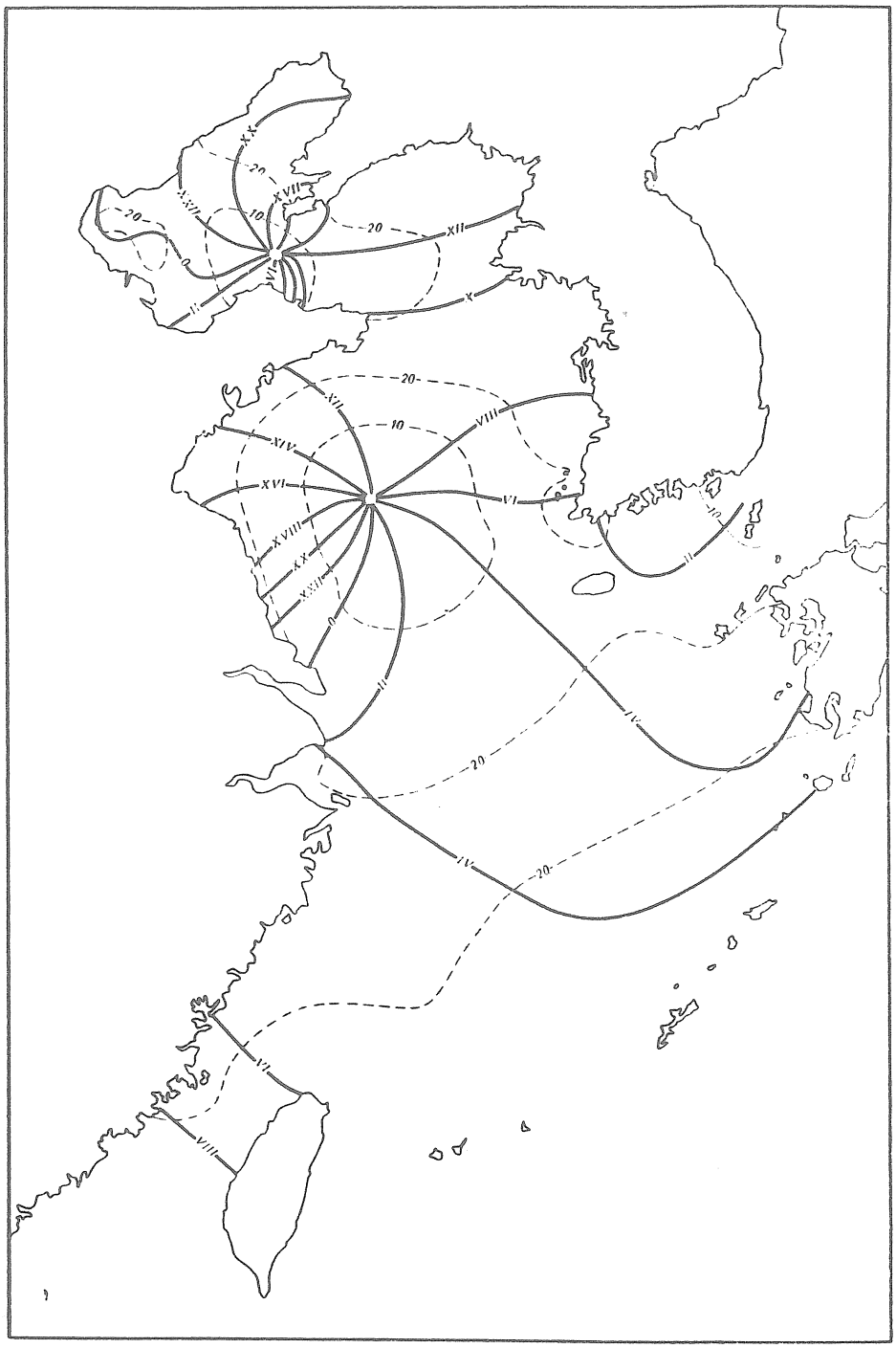

Figure 4 Carte de marée de l'onde O_1

vées depuis les nouvelles cartes de marées correspondent bien l'une avec l'autre (fig. 5). Un contrôle indépendant indique que leur précision est suffisamment élevée et elles peuvent être utilisées pour les calculs pratiques des hauteurs précalculées du niveau dans les parties ouvertes des mers, sur la rive et les îles là où il n'y a pas de série de constantes harmoniques. Dans ce cas le procédé de navigation du calcul des marées est tout à fait admissible.

Les cartes des isoamplitudes pour les ondes M_2, K_1 et O_1 donnent la possibilité de déterminer le caractère des oscillations de marées pour toute la surface des Mers Jaune et de Chine Orientale. Dans ce but la surface a été partagée en carrés de côté d'un degré. Pour le centre de chaque carré on a pris les valeurs interpolées des amplitudes (H) à partir des cartes des isoamplitudes pour les ondes M_2, K_1, O_1. Le caractère des oscillations de marées a été déterminé d'après la formule

$$\frac{H(K_1) + H(O_1)}{H(M_2)}$$

On a fait ensuite l'interpolation des valeurs calculées conformément aux critères numériques de la classification des marées de A.Y. Douvanine (0,5; 2,0; 4,0).

Il en résulte que les marées semi diurnes prédominent dans la Mer de Chine Orientale. Les marées sont sensiblement plus variées dans la Mer Jaune. On rencontre là tous les types connus jusqu'aux types anormaux, remarqués près des rives. Comme dans la Mer de Chine Orientale prédominent les marées semi diurnes imparfaites; bien que les marées avec composante diurne sensible se rencontrent également assez fréquemment. L'influence interférante des particularités morphométriques du bassin déterminant la disposition réciproque des systèmes amphidromiques et la relation des amplitudes des ondes diurnes et semi diurnes sert de facteur de solution lors de la détermination du caractère des marées dans la Mer Jaune.

Du fait que les positions des systèmes amphidromiques Sud des ondes diurnes et semi diurnes correspondent à peu près dans la partie Sud du bassin, les marées semi diurnes dominent. Il n'y a que dans la région Sud Ouest de la mer que sont sensibles les marées semi diurnes imparfaites ce qui se confirme relativement par les grandes valeurs des amplitudes des ondes diurnes et la diminution relative des amplitudes de l'onde M_2.

Le système amphidromique C des ondes semi diurnes s'applique sur un ventre des oscillations verticales diurnes. Il en résulte qu'à l'Est de l'île Shandoun on observe des marées non strictement semi diurnes mais dans le centre on observe également des ondes diurnes imparfaites. Un phénomène analogue se rencontre dans les deux Golfes du Nord, Liaotoung et Chihli (Po Hai) ou sur les systèmes amphidromiques A et B de l'onde M_2 se reporte également un ventre des ondes diurnes. Dans ces endroits apparaissent les marées non strictement diurnes et également les marées diurnes ainsi ces dernières sont notées sur une assez grande surface dans la région du système amphidromique A de l'onde M_2. Sur toute la surface restante de ces golfes les marées ont un caractère non strictement semi diurnes.

La comparaison de la nouvelle carte du caractère des marées ne réussit qu'à confirmer la carte analogue de L.Y. Boris pour la Mer

Jaune qu'elle précise (dans les travaux des autres auteurs il n'y a pas de cartes). Ainsi, sur le Sud du bassin le long du parallèle de 34° de latitude Nord il manque sur notre carte les zones avec des marées non strictement semi diurnes et par contre, la zone de ces marées découverte à l'Est de l'île Shandoun se propage vers le Sud suivant la longitude 122° Est jusqu'à 34° de latitude Nord ce qui n'est pas indiqué sur la carte de L.Y. Boris. Sur cette dernière manque également la zone de marées diurnes dans la région de l'amphidrome B pour l'onde M_2.

En outre on observe une certaine divergence dans la position des limites des autres zones du caractère des marées. Dans les régions de prédominance des marées semi diurnes et non strictement semi diurnes c'est à dire sur toute la surface de la Mer de Chine Orientale et sur la plus grande partie de la surface de la Mer Jaune, un grand rôle est joué par l'inégalité de phases pour laquelle les amplitudes maximales des marées s'observent dans les périodes de nouvelle Lune et de pleine Lune (marées de syzygie) et des amplitudes minimales dans les périodes de quadratures.

Dans les régions de prédominance des marées diurnes et non strictement diurnes, l'inégalité tropique a une grande valeur, cette inégalité résulte de la variation de la déclinaison de la Lune et du Soleil. Les petites valeurs des marées diurnes et non strictement diurnes s'observent pour une grande déclinaison de la Lune (marée tropique) et les valeurs faibles lors du passage de la Lune à l'équateur (marée équinoxiale).

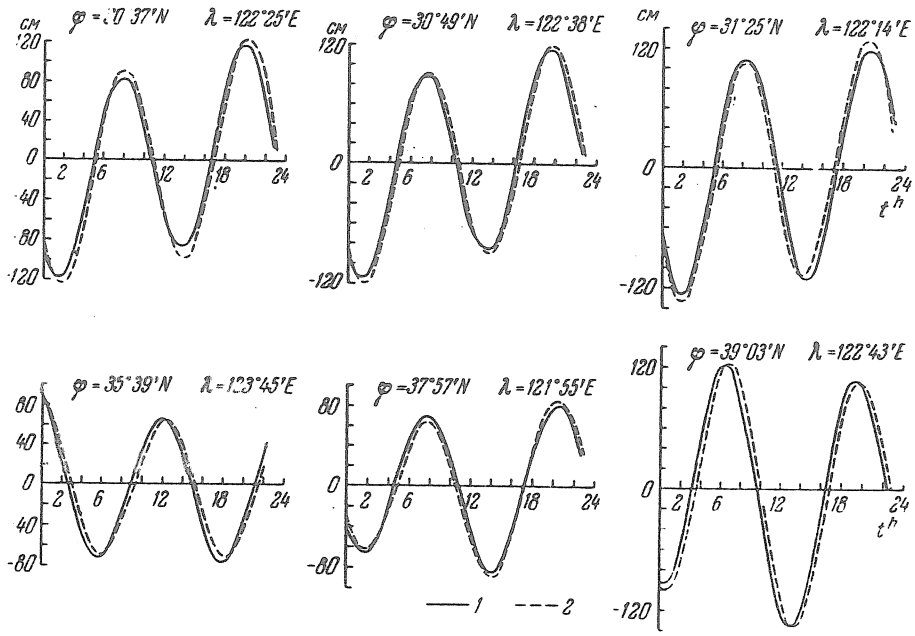

Figure 5 Courbes de l'allure diurne du niveau

1.- calculées d'après les constantes harmoniques publiées;
2.- d'après les constantes harmoniques relevées sur les cartes de marées.

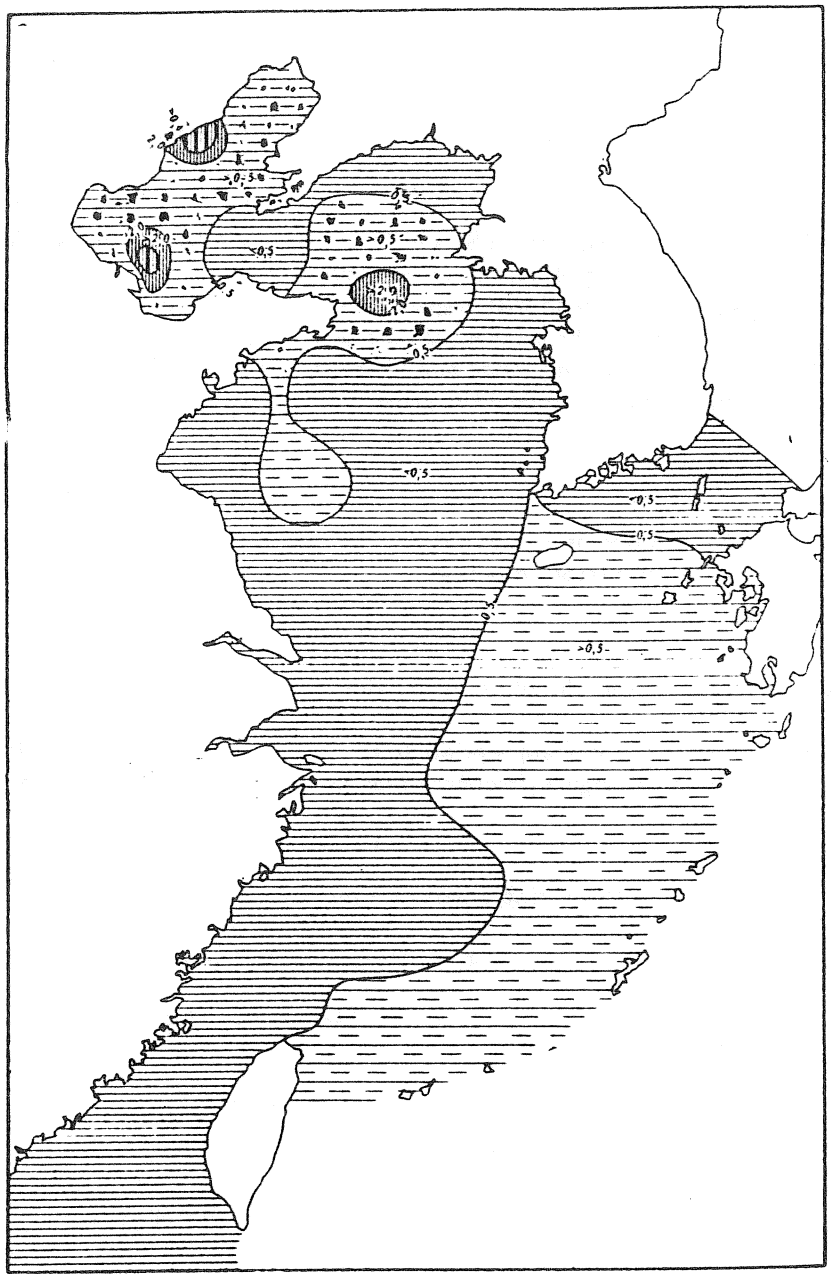

Figure 6 Carte du caractère de la marée

< 0,5 - marée semi diurne; > 0,5 à < 2,0 marée non strictement semi diurne; > 2,0 à < 4,0 marée non strictement diurne; > 4,0 marée diurne.

ЛИТЕРАТУРА

1. S. Ogura. The tides in seas adjacent to Japan.— Bull. Hydrogr. Dept., 7, Tokyo, 1933.
2. G. Dietrich. Die Schwingungssysteme der Halb und eintgigen Tiden in den Ozeanen.— Veröffentl. Inst. Meereskunde Univ. Berlin, A-41, 1—68, 1944.
3. Л. И. Борис. Расчет приливов и приливо-отливных течений для Желтого моря.— Труды ЛГМИ, вып. 7, 1958.
4. В. В. Тимонов. О кинематическом анализе приливов.— Труды ГОИН, вып. 37, 1959.
5. Таблицы приливов (зарубежные воды), ч. II. Л., Гидрометеоиздат, 1957.

THE LEAST-SQUARES AND THE WHITTAKER-ROBINSON-VONDRAK METHOD OF FILTER DESIGN IN THE COMPLEX DECONVOLUTION OF DATA SERIES

D.Djurović,Faculty of Mathematics,Studentski trg 16,11000 Belgrade

SUMMARY The least-squares (LS) and Whittaker-Robinson-Vondrak (WRV) method of filter design in the complex deconvolution of data series are analysed.

The advantages of the second with respect to the former one are: a) it may be applied to unequally spaced and weighted data series; b) the problem of data loose at both series ends,known in the LS method,does not exist; c) the condition of the amplitude and phase stability over the deconvolution subintervals is avoided.

In the frequency range examined the general formulae for the filter selectivity are found.

INTRODUCTION

Complex deconvolution is a classical method widely applied to study the amplitude and the phase variations of the quasi-oscillatory processes.

Let

$$x_t = A\cos(\lambda t + \alpha) \quad (1)$$

where the amplitude A and the phase α are slowly variable ("practically" constant) in the vincinity of t given.

The last assumption is well appropriate to the large percent of the observational series.Beside that,we remind here the variation of angular frequency may be attributed to the equivalent variation of the phase.So,for example, if

$$\lambda = \lambda_0 + \lambda_1(t),$$

where $\lambda_0 = const$ and $\lambda_1(t)$-a variable part of λ,instead of (1) we may write:

$$x_t = A\cos\{[\lambda_0 + \lambda_1(t)]t + \alpha\} =$$

$$= A\cos(\lambda_0 t + \alpha^*), \quad (1a)$$

where

$$\alpha^* = \alpha + t\lambda_1(t).$$

The process x_t may also be represented in the complex form:

$$x_t = \frac{1}{2}A[e^{i(\lambda t+\alpha)} + e^{-i(\lambda t+\alpha)}] \quad (2)$$

If the new series $\{y_t\}$ is computed by the formula:

$$y_t = x_t e^{-i\lambda t} \quad (3)$$

we say the series $\{y_t\}$ is obtained by the complex deconvolution of the series $\{x_t\}$.

From the equations (2) and (3) follows:

$$y_t = \frac{1}{2}Ae^{i\alpha} + \frac{1}{2}Ae^{-i(2\lambda t+\alpha)} \quad (4),$$

Therefore,by the complex deconvolution of an oscillatory process with angular frequency λ an another process with 2λ frequency is obtained.

The main idea in the complex deconvolution method is to extract the first term in (4).

Let by filtering of $\{y_t\}$ the second term in (4) is eliminated and the series of complex numbers

$$y_t^* = a + ib =$$

$$= 1/2Ae^{i\alpha} \qquad (5)$$

is obtained.

The *instantaneous* amplitude A and the phase α are:

$$A = (a^2 + b^2)^{1/2}$$

and

$$\alpha = arctg(b/a)$$

In the realisation of the above mentioned idea the essential technical problem is to construct the filter whoose output does not contain the "unwished" components, like the second one in (4).

By the classical, LS method of filter design this problem sometimes is not easy.

A linear filter, as we know, represents a set of positive numbers $\{W_t\}$ (weights) attributed to the input series $\{y_t\}$ such the output y_t^* is defined by the sum:

$$y_t^* = \sum_{u=r}^{s} W_u y_{t-u} \quad (6)$$

If r=-s and $W_u = W_{-u}$. the filter is known as a *symetric* one.Since this type of filters is mostly applied in astronomical practice, our attention in the present work will be devoted only to them.

According to (4) and (6) we may write:

$$y_t^* = \frac{1}{2} \sum_{u=-s}^{s} W_u[Ae^{i\alpha} + Ae^{-i(2\lambda t - 2\lambda u + \alpha)}] =$$

$$= \frac{A}{2}e^{i\alpha} \sum_{u=-s}^{s} W_u + \frac{A}{2}e^{-i(2\lambda t+\alpha)} \sum_{u=-s}^{s} W_u e^{i2\lambda u} \quad (7)$$

The function:

$$F(\omega) = \sum_{u=-s}^{s} W_u e^{-i\omega u} \quad (8)$$

($\omega = -2\lambda$) is known as the *transfer function* of the given filter.

In the case of symetric filter the imaginary terms vanish and,consequently

$$F(\omega) = W_0 + 2\sum_{u=1}^{s} W_u cos\omega u. \quad (9)$$

From (7) is clear the task of filter design consists in the search for the transfer function $F(\omega)$ making y_t^* sufficiently close to zero for ω of all "unwished" components and the well defined *the amplitude gain-factor*

$$G = \frac{1}{2} \sum_{u=-s}^{s} W_u.$$

The simplest type of filters are *low-pass* filters,sometimes called *cut-off* or *one-side* filters.For this type of filter the ideal transfer function is:

$$F_i(\omega) = \begin{cases} 1; 0 < \omega \leq \omega_c \\ 0; \omega_c < \omega \leq \pi \end{cases}$$

where ω_c and $P_c = 2\pi/\omega_c$ are *cut-off frequency* and *cut-off period.*

When the function $F(\omega)$ is known,the data filtering implies the determination of the weights W_u (see eq.6).The LS procedure starts from the idea:

$$\int_{-\pi}^{\pi} [F_i(\omega) - F(\omega)]^2 d\omega =$$

$$= \int_{-\pi}^{\pi} [F_i(\omega) - \sum_{u=-s}^{s} W_u cos\omega u]^2 = minimum$$

This idea leads to the solutions:

$$W_u = 1/\pi \int_0^{\omega_c} cos\omega u d\omega =$$

$$\frac{sin\omega_c u}{\pi u}; u \geq 1 \quad (9)$$

and

$$W_0 = \frac{\omega_c}{\pi}; u = 0$$

Since $F(\omega)$ has a pronounced overshoot with respect to $F_i(\omega)$ on either side of ω_c (*Gibbs's phenomenon*) and the subsidary ripples whoose amplitude decreases with ω increasing,Lanczos (1961) proposed how to overcome this problem by the introducing the weight corrections C_u, called *the convergence factors*:

$$C_u = \frac{sin\frac{2\pi u}{2s+1}}{\frac{2\pi u}{2s+1}} \quad (10)$$

So,the weights W_u in (6) need be replaced by

$$W_u^* = C_u W_u \qquad (11)$$

and the transfer function $F(\omega)$ by:

$$F^*(\omega) = W_0^* + 2\sum_{u=1}^{s} W_u^* cos\omega u \quad (12)$$

In fact,$F^*(\omega)$ represents an approximation (by the Fourier polynome) of the modified (smoothed) transfer function $F_s(\omega)$ deduced from $F_i(\omega)$ where the vertical fall at $\omega = \omega_c$ is replaced by the linear decay from 1 at $\omega = \omega_c - \frac{2\pi}{2s+1}$ to 0 at $\omega = \omega_c + \frac{2\pi}{2s+1}$ (Bloomfield 1974).

THE SELECTIVITY OF LEAST-SQUARES AND WHITTAKER-ROBINSON-VONDRAK FILTERS

When the series $\{y_t\}$ contains two or more processes whoose frequencies are close,the quality of data filtering depends on the filter selectivity and,indirectly, on the accuracy of the $F_s(\omega)$ approximation. Since $\{W_u^*\}$ are the coefficients in the Fourier polynome for $F_s(\omega)$,it may easily be proven that the accuracy of the approximation increases with the increasing of s (see,for example,Smirnov 1974).Instead of proof,in Fig.1 are illustrated $F_i(\omega)$ and $F^*(\omega)$ for P_c=11 and s=5,15,25 and 35.

From the above discussion and Fig.1 seems that we have an interest to take s as large as possible.However,we also need to have in mind that the computation of the series $\{y_t^*\}$ is followed by the loose of s data at both ends of the series $\{y_t\}$.Therefore,over subintervals $t \leq s$ and $t \geq n - s$ we are unable to observe how A and α change.Beside that. the choice of s is related with the assumption that A and α are constant inside the subintervals of s data.

From the equations (9)-(12) is evident that ω_c is a second parameter which defines $F^*(\omega)$.Therefore,$F^*(\omega)$ represents the s filter families (one family has the same s and different ω_c). Let absolute deviations of the real transfer function from the ideal one be

$$\delta = |F^*(\omega) - F_i(\omega)|$$

and δ_{tol} the limit of δ tolerated (if $\delta \leq \delta_{tol}$, $F^*(\omega)$ is considered "practically" equal to $F_i(\omega)$).

The selectivity of filter is usually defined by the width of range $\omega \in (\omega_1, \omega_2)$ where $\delta > \delta_{tol}$;it is inverse to $D\omega = \omega_2 - \omega_1$.

To see is there any common in different families of $F^*(\omega)$,we have examined how the *relative selectivity*,defined as $R = DP/P_c$ (DP-the period span where $\delta > \delta_{tol}$), changes in function of $r = s/P_c$.

In Fig.2 are represented the curves $R = R(r)$ for P_c=5.5,11,88 and 176 and δ_{tol}=0.05 (upper curve),0.10,0.15,0.20 and 0.30 (lower curve).The full lines are their LS approximations by the power function:

$$\hat{R}(r) = Qr^q \qquad (13)$$

From the Fig.2 seems that the shape of any curve mainly depends on δ_{tol}.How many this assumption holds we can verify by the results obtained for Q and q (Table 1).Since Q and q practically do not change in function of P_c (in the range of P_c analysed) the mentioned assumption may be accepted as a rule.Beside that,the mean values of Q and q for δ_{tol} given may be accepted as the best approximations.

From the results in Fig.2 and the above discussion concerning the accuracy of $F_s(\omega)$ approximation is clear that high selectivity of LS filter must be paid by the great loose of data accompained by the risk of important variations of A and α.Beside that,the LS method may be applied only if data are equally spaced and weighted:this restriction provides from the fact that $\{W_u\}$ are the coefficients of Fourier polynome. If the above mentioned lacks make the LS method unappropriate,it worth to examine whether the method of data smoothing proposed by Whittaker and Robinson (1946),later extended by Vondrak (1969;1977) on unequally spaced and weighted data, may be useful.This method is developed on the principle:

$$\sum_i (f_i - \hat{f}_i)^2 + \epsilon^{-2} \sum_i (\delta^3 \hat{f}_i)^2 = minimum \qquad (14)$$

where ϵ is the parameter choosen according to the wished level of smoothing,f_i, $\hat{f}_i$-raw and smoothed values of a function $f(t)$ and $\delta^3 \hat{f}_i$-the third order differences of $\hat{f}_i$.

The system of linear equations corresponding to (14) and other details about its solution are well explained in Vondrak (1969;1977).From the practical raisons their reproduction in this paper is missed (even a concise form contains too equations and inevitable coments).

Let the series $\{f_i\}$ has a sinusoidal component whoose amplitude is A and the period P. After the WRV smoothing of $\{f_i\}$ the amplitude of the output sinusoid will be $\bar{A}$, defined by the formula of Kun-Yi and Zhou (1981):

$$\bar{A}/A = G = \frac{\epsilon P^6}{64\pi^6 + \epsilon P^6} \qquad (15)$$

Since the gain factor G is a function of the period P (or frequency) by the smoothing we attempt a selective filtering of data.Varying the parameter ϵ we obtain a family of filters whoose performances are illustrated in Fig.3.

The selectivity of the WRV filters is the main practical question which need be well understood before we decide what kind of filter will be applied to the series $\{f_i\}$.

Let G_1 and G_2 the values of gain-factor G for ϵ given and the periods P_1 and P_2,respectively.If $G_1 = \delta_{tol}$ and $G_2 = 1 - G_1$, from (15) follows:

$$R_{WRV} = \frac{DP}{P_m} = \frac{2(k-1)}{k+1}, \qquad (16)$$

where

$$k = \left(\frac{1 - \delta_{tol}}{\delta_{tol}}\right)^{1/3}$$

and $P_m = \frac{1}{2}(P_1 + P_2)$.

From the above equations follows *the relative selectivity of any WRV filter is independent neither the ϵ nor the frequency.*

When the approximation of $F_s(\omega)$ by the polynome (12) is sufficiently accurate,from the definitions of $F_i(\omega)$ and $F_s(\omega)$ follows that P_m must be close to P_c.So,by the simple computation $\hat{R}$ and R_{WRV} from (13) and (16) (taking $P_c = P_m$) we can compare the selectivity of two filter type.

The WRV method can also be applied for the narrow band-pass filter design.

Let A_0 and P_0 be the amplitude and the period of an oscillatory process wich we wish to extract from the series $\{y_t\}$.With $G = G_1$ arbitrary choosen,positive and close to zero,and P_0 given,by the formula (14) one detrmine the smoothing parameter $\epsilon = \epsilon_1$.In the smoothed series $\{\hat{y}_i\}$ all oscillatory processes with the periods $P_i \leq P_0$ are damped:their amplitudes are reduced by the factors $G \leq G_1$.Therefore, in the residuals $Dy_i = y_i - \hat{y}_i$ they are "practcally" saved.

In the second step,by the smoothing of the residuals Dy_i with $\epsilon = \epsilon_2$,computed with the gain factor G_2,now close to 1,and $P = P_0$ one obtains the series $\{D\hat{y}_i\}$ in which the oscillatory process with the period P_0 is saved.So,by the double WRV smoothing the narrow band-pass filter,centered at given period P_0,may be realised.

The selectivity function of the above type of filter is:

$$G = (1 - G_1)G_2$$

As an example, in Fig.4 is illustrated the selectivity curve corresponding to $P_0 = 10, G_1 = 0.05$ and $G_2 = 1 - G_1$.

Since the selectivity functions $G = G(\epsilon, P_0)$ are not ideal,like the Dirac's function $\delta(P - P_0)$,neither the residuals Dy_i nor the residuals $D\hat{y}_i$ are free the reminders of other components whoose periods lie at both sides of P_0.Therefore, the high quality of filtering may be attempted if the periods of oscillatory processes in $\{y_t\}$ are not too close to P_0 and if their amplitudes are not too large with respect to A_0.

CONCLUSIONS

The WRV method of filter design is more general than the LS method:it may be applied on equally as well as on unequally spaced and weighted data series. Beside that,it is free of the data loose at ends of data series:in LS method it is important if the high filter selectivity is needed.Yet one advantage of the WRV method ought to be pointed out:WRV filters have the "instantaneous" reaction.Namely, any $\hat{y}_i$ is updated over 4 successive data:the method is based on the interpolation by the 3-rd order Lagrange polynome and the computation of its 3-rd order derivative over subintervals (t_i, t_{i+3}). So, the hypothesis (A, α)=const need be satisfied over these subintervals.

The relative selectivity of low-pass LS filters may be accurately approximated by the power functions (13), while in the case of WRV filters it is independent neither the smoothing parameter ϵ, nor the frequency.

TABLE 1

The coefficients Q and q of the power function which approximates the relative selectivity of LS filters

δ_{tol}:	0.05		0.10		0.15	
P_c	Q	q	Q	q	Q	q
5.5	1.111	-1.102	0.846	-1.048	0.696	-1.055
11.0	1.146	-1.112	0.877	-1.062	0.728	-1.076
22.0	1.214	-1.157	0.915	-1.095	0.755	-1.103
44.0	1.214	-1.153	0.918	-1.092	0.769	-1.116
88.0	1.244	-1.174	0.955	-1.127	0.777	-1.124
176.0	1.220	-1.156	0.924	-1.097	0.780	-1.130

mean	1.192	-1.142	0.906	-1.087	0.751	-1.101
σ_1	0.051	0.029	0.038	0.028	0.033	0.029

δ_{tol}:	0.20		0.25		0.30	
P_c	Q	q	Q	q	Q	q
5.5	0.548	-1.014	0.431	-0.985	0.330	-0.972
11.0	0.576	-1.042	0.453	-1.017	0.348	-0.999
22.0	0.595	-1.065	0.466	-1.037	0.357	-1.019
44.0	0.604	-1.079	0.473	-1.049	0.362	-1.028
88.0	0.609	-1.082	0.476	-1.052	0.364	-1.032
176.0	0.612	-1.086	0.478	-1.055	0.365	-1.034
mean	0.591	-1.061	0.463	-1.032	0.354	-1.014
σ_1	0.025	0.028	0.018	0.027	0.013	0.024

REFERENCES

Bloomfield P.:1976,*Fourier Analysis of Time Series:An Introduction*, J.Wiley & Sons,New York.
Kun-Yi H.,Zhou X.:1981,Acta Astronomica Sinica **23**,3,286.
Smirnov V.I.:1974,*The Advanced Mathematics*,tome II,p.454,"Naouka",Moscou.
Vondrak J.:1969,Bull.Astron.Inst.Czechoslovakia **20**,349.
Vondrak J.:1977,Bull.Astron.Inst.Czechoslovakia **28**,84
Whittaker E.,Robinson G.:1946,*The Calculus of Observations*,Monograph (4-th ed),Blackie and Son,London.

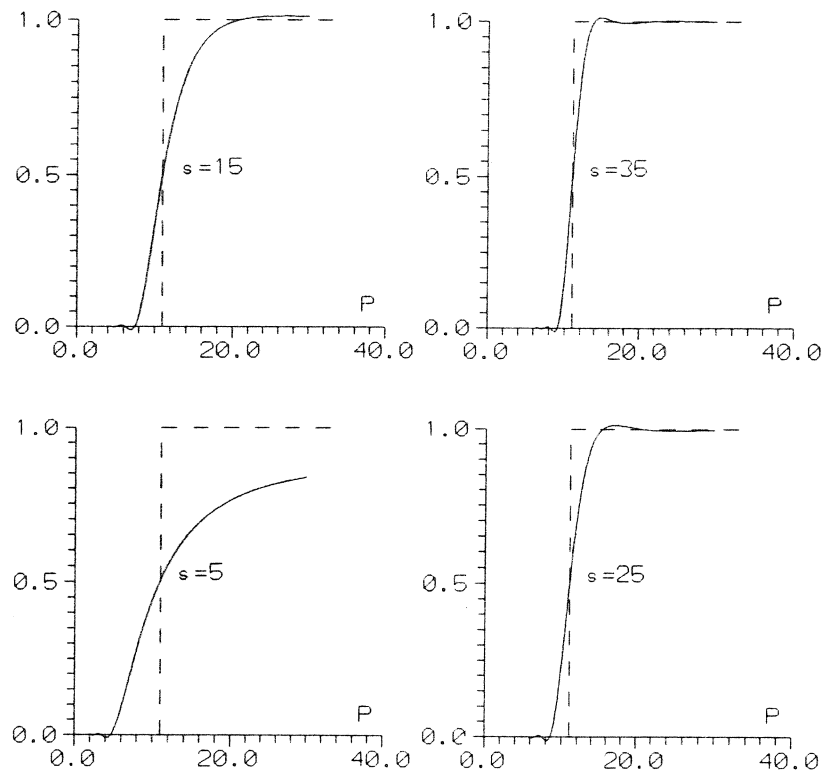

FIG.1

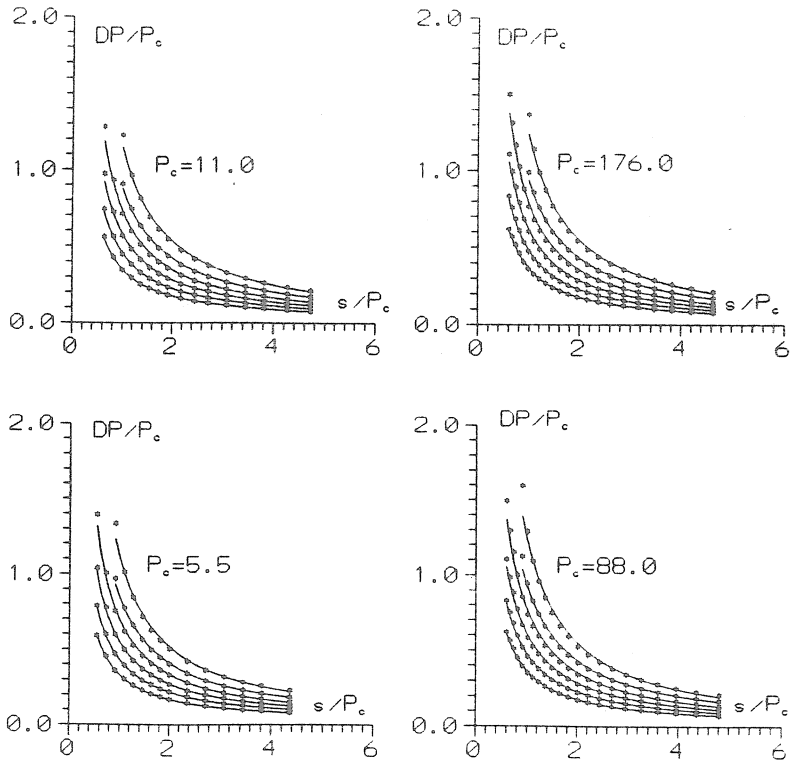
2.0
1.0
0.0
DP/Pc
Pc=11.0
s/Pc
0
2
4
6
Pc=176.0
Pc=5.5
Pc=88.0

FIG.2

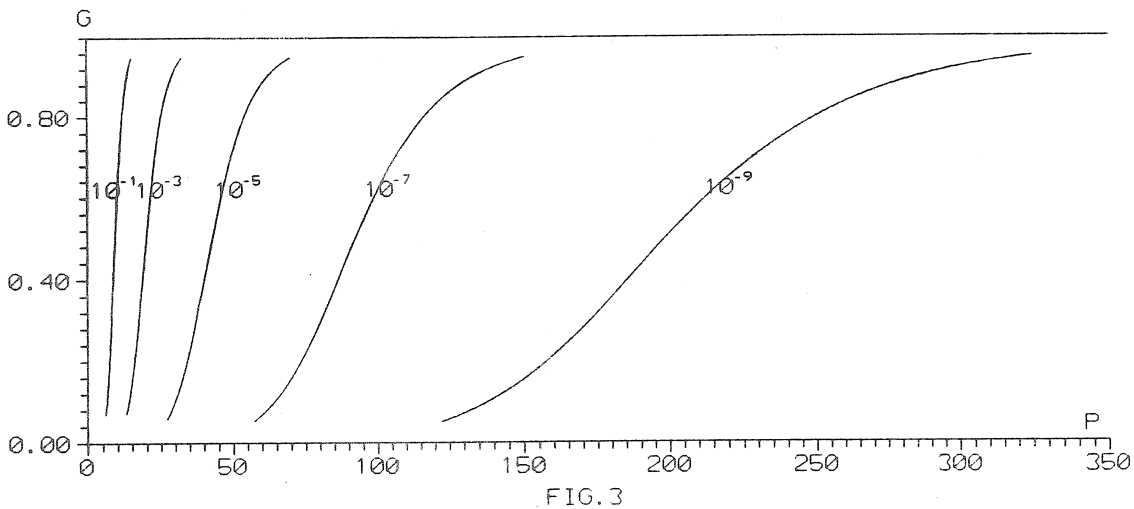
G
0.80
0.40
0.00
10-1
10-3
10-5
10-7
10-9
P
0
50
100
150
200
250
300
350

FIG.3

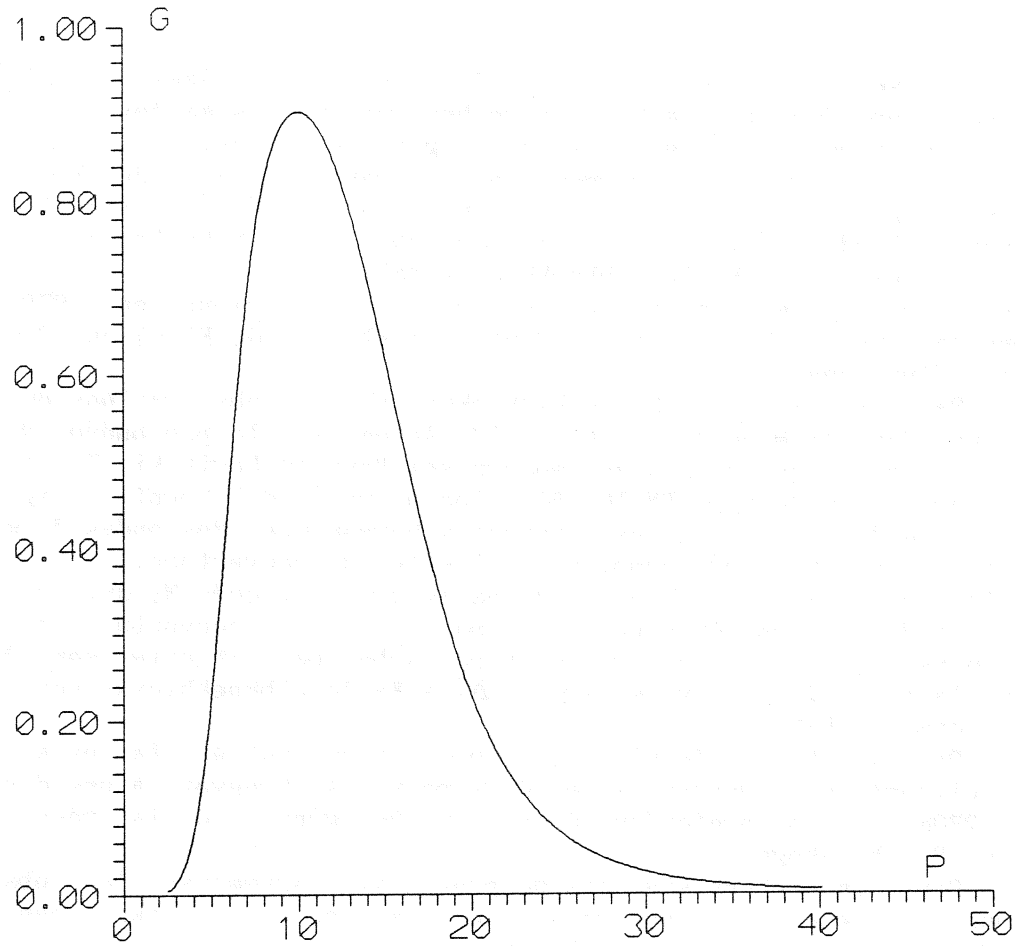

FIG. 4

Traduction

Observations des marées terrestres par l'Observatoire gravimétrique de Poltava suivant un profil Kiev-Artemovsk

V.G. Balenko, A.M. Koutnii, V.G. Boulatsen
Observatoire gravimétrique de Poltava
Institut de Physique Soubbotine
de l'Académie des Sciences d'Ukraine

Prévision des tremblements de Terre N° 8 pp 158-166 - 1988

L'Observatoire Gravimétrique de Poltava situé dans la région du fossé Dniepr-Donetz effectue des recherches sur les marées terrestres sous deux aspects : clinométriques et gravimétriques.

Les observations clinométriques suivant le profil de Kiev-Artemovsk (fig. 1) sont à présent terminées en six points : Kiev [1], Beresovaïa Roudka [2], Pokrovskaïa Bagatehka [3], Schevtchenkovo [4], Katerinovka [5] et Karlo-Libknekhtovsk [6].
Les travaux y ont commencé en 1963 et se sont terminés en 1979. Les observations en chaque station (outre la station de Kiev) ont duré pas moins d'une année.

Dans la station de Karlo-Libknekhtovsk les observations ont été faites dans la mine de sel N° 1 II/o Artemsol à la profondeur de 120m avec des pendules horizontaux modernisés Repsold-Levitski [7] et avec des appareils du type RMIIO [8] selon un petit microprofil (fig. 2). Outre la détermination des constantes harmoniques des ondes de marées on a réalisé une étude complexe de l'effet de couverture.
Le facteur d'amplitude γ et le déphasage $\Delta\varphi$ de l'onde M_2 qui, en théorie, ne doivent pas être perturbés par l'effet de couverture sont donnés dans la table 1. Ceux qui sont perturbés par cet effet sont donnés dans la table 2. Les valeurs γ et $\Delta\varphi$ à Karlo-Libknekhtovsk sont données dans la table 3.

Dans la station de Kiev, les observations ont été faites à l'aide de clinomètres d'Ostrovskii en deux points se trouvant à une distance de 270m, à une profondeur d'environ 15m (grottes de la réserve de Lavro-Petcherskogo).

Dans les autres stations du profil Kiev-Artemovsk les observations ont été réalisées par les clinomètres d'Ostrovskii dans des mines à une profondeur de 12 à 16m.
Les résultats obtenus pour l'onde M_2 après introduction de toutes les corrections nécessaires [10] sont donnés dans la table 3 pour toutes les stations du profil.

Des recherches clinométriques suivant le profil Kiev-Artemovsk on a tiré les résultats principaux suivants :

1. On a déterminé pour ce territoire d'une étendue de plus de 600 km les paramètres régionaux de la marée élastique γ et $\Delta\varphi$ avec une erreur ne dépassant pas 0,5 %.
   On a élaboré une méthode pour ces recherches [10].

2. On a confirmé qualitativement les conclusions principales de la théorie de l'effet de couverture [9].

3. On a déterminé les conditions du relief de l'endroit lors de l'établissement des stations clinométriques dans le but de déterminer les paramètres régionaux de la marée élastique [11].

Depuis 1977, l'Observatoire Gravimétrique de Poltava effectue des observations clinométriques pour contrôler l'affaissement de la surface de la Terre sur les excavations minières à Karlo-Libknekhtovsk [12]. Les clinomètres d'Ostrovskii ont été placés dans les mines à une profondeur de 6m suivant les bords d'une zone fortement éboulée (fig. 3). Les résultats préliminaires de l'analyse harmonique sont donnés pour l'onde M_2 dans la table 4. Il s'ensuit que les relâchements technogéniques de l'écorce terrestre perturbent sensiblement la valeur du facteur dans la direction nord-sud. Le signe des perturbations correspond à la théorie de cet effet.

Les observations des marées de la pesanteur à Poltava qui est situé au centre du fossé Dniepr-Donetz, ont commencé en 1955 et se poursuivent. On peut les répartir en quatre étapes d'après la précision atteinte (table 5).

A la suite des recherches instrumentales faites de 1974 à 1978 [13, 14] on a établi que les appareils Askania GS 11 et 12 peuvent introduire dans le facteur d'amplitude déterminé δ une erreur systématique atteignant 2 %, à cause de l'imperfection de construction du micromètre. Pour l'éliminer on a élaboré une nouvelle méthode de mesure de la sensibilité du gravimètre [13, 14].

En utilisant cette méthode, en 1980-1981 (quatrième étape de la table 5) on a réalisé avec l'appareil Askania GS 12 n° 185 une série d'un an et demi d'observations des marées à l'Observatoire de Poltava. Les constantes harmoniques des ondes de marées obtenues par cette série sont donnés dans la table 6.

Des observations des variations de la pesanteur à Poltava on peut tirer les conclusions principales suivantes :

1. Les résultats des observations avec les gravimètres Askania GS 11 et 12 renferment une certaine erreur systématique lors de la mesure de leur sensibilité par le micromètre. Il faut donc les utiliser avec beaucoup de précautions. Dans la suite il a fallu considérer cette méthode de détermination de l'échelle d'enregistrement comme non utile.

2. La nouvelle méthode de détermination de la sensibilité des gravimètres Askania GS 11 et 12 utilisée à l'Observatoire de Poltava n'élimine pas seulement l'erreur systématique introduite par le micromètre mais augmente aussi sensiblement la précision de détermination des paramètres de la marée élastique (tables 5 et 6). Les nombres de Love déterminés par ces observations diffèrent des valeurs théoriques tout au plus de quelques pourcents (table 7).

3. Les constantes harmoniques des ondes de marées obtenues par les observations en 1980-1981 (table 6) doivent être considérées comme représentatives pour Poltava et le fossé Dniepr-Donetz.

Table 1

Constantes harmoniques de l'onde M_2 obtenues par les observations clinométriques dans la mine n° 1 m/o Artemsol (station Karlo Libknekhtovsk) dans les salles 2, 3, 4 dans les directions affranchies de l'effet de couverture.

Salle	Socle	Nord - Sud		Salle	Socle	Ouest - Est	
		γ	$\Delta\varphi^\circ$			γ	$\Delta\varphi^\circ$
2	-	0,696	+2,70	2	-	0,717	-3,16
		±0,004	±0,25			±0,004	±0,26
3	1	0,679	-2,89	3	1	0,714	+0,16
		±0,004	±0,21			±0,006	±0,32
	2	0,679	-1,56	4	4	0,720	-1,04
		±0,006	±0,52			±0,005	±0,40
	3	0,699	-0,91				
		±0,007	±0,55				
Moyenne		0,688	-0,32			0,718	-1,11
Vectorielle		±0,004	±1,26			±0,004	±1,30

Table 2

Constantes harmoniques de l'onde M_2 obtenues par les observations clinométriques dans la mine n° 1 m/o Artemsol (station Karlo Libknekhtovsk) dans les salles 1, 3, 4 dans les directions affranchies de l'effet de couverture.

Salle-pa	Socle-MeHT	Nord - Sud		Salle-pa	Socle-MeHT	Ouest - Est	
		γ	$\Delta\varphi^\circ$			γ	$\Delta\varphi^\circ$
1		0,476	-1,38	1		0,682	0,00
		±0,005	±0,47			±0,004	±0,52
				3	2	0,665	+2,01
						±0,010	±0,90
					3	0,700	-3,03
						±0,007	±0,61
4	4	0,814	-1,32				
		±0,007	±0,51				
	6	0,641	-0,13				
		±0,006	±1,24				

Table 3

Facteurs d'amplitude γ et phase $\Delta\varphi$ pour les stations clinométriques du profil Kiev-Artemovsk

Stations	Nord - Sud		Ouest - Est	
	γ	$\Delta\varphi°$	γ	$\Delta\varphi°$
Kiev	0,704±0,026	+1,62±2,26	0,718±0,046	-5,48±2,51
B. Roudka	0,712±0,005	-1,20±0,78	0,718±0,005	-4,23±0,51
P. Bagatchka	0,684±0,008	-1,00±0,62	0,717±0,008	-4,90±0,74
Schevtchenkovo	0,699±0,008	+0,57±1,01	0,710±0,007	-4,18±1,08
Katerinovka	0,689±0,009	-1,12±0,94	0,714±0,006	-0,53±0,48
Karlo-Libknekhtovsk	0,688±0,003	-0,32±1,26	0,718±0,003	-1,11±1,39
Moyenne Vectorielle	0,6936 ±0,0044	-0,52 ±0,24	0,7163 ±0,0013	-2,19 ±0,73

Table 4

Résultats de l'analyse harmonique des inclinaisons de marées dans la zone fortement éboulée de Karlo-Libknekhtovsk

Mine	Nord - Sud		Ouest - Est	
	γ	$\Delta\varphi°$	γ	$\Delta\varphi°$
N° 1	0,563 ± 0,034	-1,0 ± 2,4	0,737 ± 0,016	-5,7 ± 2,4
N° 2	0,506 ± 0,024	-2,9 ± 2,4	0,705 ± 0,012	-5,8 ± 1,4
N° 4	0,761 ± 0,025	-3,4 ± 1,7	0,744 ± 0,013	-4,6 ± 0,8

Table 5

Constantes harmoniques de l'onde M_2 tirées des observations des variations de marées à Poltava.

Appareils	Opérateur	Moniteur	Durée des observations	δ	$\Delta\varphi^\circ$
1 Граф-2	Z.N. Aksentieva B.A. Sokolov	Z.N. Aksentieva	8.09.55 - 4.11.55	1,17	-8,9
2 G_s -11 № 159	J.A. Ditchko	Z.N. Aksentieva	6.11.61 - 1.01.64	1,182 ± 0,005	0,80 ± 0,20
3 G_s -11 № 159	V.G. Balenko V.G. Boulatsev	V.G. Balenko	27.12.73 - 24.12.74	1,1800±0,0024	0,33 ± 0,12
			25.09.74 - 29.09.75	1,1943±0,0020	0,38 ± 0,10
	P.S. Korba J.A. Ditchko		16.11.75 - 26.12.76	1,2016±0,0024	0,57 ± 0,11
			25.11.73 - 13.04.74	1,1801±0,0059	0,08 ± 0,21
G_s -12 № 185	V.P. Schliakhovii		8.01.76 - 26.11.76	1,2003±0,0029	0,28 ± 0,14
4 G_s -12 № 185	V.G. Balenko V.G. Boulatsev A.N. Novikova	V.G. Balenko	21.04.80 - 30.09.81	1,1749±0,0010	-0,47 ± 0,05

Remarque : on a introduit les corrections au retard instrumental, d'inertie et à la normale ellipsoïdale.

Table 6

Paramètres δ et $\Delta\varphi$ tirés des observations des variations de la pesanteur à Poltava (1980-1981)

Ondes	δ	$\Delta\varphi$
Q_1	1,1421 ± 0,0108	-0,40 ± 0,54
O_1	1,1521 ± 0,0021	-0,13 ± 0,11
M_1	1,1834 ± 0,0216	-3,01 ± 1,05
P_1	1,1385 ± 0,0040	-0,15 ± 0,20
K_1	1,1319 ± 0,0014	-0,24 ± 0,07
J_1	1,1376 ± 0,0247	0,96 ± 1,25
OO_1	1,1052 ± 0,0614	-5,61 ± 2,75
$2N_2$	1,1836 ± 0,0530	-1,73 ± 1,33
N_2	1,1595 ± 0,0052	-0,91 ± 0,26
M_2	1,1749 ± 0,0010	-0,47 ± 0,05
L_2	1,2831 ± 0,0491	-9,08 ± 2,20
S_2	1,1668 ± 0,0022	-0,77 ± 0,11
K_2	1,1567 ± 0,0098	-1,16 ± 0,48
M_3	1,072 ± 0,054	1,46 ± 2,88

Remarque : on a introduit les corrections de retard instrumental, d'inertie, à la normale ellipsoïdale et de la nutation forcée de la Terre

Table 7

Nombre de Love k calculé d'après les observations des variations de marées à Poltava en 1980-1981 en tenant compte des corrections de l'influence des zones lointaines de la marée océanique [15] et leurs analogies théoriques.

Ondes	Calculées d'après les observations			Théoriques		
	1	M	W	1	M	W
M_2	0,303	0,289	0,306	0,307	0,302	0,284
O_1	0,298	0,285	0,298	0,305	0,300	0,283
K_1	0,258	0,247	0,256	0,260	0,261	0,241

Remarque : le nombre de Love k dans les colonnes 1, M et B est calculé d'après les rapports h/k pour le modèle de Terre 1 de Molodenski et 1066 A et PEM - C (d'après J.M. Wahr [16]).

Figure 1 Schéma du profil de Kiev-Artemovsk

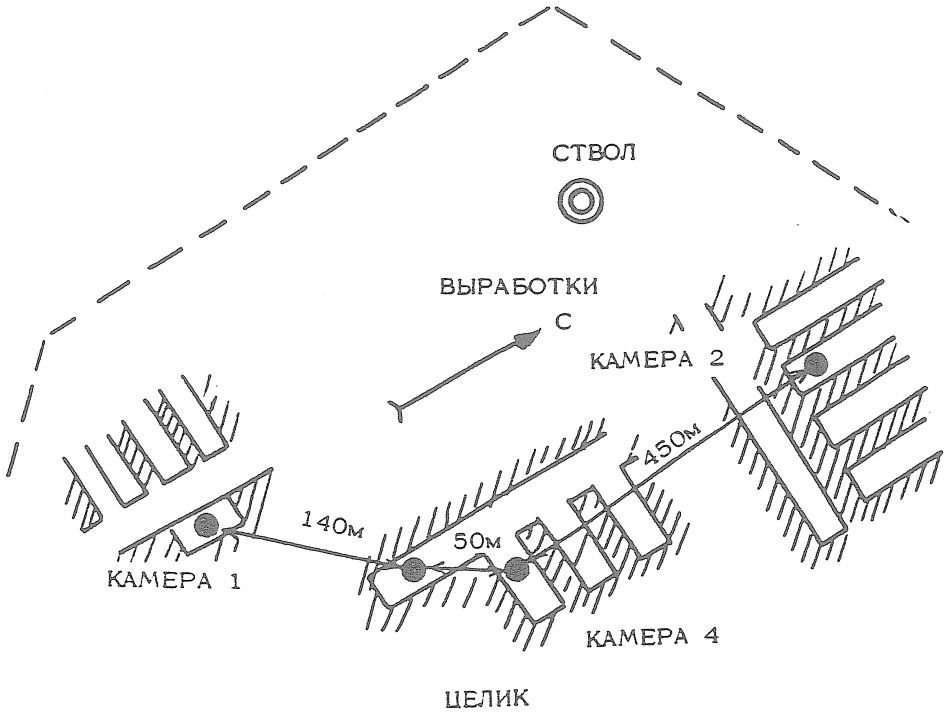

Figure 2 Schéma de la situation des salles clinométriques dans la station de Karlo-Libknekhtovsk.

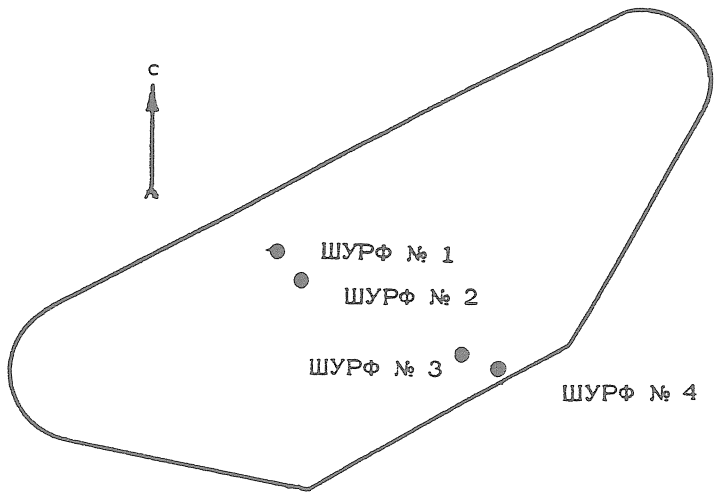

Figure 3 : Schéma de disposition des mines dans la zone fortement éboulée.

BIBLIOGRAPHIE

1. Баленко В.Г., Кутный А.М., Новикова А.Н. Результаты наклономерных наблюдений в Киево-Печерской Лавре в 1964-1966гг. - В сб.: Вращение и приливные деформации Земли. М.: Наука, 1970, вып. 1, с. 249-264.

2. Баленко В.Г., Кутный А.М., Новикова А.Н. Наблюдения приливных наклонов на станции Березовая Рудка. - В сб.: Вращение и приливные деформации Земли. М.: Наука, 1978, вып. 10, с. 14-22.

3. Баленко В.Г., Кутный А.М., Новикова А.Н. Результаты наблюдений приливных наклонов на станции Покровская Багачка. - В сб.: Вращение и приливные деформации Земли. М.: Наука, 1975, вып. 7, с. 15-21.

4. Баленко В.Г., Кутный А.М., Новикова А.Н. Наклономерные наблюдения на станции Шевченково Карловского района Полтавской области. - В сб.: Вращение и приливные деформации Земли. М.: Наука, 1970, вып. 2, с. 41-57.

5. Баленко В.Г., Кутный А.М., Новикова А.Н. Результаты наблюдений приливных наклонов на станции Катериновка. - В сб.: Вращение и приливные деформации Земли. М.: Наука, 1972, вып. 4, с. 65-75.

6. Баленко В.Г., Кутный А.М., Новикова А.Н. и др. Наклономерные наблюдения в шахте № 1 рудоуправления Артемсоль. - В сб.: Вращение и приливные деформации Земли. М.: Наука, 1972, вып. 4, с. 20-44.

7. Орлов А.Я. Первый ряд наблюдений с горизонтальными маятниками в Юрьеве над деформациями Земли под влиянием лунного притяжения. - Избр. тр., Киев: Изд-во АН УССР, 1961, т. 2, с.156-215.

8. Баленко В.Г., Овчинников В.А., Кутный А.М. и др. Горизонтальный маятник с цельнеровским подвесом на металлических нитях. - В сб.: Вращение и приливные деформации Земли. М.: Наука, 1974, вып. 6, с. 3-15.

9. Баленко В.Г., Кутный А.М., Новикова А.Н. Наклономерные наблюдения в Карло-Либкнехтовске по программе изучения эффекта полости. - В сб.: Вращение и приливные деформации Земли. М.: 1979, вып. 11, с. 18-23.

10. Баленко В.Г. Исследования наклонов земной поверхности по профилю Киев-Артемовск. Киев: Наукова думка, 1980, 174 с.

11. Баленко В.Г. Эффект топографии в приливных наклонах на станциях профиля Киев-Артемовск. - В сб.: Вращение и приливные деформации Земли. М.: Наука, 1981, вып. 13, с. 3-10.

12. Кутный А.М. Наклономерные наблюдения в обвалоопасной зоне. - В сб.: Вращение и приливные деформации Земли. М.: Наука, 1979, вып. 11, с. 3-9.

13. Баленко В.Г., Булацен В.Г., Шляховый В.П. и др. Приливные изменения силы тяжести в Полтаве с 1973 по 1976гг. - В сб.: Вращение и приливные деформации Земли. М.: Наука, 1978, вып. 10, с. 3-14.

14. Баленко В.Г., Булацен В.Г. О повышении точности приливных наблюдений с гравиметрами G_s -11 и G_s -12. - В сб.: Вращение и приливные деформации Земли. М.: Наука, 1980, вып. 12, с. 75-84.

15. Парийский Н.Н., Барсенков С.Н., Волков В.А. и др. Приливные вариации силы тяжести в СССР. - В кн.: Изучение земных приливов. М.: Наука, 1980, с. 65-85.

16. Wahr J.M. Body tides on an elliptical, rotating, elastic and oceanless earth.- Geoph. Journ. Roy.Astron.Soc., 1981, v.64, No 3, p.677-703.

Traduction

Paramètres de marées et composition spectrale des inclinaisons de l'écorce terrestre d'après les observations dans les puits

J.A. Chirokov, K.M. Anokhina, K. Arlt
Institut de physique de la Terre
de l'Académie des Sciences, Moscou
Institut d'Astrophysique
de l'Académie des Sciences, Potsdam

Prévision des tremblements de terre N° 8 pp 167-181 - 1988

La détermination des propriétés élastiques de la Terre d'après les observations des inclinaisons de marées et les variations de la pesanteur constitue un problème classique des marées terrestres. Le fait que la force génératrice de marée soit connue avec une haute précision a toujours servi de condition. Les observations des inclinaisons de marées ont été faites jusqu'à ces derniers temps exclusivement à l'aide de pendules horizontaux installés dans des sites souterrains. La diversité des conditions d'installation des clinomètres dans les sous-sol, les galeries de mines, les mines et les galeries de recherche a conduit à la divergence et à la faible comparabilité des résultats obtenus. La dispersion des valeurs du facteur d'amplitude obtenue dans les différentes stations du monde pour l'onde M_2 atteint 40%.

On peut apparemment diminuer cette dispersion en installant les clinomètres dans un puits ce qui garantit un procédé standard d'installation de l'instrument dans n'importe quelles conditions géologiques. Une influence positive sur la précision des mesures est exercée par la base de mesure relativement grande et orientée verticalement du clinomètre de puits avec pendule vertical, augmentant la relation signal/bruit.

Pose du problème

La méthode élaborée ces dernières années pour les observations clinométriques de campagne dans les puits [1] permet d'estimer son efficacité. C'est à dire la capacité de la méthode de garantir l'obtention d'un résultat représentatif. Le degré de concordance des paramètres des inclinaisons de marées en un point donné peut servir de critère. Sous ce rapport, la comparaison des résultats a une valeur particulière d'après les observations dans un groupe de puits situés à proximité, dans des puits de différentes constructions, dans des puits où les conditions hydrogéologique sont différentes etc .

Conditions des observations

Au cours d'une série d'un an dans la station clinométrique voisine de Moscou "Polouchkino" on a utilisé dans les puits le clinomètre "Askania" et les clinomètres HCO-C [203].

Les puits n° 1 et n° 4 ont été forés en 1973 dans le sable argileux jusqu'à une profondeur de 30m et dans des dépôts calcaire jusqu'à une profondeur de 50m. Ils sont distants l'un de l'autre de 20m. Les tubages hermétiques des puits sont reliés avec le terrain par cimentation. L'épaisseur de l'anneau de ciment est en moyenne d'environ 3 cm. Les tubes sont pourvus de saillies spéciales sur lesquelles on peut installer les clinomètres de type "Askania" et HCO-C. L'orifice du puits n° 1 est situé à la profondeur de 12m pour créer un régime isothermique dans la colonne des tubes. L'orifice du puits n° 4 sort en surface et est protégé des perturbations de température par un tube supplémentaire en acier et par une couverture isolante de la chaleur.

Les clinomètres sont descendus dans les puits par un treuil, après quoi on les a orientés à l'aide d'une barre spéciale du type YYCH-1 dans l'azimut N.S et E.W avec une précision de ± 0,5° et on a ensuite fait un ajustage des pendules. Le site d'enregistrement se trouvait dans un local souterrain éloigné de 10 à 30m. L'enregistrement a été fait simultanément aussi bien par procédé photographique que sur autoenregistreurs à plusieurs canaux du type "Siemens compensographe" et "Vatanabe".

Simultanément aux inclinaisons on a enregistré sans interruption la température de l'air dans les deux puits avec des thermographes à résistance ayant la sensibilité de 0,001° c/mm.

Les observations dans le puits n° 4, à la profondeur de 50m, avec le clinomètre Askania, ont duré 252 jours; la durée des observations dans le puits n° 1, à la profondeur de 30m, avec les clinomètres Askania et HCO-C-72 étaient de 76 et 92 jours respectivement et les observations de contrôle dans le puits n° 1, à la profondeur de 30m, avec l'appareil HCO-C-51 ont duré 40 jours.

Analyse harmonique

L'analyse harmonique a été faite par les méthodes Pertsev (méthode de 29 jours) [4, 5], Venedikov (version BM.65) [6] et Chojnicki (version XA 15H et Xa 150) [9].

L'analyse par la méthode Chojnicki et l'analyse spectrale ont été faites sur EBM EC 1040 à l'Institut d'astrophysique de Potsdam.

Nous donnons dans les tables 1 et 2 les valeurs du facteur d'amplitude et du retard de phase obtenues avec le clinomètre "Askania" dans le puits à la profondeur de 50m. Les résultats de l'analyse selon la méthode Pertsev représentés par les valeurs moyennes de 6 séries indépendantes mensuelles sont déterminés avec une erreur quadratique moyenne bien plus importante que par les autres méthodes. Les résultats obtenus par la méthode Venedikov, sans élimination préliminaire de la dérive ont, comparativement à la méthode Pertsev une erreur sensiblement moindre pour les composantes E.W et la même pour les composantes N.S.

Une supériorité de la méthode Chojnicki est apparue dans le fait qu'on a réussi à déterminer avec assez de précision le facteur d'amplitude et le retard de phase des ondes à longue période S_{sa}, M_m, Mf, Mt_m. Un intérêt particulier est représenté par les résultats pour l'onde de 14 jours Mf qui n'existe dans les inclinaisons que dans l'azimut N.S. Il est à noter que l'effet de charge provoqué par l'onde Mf de la marée océanique doit être observé pour les deux composantes des inclinaisons. Cette circonstance crée une possibilité de principe d'étudier les hétérogénéités horizontales de l'écorce terrestre sur les continents par la mesure des inclinaisons à la fréquence de l'onde Mf dans l'azimut E.W. La présence de limites verticales du partage et des régions des paramètres élastiques anormaux sera marquée dans ce cas par l'écart des amplitudes de l'onde Mf - EW en fonction de déformations, inclinaisons de charge océanique calculées, apparaissant au point d'observation. Cependant pour séparer l'onde à longue période il faut de longues séries d'observations avec une dérive préliminairement soustraite par la méthode des points nuls [7]. L'application de cette méthode ne diminue pas la précision de la détermination des caractéristiques des ondes principales diurnes et semi diurnes (tables 1 et 2) uniquement pour la séparation des petites ondes de périodes diurne, semi diurne et terdiurne il est préférable de faire la soustraction préliminaire de la dérive par la méthode de Pertsev [8].

Analyse spectrale

Toutes les méthodes d'analyse harmonique à l'aide desquelles on détermine les paramètres de marées γ et $\varkappa$, sont basées sur la séparation des ondes dont les fréquences sont connues. Cependant les observations peuvent être soumises à l'influence de facteurs non dus aux marées mais qui leur sont voisins en fréquence et qui diminuent la sûreté des résultats de l'analyse harmonique. C'est pourquoi il est apparu intéressant d'étudier la composition spectrale des inclinaisons observées dans les azimuts N.S. et E.W.

Pour réaliser l'analyse spectrale de Fourier, on a choisi un intervalle continu de 6 mois d'observations avec le clinomètre "Askania" dans le puits n° 4.

Nous donnons sur les figures 1, 2, 3, 4 les spectres d'amplitude des inclinaisons de marées dans les azimuts N.S et E.W dans les gammes de fréquence des ondes à longue période, diurnes semi diurnes et terdiurnes.

Sur chaque figure les courbes "A" et "a" qui représentent les spectres des inclinaisons observées dont on a éliminé la dérive par le procédé des points nuls.

Les courbes "B" et "b" sont les spectres du "résidu" qui est le résultat de l'élimination de la "marée théorique" calculée en tenant compte des paramètres de marées obtenus par les observations elles-mêmes par la méthode de Chojnicki. La dérive a été éliminée par la méthode des points nuls.

Les courbes "C" et "c" sont les spectres de ces mêmes "résidus" mais avec élimination préliminaire de la dérive par la combinaison Pertsev.

La courbe "A" indique que sur l'intervalle de 6 mois en composante NS on sépare bien les ondes à longue période malgré leurs faibles amplitudes : l'onde solaire de déclinaison Ssa de période semi annuelle et dont l'amplitude théorique dans la station n'est que de 0,88 mseca; l'onde Mm elliptique lunaire de période 27 jours et d'amplitude théorique 1,00 mseca; l'onde lunaire de déclinaison Mf de période 14 jours et d'amplitude théorique 1,89 mseca, l'onde Mtm d'amplitude 0,36 mseca et de période 9 jours.

Le spectre des résidus indique qu'on n'observe pas d'ondes qui ne sont pas dues aux marées ayant une amplitude de plus de 0,1 mseca. La courbe "c" indique que dans le spectre du résidu, après application de la combinaison Pertsev, comme il fallait s'y attendre il n'y a pas en général d'ondes à longue période car elles entrent entièrement dans la dérive. Un certain bruit apparaît uniquement à partir des périodes de 90 heures c'est à dire quand le facteur d'éjection de la combinaison Pertsev devient plus petit que l'unité.

Dans la gamme diurne il est évident qu'on sépare les quatre ondes principales Q_1, O_1, $(K_1\ P_1)$, J_1. Les ondes K_1 et P_1, n'ont pas été séparées à cause de la longueur insuffisante de la série. Le spectre du résidu indique qu'à la fréquence des ondes K_1 P_1 l'amplitude du bruit augmente jusqu'à 0,2 mseca soit 6% de l'amplitude théorique de K_1. Aux autres périodes, le bruit ne dépasse pas 0,1 mseca.

Dans la gamme semi diurne on a également séparé quatre ondes: μ_2, N_2 M_2 et S_2. Pour la séparation des ondes S_2 et K_2 la longueur de la série était également insuffisante.
Les spectres des résidus ont montré que le bruit ne dépasse pas 0,1 mseca dans la gamme semi diurne.

Dans le spectre des ondes terdiurnes on a bien séparé l'onde M_3 qui a une amplitude théorique de 0,082 mseca. Le bruit y est très faible et ne dépasse pas 0,03 mseca.

Observations comparatives

La bonne concordance des valeurs γ et α présentées dans les tables 1 et 2, obtenues par les trois méthodes différentes, témoigne de l'exactitude des résultats dans les puits n° 4. Cependant on ne peut pas ne pas noter que le facteur d'amplitude des ondes semi diurnes est exagéré de 5 ÷ 10 % pour les deux composantes tandis que pour les ondes diurnes un résultat exagéré ne se note que dans l'azimut N.S. Pour éclaircir le rôle de l'influence instrumentale comme cause possible on a fait des observations comparatives avec trois clinomètres de construction différente, notamment les clinomètres "Askania" HCO-C-72 et HCO-C-51. Les deux derniers appareils n'ont pû être installés que dans le puits de diamètre 300mm pour des raisons de construction. Le puits n° 4 avait un diamètre de 200mm ce qui a éliminé la possibilité d'y installer les clinomètres du type HCO-C. Les observations comparatives ont été faites dans le puits voisin n° 1 de diamètre 300mm et à la profondeur de 30m. Elles ont été faites par remplacement successif des appareils dans le puits. La durée moyenne de la série d'observations de chaque appareil était de plus de deux mois ce qui permettait d'estimer avec sécurité les paramètres de l'onde M_2 dans l'azimut EW.

La table 3 donne les résultats des observations comparatives pour les cinq ondes principales dans le puits n° 1 avec les trois appareils. L'analyse harmonique a été faite par les méthodes de Venedikov et Chojnicki.
De la table 3 il résulte que, pour l'onde M_2, les trois appareils ont donné des résultats ne différant pas l'un de l'autre de plus de 1% ce qui ne sort pas des limites des erreurs. La comparaison des résultats pour les ondes diurnes a été difficile à cause de la durée différente des séries et de la non concordance des époques d'observation.

Ainsi, les observations comparatives ont montrée le rôle insignifiant de l'influence instrumentale comme cause possible des divergences dans les puits n° 1 et n°4. C'est pourquoi on peut émettre une hypothèse sur le fait que les valeurs exagérées des paramètres de marées dans le puits n° 4 sont dues à la présence de la couche de calcaire dur se trouvant à la profondeur de 50m. Le puits n° 1, moins profond, se trouve complètement dans l'épaisseur de masses friables, ce qui influence favorablement les résultats. Les observations dans les puits voisins de 30 mètres n° 2 et n° 3 situés également dans les masses friables ont donné les valeurs de γ pour l'onde M_2 correspondant pratiquement aux valeurs de la table 3 [9, 10]. Ce fait montre la nécessité de tenir compte de l'influence de la fracture géologique sur le choix du puits.

Conclusions

1. Les observations clinométriques dans deux puits voisins de construction différente ont permis de découvrir une divergence systématique des paramètres des inclinaisons de marées.

2. Comme l'ont montré les expériences, l'effet instrumental n'est pas la cause de cette divergence.

3. Le procédé d'installation des clinomètres dans le puits en possédant une série d'avantages importants vis à vis des autres procédés d'installation n'élimine pas l'influence perturbatrice des facteurs géologiques et hydrogéologiques.
   On peut diminuer sensiblement l'influence perturbatrice si on tient compte de la structure géologique au site d'observation.

Table 1

Facteur d'amplitude γ avec le clinomètre "Askania" dans le puits n° 4.

Onde	N.S					E.W				
	Ат мсек	П	ВМ65	Х15Ф ФП	Х15Ф МНП	Ат мсек	П	ВМ65	Х15Ф ФП	Х15Ф МНП
Ssa	0,882	-	-	-	0,742 13	-	-	-	-	-
Mm	1,000	-	-	-	0,773 11	-	-	-	-	-
Mf	1,895	-	-	-	0,741 7	-	-	-	-	-
Mtm	0,363	-	-	-	0,592 35	-	-	-	-	-
$2Q_1$	0,059	-	-	1,203 122	1,228 141	0,136	-	-	0,865 45	1,145 60
θ_1	0,447	-	0,645 159	0,652 25	0,684 29	1,029	-	0,677 63	0,613 9	0,656 12
Q_1	2,337	0,737 25	0,729 29	0,758 5	0,754 6	5,373	0,663 18	0,666 12	0,653 2	0,692 2
M_1	0,184	-	0,435 288	0,476 46	0,509 53	0,422	-	0,650 126	0,612 18	0,623 24
$P_1 S_1$	1,088	-	-	0,862 10	0,806 11	2,500	-	-	0,699 4	0,740 5
K_1	3,287	0,788 18	0,763 19	0,788 3	0,773 4	7,556	0,684 18	0,681 8	0,692 1	0,713 2
J_1	0,184	-	1,459 392	0,966 62	0,876 71	0,422	-	0,874 144	0,797 22	0,827 30
OO_1	0,101	-	0,743 644	0,814 104	1,027 120	0,231	-	0,571 265	0,494 39	0,688 55
$2N_2$	0,187	-	0,838 97	0,831 35	0,859 41	0,226	-	0,654 78	0,698 25	0,728 33
N_2	1,410	0,736 18	0,722 18	0,741 7	0,740 8	1,709	0,799 17	0,797 15	0,794 5	0,792 7
M_2	7,366	0,742 5	0,744 4	0,743 1	0,742 2	8,929	0,773 5	0,777 3	0,775 1	0,770 1
L_2	0,208	-	1,023 188	0,944 65	0,955 74	0,252	-	0,871 164	0,740 46	0,714 62
S_2	3,427	0,757 3	0,754 7	0,742 3	0,744 3	4,154	0,781 8	0,784 6	0,784 2	0,782 3
M_3	0,082	-	-	0,807 123	0,912 143	0,099	-	-	0,780 88	0,790 88

Table 2

Retard de phase φ avec le clinomètre "Askania" dans le puits n° 4.

Onde	N.S				E.W			
	П	ВМ65	Х15Ф ФП	Х15Ф МНП	П	ВМ65	Х15Ф ФП	Х15Ф МНП
Sso	-	-	-	0,4 9	-	-	-	-
Mm	-	-	-	2,9 8	-	-	-	-
Mf	-	-	-	-1,5 6	-	-	-	-
Mtm	-	-	-	-3,4 3,4	-	-	-	-
$2Q_1$	-	-	38,8 5,8	45,8 6,6	-	-	-9,9 3,0	-16,1 3,0
Q_1	-	9,2 9,1	-0,1 2,2	-6,3 2,4	-	-3,3 3,6	-5,5 9	-3,0 1,1
O_1	5,0 1,6	5,9 1,6	4,6 4	3,5 4	-4,3 1,5	-2,0 7	-1,8 2	-1,7 2
M_1	-	-35,0 16,5	-13,3 5,5	-31,6 5,9	-	9,2 7,2	-2,8 1,7	-1,4 2,2
P_1S_1	-	-	5,0 0,6	5,9 8	-	-	0,5 3	0,3 0,4
K_1	-3,0 3,1	-2,1 1,1	-3,2 3	-3,7 3	-4,0 5	-4,3 5	-5,4 1	-5,5 1
J_1	-	5,4 2,4	9,4 3,7	5,2 4,7	-	14,8 8,2	1,5 1,6	2,3 2,1
OO_1	-	11,1 16,9	34,5 7,3	31,1 6,7	-	20,2 15,2	-6,8 4,6	-6,4 4,4
$2N_2$	-	-7,5 5,5	0,7 2,4	-1,7 2,7	-	-8,2 4,5	-7,0 2,0	-2,9 2,6
N_2	-2,0 1,8	-0,9 1,0	-0,2 0,6	-0,6 0,6	-2,1 4	-2,5 8	-2,2 4	-2,7 5
M_2	1,4 5	1,4 2	1,6 1	1,5 1	-3,5 2	-3,5 2	-3,1 1	-3,1 1
L_2	-	2,5 7,3	-3,9 3,9	-9,6 4,5	-	19,5 9,4	-0,3 3,6	-1,4 4,9
S_2	2,3 1,4	0,1 4	3,3 2	2,8 3	-2,0 5	-2,2 3	-1,6 1	-1,7 2
M_3	-	-	13,1 8,8	9,9 8,9	-	-	2,4 6,4	-5,9 7,6

Table 3

Facteur d'amplitude γ des inclinaisons de marées d'après les observations avec des appareils de différents types dans le puits N° 1.

Ondes	"Askania" vertic 73 jours		N° 72 - horiz. 92 jours		N° 51 horiz. 40 jours
	XA15H	BM65	XA15H	BM65	BM65
M_2	0,726 6	0,727 12	0,731 8	0,729 11	0,719 31
S_2	0,771 11	0,760 24	0,772 15	0,758 23	0,709 76
N_2	0,829 36	0,825 83	0,696 39	0,754 58	
K_1	0,754 9	0,741 41	0,719 11	0,729 35	0,676 73
O_1	0,672 12	0,632 56	0,802 16	0,785 57	0,760 122

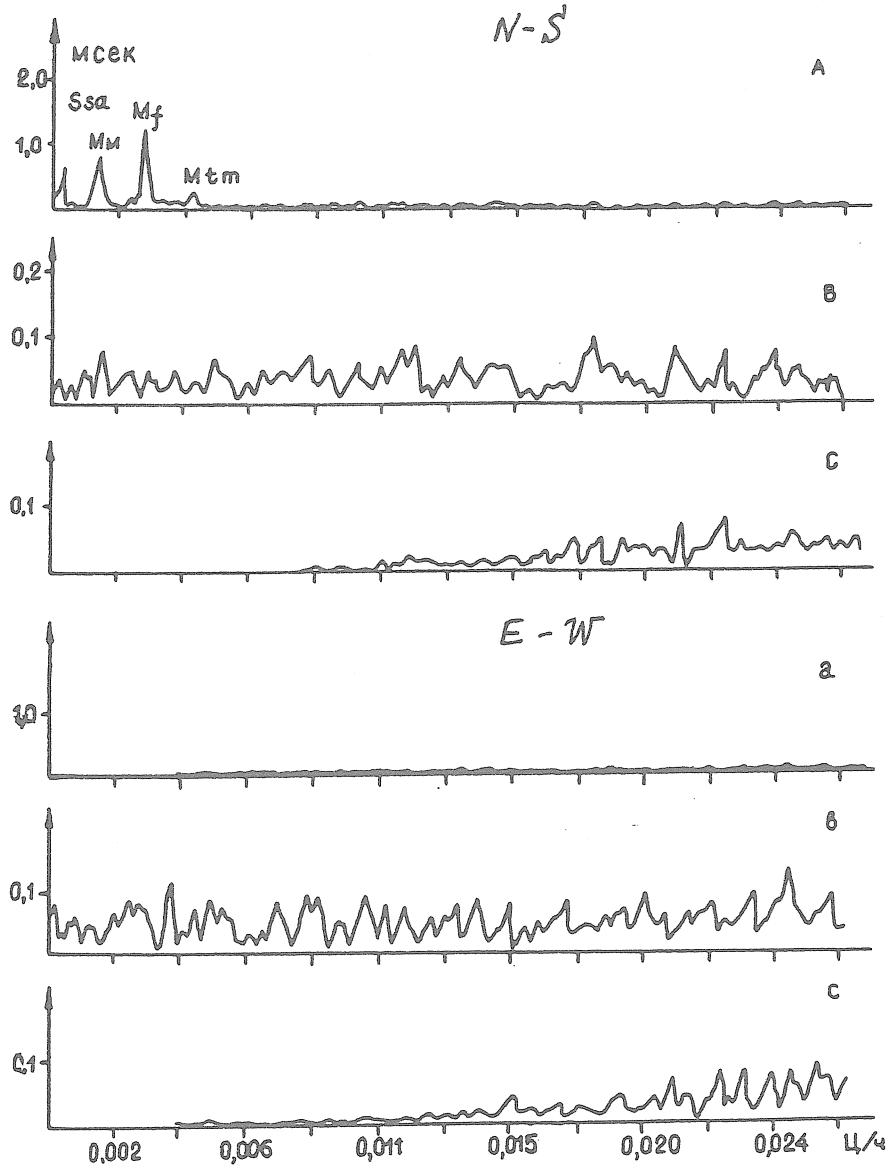

Figure 1 : Spectre d'amplitude des inclinaisons de marées dans les azimuts N.S et E.W dans la gamme des ondes à longue période.
A et a : spectre des inclinaisons observées;
B et b : spectre du "résidu" avec soustraction préliminaire de la dérive par la méthode des points nuls;
C et c : spectre du "résidu" avec soustraction préliminaire de la dérive d'après Pertsev.

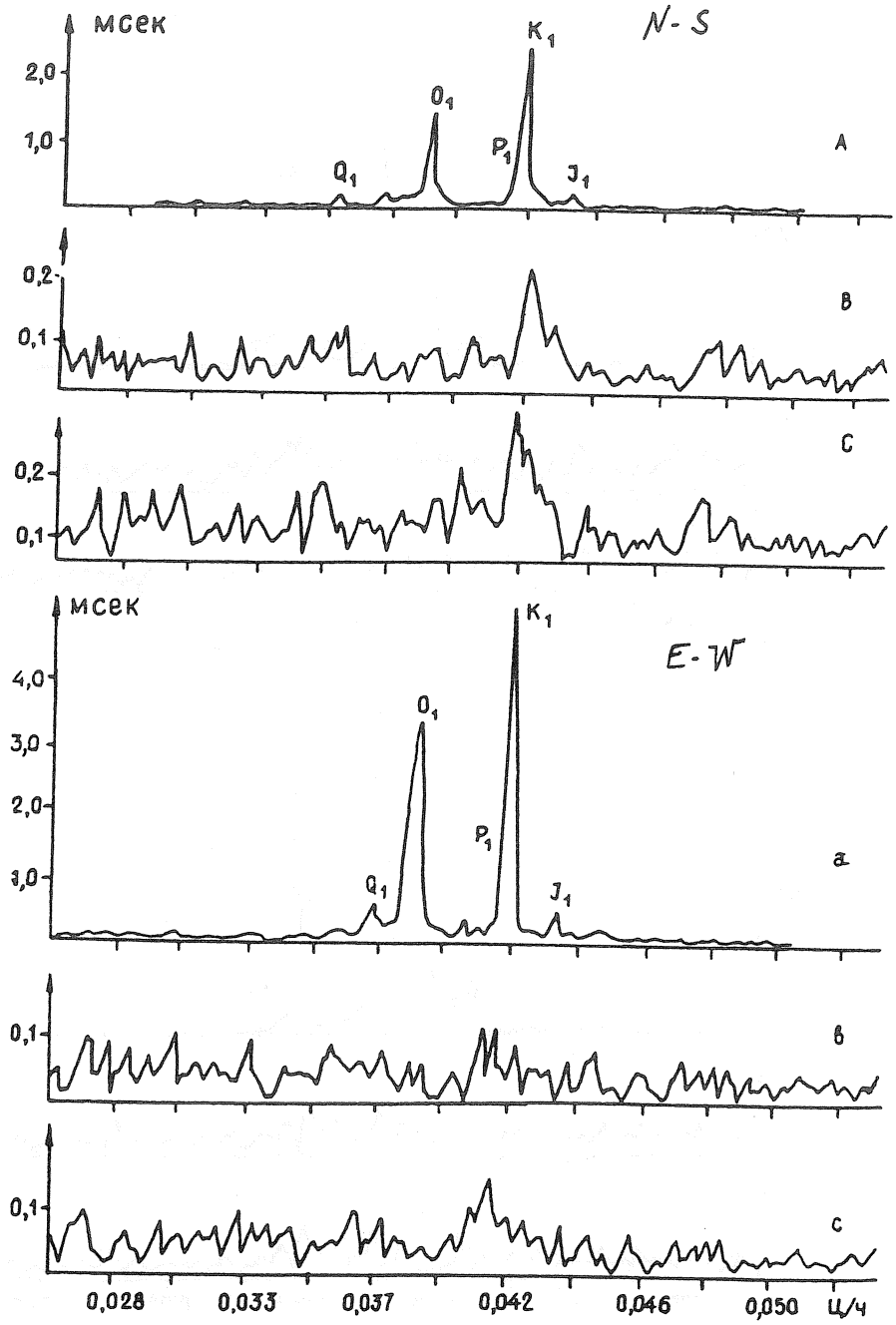

Figure 2 : Spectre d'amplitude des inclinaisons de marées dans les azimuts N.S. et E.W. dans la gamme des ondes diurnes.

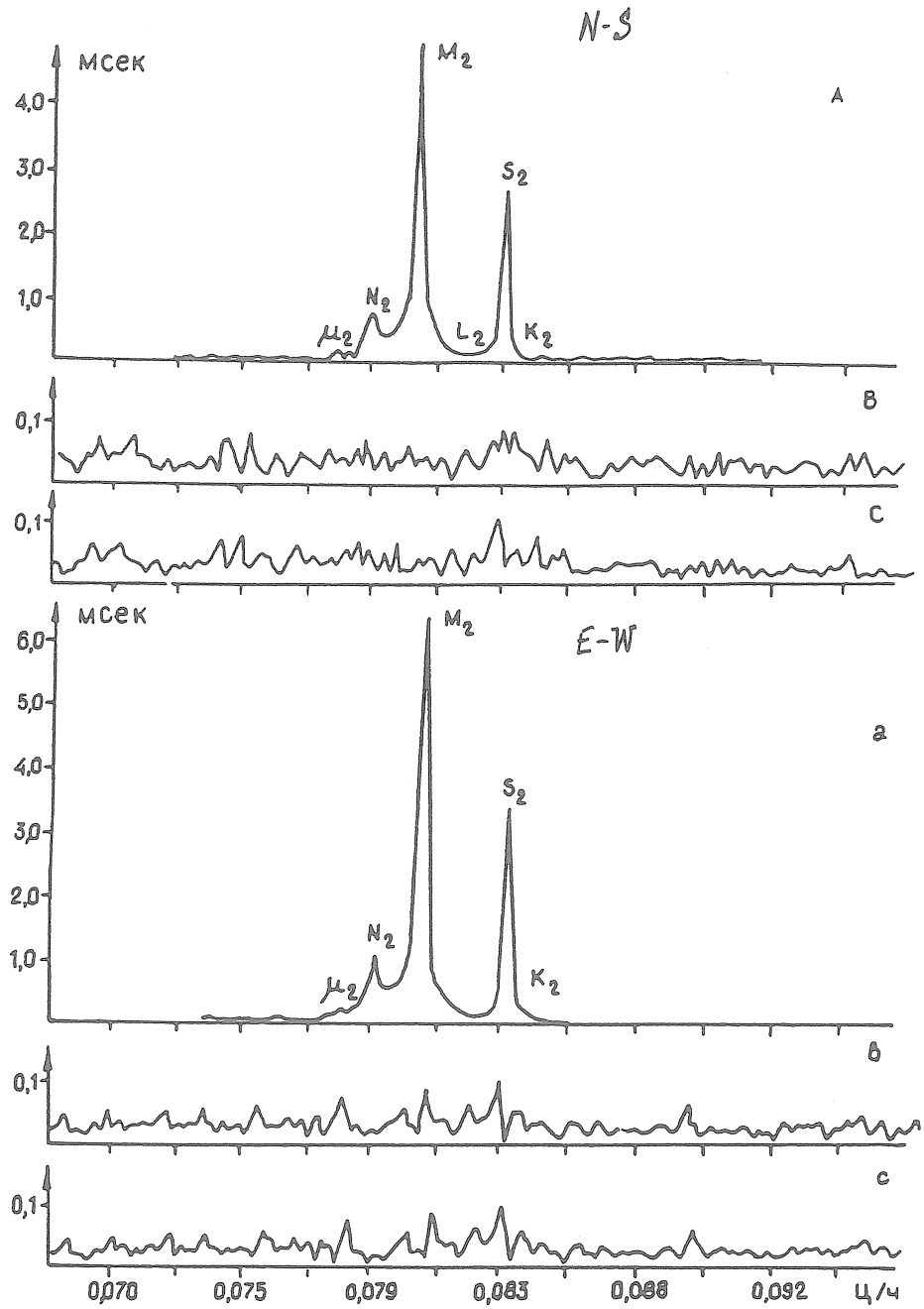

Figure 3 : Spectre d'amplitude des inclinaisons de marée dans les azimuts N.S et E.W dans la gamme des ondes semi diurnes

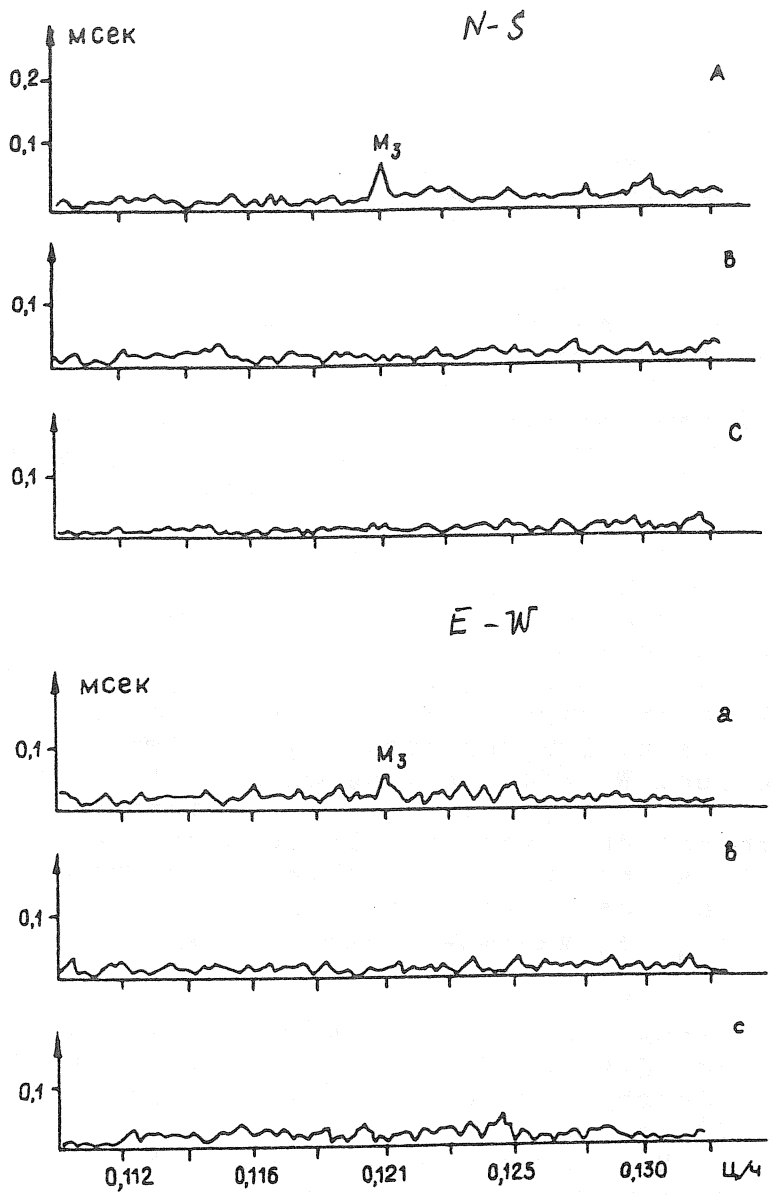

Figure 4 : Spectre d'amplitude des inclinaisons de marées dans les azimuts N.S et E.W dans la gamme des ondes terdiurnes.

Bibliographie

1. Широков И.А., Анохина К.М. Методика и результаты наклономерных наблюдений в скважинах. – В кн.: Современные движения земной коры. Новосибирск, Изд-во Института геологии и геофизики СО АН СССР, 1976, с.98.

2. Широков И.А., Анохина К.М. О сравнительных земноприливных наблюдениях скважинным наклономером "Аскания" и наклономерами Островского. – В кн.: Вращение и приливные деформации Земли. Киев: Наукова думка, № 7, 1974.

3. Широков И.А., Анохина К.М. Результаты наблюдений приливных наклонов скважинным наклономером "Аскания". – В кн.: Современные движения земной коры. Новосибирск, Изд-во Института геологии и геофизики СО АН СССР, 1976, с.114.

4. Перцев Б.П. Гармонический анализ упругих приливов. – Изв. АН СССР, Геофизика, № 8, 1958, с.946.

5. Перцев Б.П. Об учете сползания нуля при наблюдениях земных приливов. – Изв.АН СССР, Геофизика, № 4, 1959, с.547.

6. Venedikov A.P. Une méthode pour l'analyse des marées terrestres à partir d'enregistrements de longuer arbitraire. Comm. Obs. Royal Belgique., No 250, Ser. Geoph., No 71, 1966, p.3.

7. Chojnicki T. Determination des paramétres des marée par la compensation des observations au moyen de la methode de moindres carrés. Publications of the Inst. of Geophysics Polich Acad.of Sci., 55. Warszawa, 1972, p. 43.

8. Chojnicki T. Determination de la derive dans les mesures des marées au moyen de la methode des points neutres. Publications of the Inst. of Geophysics Polish Acad. of Sci, 71. Warszawa, 1973, p. 3.

9. Широков И.А., Анохина К.М. Наблюдения приливных наклонов в скважинах. – В кн.: Изучение земных приливов. М.: Наука, 1980, с.188.

10. Широков И.А., Анохина К.М. Наклономерные наблюдения с вертикальным маятником "Аскания" в скважине вблизи Москвы. – В кн.: Изучение земных приливов. М.: Наука, 1980, с.193.